1983

Reinforced composite masonry shear walls

Mahmoud Hussien Ahmed
Iowa State University

Ahmed, Mahmoud Hussien

REINFORCED COMPOSITE MASONRY SHEAR WALLS

Iowa State University PH.D. 1984

PLEASE NOTE:

In all cases this material has been filmed in the best possible way from the available copy. Problems encountered with this document have been identified here with a check mark __√__.

1. Glossy photographs or pages _____
2. Colored illustrations, paper or print _____
3. Photographs with dark background __√__
4. Illustrations are poor copy _____
5. Pages with black marks, not original copy _____
6. Print shows through as there is text on both sides of page _____
7. Indistinct, broken or small print on several pages __√__
8. Print exceeds margin requirements _____
9. Tightly bound copy with print lost in spine _____
10. Computer printout pages with indistinct print _____
11. Page(s) _____ lacking when material received, and not available from school or author.
12. Page(s) _____ seem to be missing in numbering only as text follows.
13. Two pages numbered _____. Text follows.
14. Curling and wrinkled pages _____
15. Other _____

Reinforced composite masonry shear walls

by

Mahmoud Hussien Ahmed

A Dissertation Submitted to the

Graduate Faculty in Partial Fulfillment of the

Requirements for the Degree of

DOCTOR OF PHILOSOPHY

Department: Civil Engineering
Major: Structural Engineering

Approved:

Signature was redacted for privacy.

In Charge of Major Work

Signature was redacted for privacy.

For the Major Department

Signature was redacted for privacy.

For the Graduate College

Iowa State University
Ames, Iowa

1983

TABLE OF CONTENTS

LIST OF FIGURES

LIST OF TABLES

INTRODUCTION

Masonry is one of the oldest construction materials known to man. However, reinforced masonry, as a construction material, has only recently been developed. Extensive theoretical and experimental research investigations have been conducted for the development of reinforced masonry for construction of multi-story buildings. Reinforced structural walls efficiently resist lateral loads resulting from wind or earthquakes in addition to vertical gravity loads [1]. The resistance to wind or earthquake loads is provided most generally by a masonry wall's strength in diaphragm action (i.e., in-plane shear). Reinforcement was used in the masonry buildings to eliminate the need for thick, massive sections; for walls needing greater load resistance, multi-wythe masonry or composite walls were introduced. Composite can be accomplished by combining masonry wythes and/or a grouted collar joint (in between) to act as one wall. This study investigates these composite multi-wythe walls subjected to combined in-plane shear and gravity loads.

Objectives

This research was undertaken to study the strength and behavior of the new concept of multi-wythe composite reinforced masonry. Composite shear walls were subjected to in-plane lateral loads, in addition to the gravity load. This study is similar to research proposed by Masonry Research Foundation [2].

The detailed objectives were:

(1) to determine the failure modes;

(2) to determine the behavioral and strength characteristics due to the in-plane loads in combination with gravity loads;

(3) to study the effect of the following parameters on the behavioral and strength characteristics of the composite walls:

   (a) the arrangement of the wall, i.e., brick-to-brick and brick-to-block;

   (b) effect of the precompression load; and

   (c) type of reinforcement.

(4) to analyze the wall using the finite element technique;

(5) to compare the experimental results to both analytic results and to the ACI Code; and

(6) to make recommendations for design of composite diaphragm masonry walls.

Research Plan

Composite wall tests were conducted and analyzed. Each wall tested was made from two wythes of eithr brick-to-brick or brick-to-block with a two-inch collar joint. The collar joint was grouted and reinforced. The wall panels were approximately 4 feet wide, 6 feet high, and 9 inches thick. The walls were fixed at the base but free to displace at the top. The in-plane and gravity loads were applied as distributed loads at the top of the wall. To determine the gravity load, an example for a proposed real building was solved in a similar manner to that given in [3] (see the Appendix). The results were analyzed comparatively using the finite element technique and the theory for flexural strength. In addition to the composite walls, a number of unit and prism tests were

conducted to serve as control specimens for determination of material strength.

The following chapters were written in a way that can be published as papers (as suggested in the University thesis manual [4]) as given below:

Paper 1: Behavior of reinforced brick-to-block walls. This paper contains Part 2A and Part 1, which will be placed after the abstract.

Paper 2: Behavior of reinforced brick-to-brick walls. This paper contains Part 2B and Part 1, which will be placed after the abstract.

Paper 3: Analysis of composite masonry walls: Part I. This paper contains Part 3.

Paper 4: Analysis of composite masonry walls: Part II. This paper contains Part 4.

The first two papers deal with the experimental results; the last two deal with the analytical results and compare analytical with experimental results.

These four papers are followed by a tentative design criterion for reinforced composite masonry walls and the overall conclusions and recommendations based on the results of this study.

This research was funded by:

(1) the Agency for International Development, Washington, D.C.;

(2) the Masonry Institute of Iowa;

(3) the Masons Union of Iowa;

(4) the Civil Engineering Department at Iowa State University; and

(5) the Engineering Research Institute at Iowa State University.

PART 1. LITERATURE REVIEW AND CONTROL TESTS

INTRODUCTION

Extensive experimental investigations have been made toward the development of reinforced masonry. Reinforced masonry elements can provide taller and stronger buildings which resist lateral loads caused by earthquakes and strong winds. Generally, lateral load resistance in a masonry wall's strength is provided by diaphragm action (i.e., in-plane shear). For walls needing more lateral load resistance, multi-wythe masonry walls or composite walls were introduced. The purpose of this study was to investigate the strength and behavior of the brick-to-block composite reinforced walls.

LITERATURE REVIEW

The use of reinforced masonry structures was first proposed by Brunel in 1813. In 1923. Brebner, as cited by Grogan [1], studied the performance of reinforced brick masonry and concluded that reinforced brick masonry was analogous to reinforced concrete, so that the same working stress design could be used for many reinforced masonry members. Tests by Benjamin and Williams [2] studied the effectiveness of unreinforced brick masonry walls in resisting in-plane shear forces by using scale models to test this type of wall. The tested walls ranged from 0.34 scale to full size (one-story). However, brick units and mortar joints were of actual size, regardless of model size. Benjamin and Williams concluded that no significant errors resulted from the model scaling. In 1959, Schneider [3] evaluated the behavior of the three basic types of masonry units forming integral parts of a composite masonry wall. The tested units were clay brick, concrete block, and shel-brick. Reinforcement used in these walls consisted of vertical and horizontal bars. When loaded with in-plane loads at the upper end, the walls failed through diagonal tension. Schneider concluded that:

(1) the reinforced grouted masonry was highly recommended for resisting lateral in-plane loading;

(2) the ultimate shear index (i.e., the shear force divided by the gross area of the wall) was 143 psi with a height-to-width ratio approximately equal to one; and

(3) the type of mortar mix used had little effect on the overall shear

resistance of brick walls.

Nilsson and Losberg [4] (1970) tested prefabricated brick panel walls 6.5 ft. wide and 9.2 ft. high, having a thickness of 5.51 inches. These walls consisted of two wythes with mesh reinforcement in the middle (Fig. 1). The walls were simply supported along all four edges, then loaded in the out-of-plane direction by plastic bags filled with compressed air. After large deflections, gradual failure occurred. Nilsson and Losberg concluded that load capacity can be raised significantly after cracking pressure is reached with mesh-reinforced walls.

Meli [5] (1974) tested 56 walls, of about (6'-6"x6'-6"), built on stiff concrete beams. The walls were either brick or concrete block, vertically reinforced through holes in the units. The walls were tested as cantilevers fixed at the base and free at the top. The loads were applied in-plane with or without precompression applied before the horizontal load or in cycles of alternate loads. For walls with low vertical reinforcement ratios and low vertical precompression, failure was governed by flexure (horizontal crack at the bed joints). The behavior of these walls was similar to that of an underreinforced concrete beam. Precompression on this type of wall caused a small increase in horizontal strength, compared to a large increase in vertical stresses. Failure was governed by diagonal shear for walls with high vertical reinforcement ratios. The cracking loads increased due to precompression of approximately 40% of the total applied vertical load (providing that this vertical load did not exceed one-third of the ultimate vertical strength of the wall. Cracks gradually formed through the joints. Crack

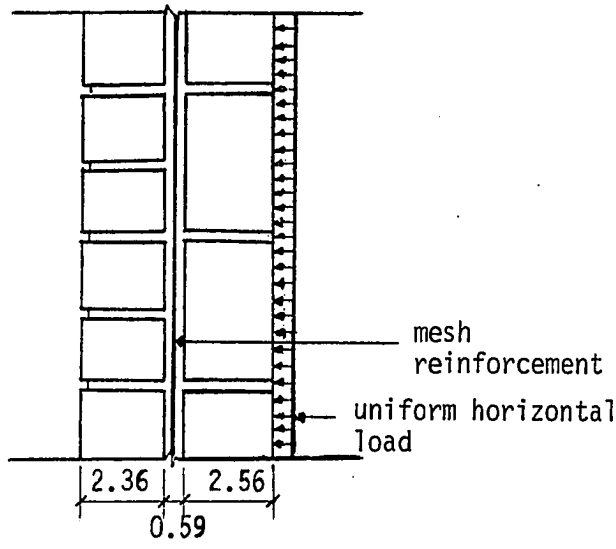

Figure 1. Section of the prefabricated brick wall panel [4]

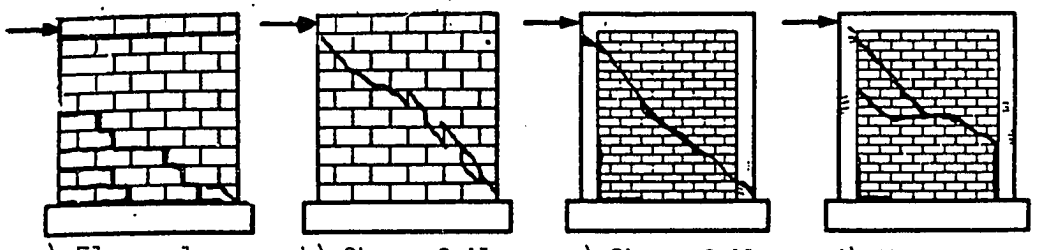

Figure 2. Cracking patterns at failure [5]

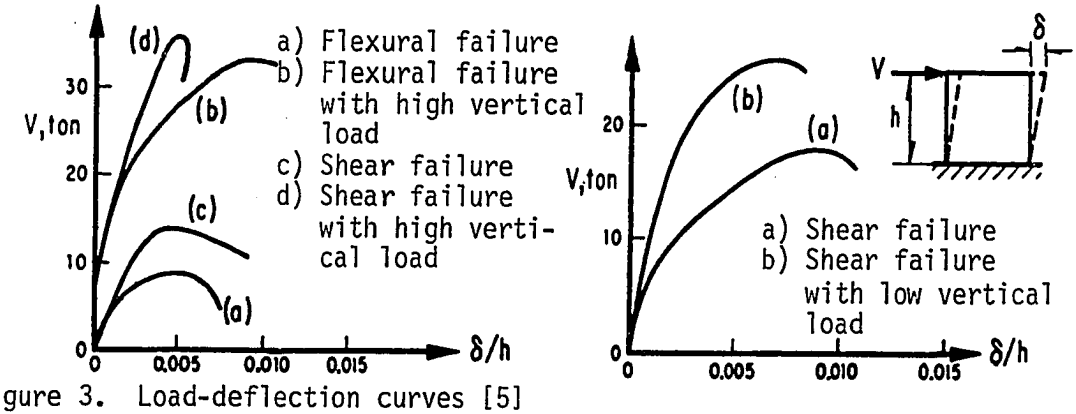

Figure 3. Load-deflection curves [5]

patterns and some of the results are shown in Figs. 2 and 3. The crack patterns in Fig. 2 (2a through 2d) are associated with each particular failure made. Fig. 3 illustrates some of the load-deflection behavior associated with these failure modes.

Meli [5] proposed a trilinear load-deflection curve to describe the behavior of the wall (Fig. 4); the author gave different values for the constants (β, γ_0, a_1 and a_2) defining the curve. He concluded that in walls with interior vertical reinforcement, behavior was nearly elasto-plastic with remarkable ductility, i.e., failure was governed by bending. If failure was governed by diagonal cracking, ductility was small and behavior was brittle when high vertical loads were applied (Fig. 3(a)).

Hatzinikolas et al. [6] tested the effect of joint reinforcement on the vertical load capacity of masonry walls built of hollow concrete blocks and loaded vertically (only). The authors concluded that joint reinforcement produced stress concentration, reducing the ultimate load bearing capacity of the wall.

Williams and Geschwindner [7] studied shear transfer between a concrete masonry wythe and a brick wythe. The shear transferred through a 3/8-in. collar joint of three different mixes of mortar and grout. Based on the results of their tests of assemblies with and without joint reinforcement, they proposed an equation for shear-bond strength in the collar joint:

$$V_{SB} = 38.9 + 0.0103\ f'_m \qquad (1)$$

where: V_{SB} = the shear-bond strength (psi)

f'_m = the ultimate compressive strength of the collar joint (psi).

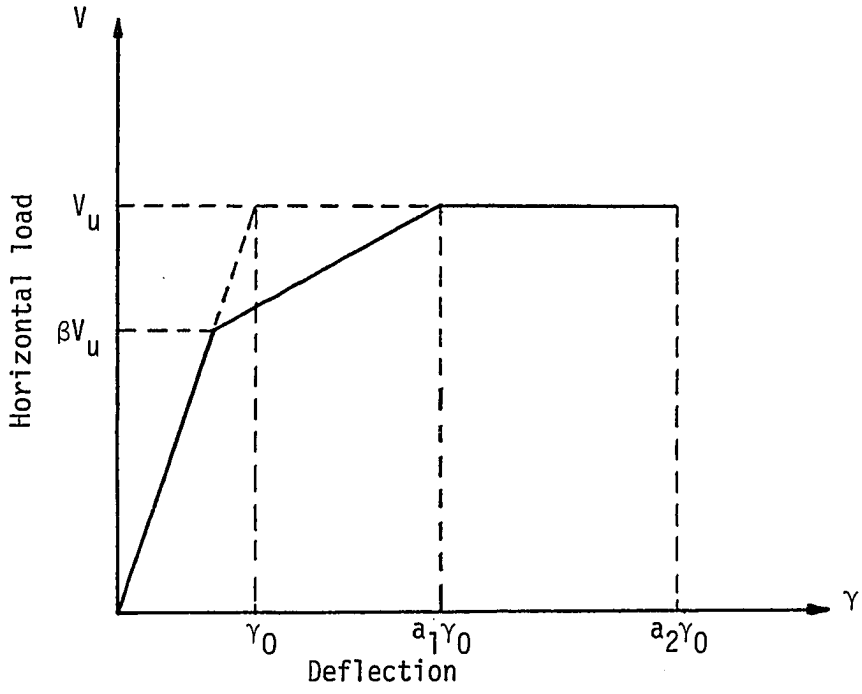

Figure 4. Proposed load-deflection curve for masonry walls [5]

Scrivener [8] tested six full-scale reinforced brick masonry walls of two wythes (4-in.) each, having a cavity of about 1.4-in. filled with mortar and reinforced with vertical and horizontal bars. The walls were constructed on a reinforced concrete beam and topped with another beam. The walls were loaded in-plane at the top until failure occurred. The failure can be described as a crack along the joints near the base as a result of excessive tensile stresses caused by the bending moment, followed by a major diagonal crack accompanied by vertical splitting. An example of this failure is shown in Fig. 5. Scrivener concluded that the first shear cracks were consistent for all walls, with an average value for lateral loads of 47.6 psi and that no effect was attributed to different aspect ratios. Maximum shear strengths were in the range of 49.6 to 79.3 psi.

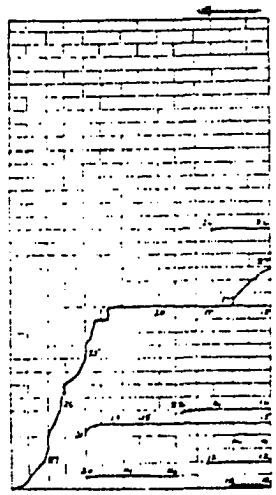

Wall A1: Cracks

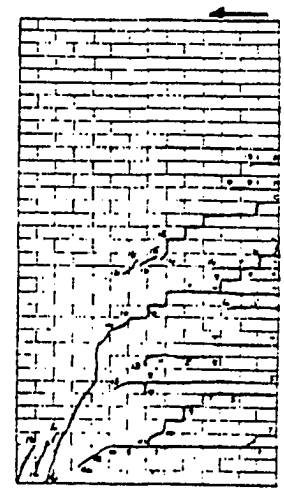

Wall A2: Cracks

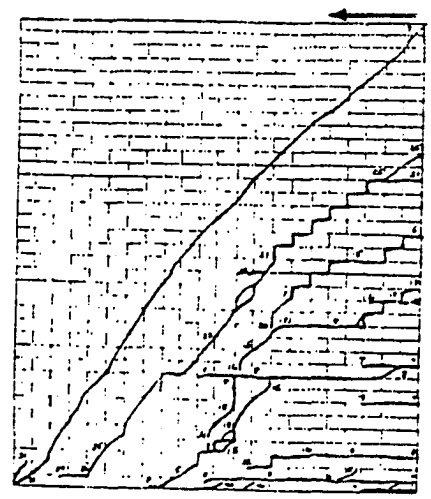

Wall B1: Cracks

Figure 5. Shear tests on reinforced brick masonry walls [8]

TEST PROGRAM AND CONTROL SPECIMENS

General

The composite walls were built in three groups. An average of 10 one-wythe prisms were built with each group, in addition to the mortar and grout cubes. Five composite prisms similar to each wall were also built. The wall panels (consisting of two wythes each with a two-inch reinforced collar joint) were approximately 6 ft. high and 4 ft. wide.

Test Frame

A rigid steel frame with a horizontal maximum capacity of 400,000 lbs. and a vertical maximum capacity of 250,000 lbs. was designed at Iowa State University. The horizontal load was adjusted vertically to meet the height of the specimen. The frame was fixed to the structural laboratory floor which is of the tie-down type with a maximum capacity of 1,000,000 lbs. (either applied per hole or in combination for the overall floor). A horizontal load was applied using a hydraulic cylinder of 200,000 lbs. Vertical loads were applied at two points using hydraulic cylinders of 100,000 lbs. each. Figs. 6 and 7 show the frame and load set-up. Fig. 6 shows photographs for the test frame and the wall before test. Fig. 7 shows the details of the test frame.

Materials

All materials used in construction of the test specimens were commercially available and were typical of those commonly used in buildings. All tests were carried out according to the ASTM-Specifications [9].

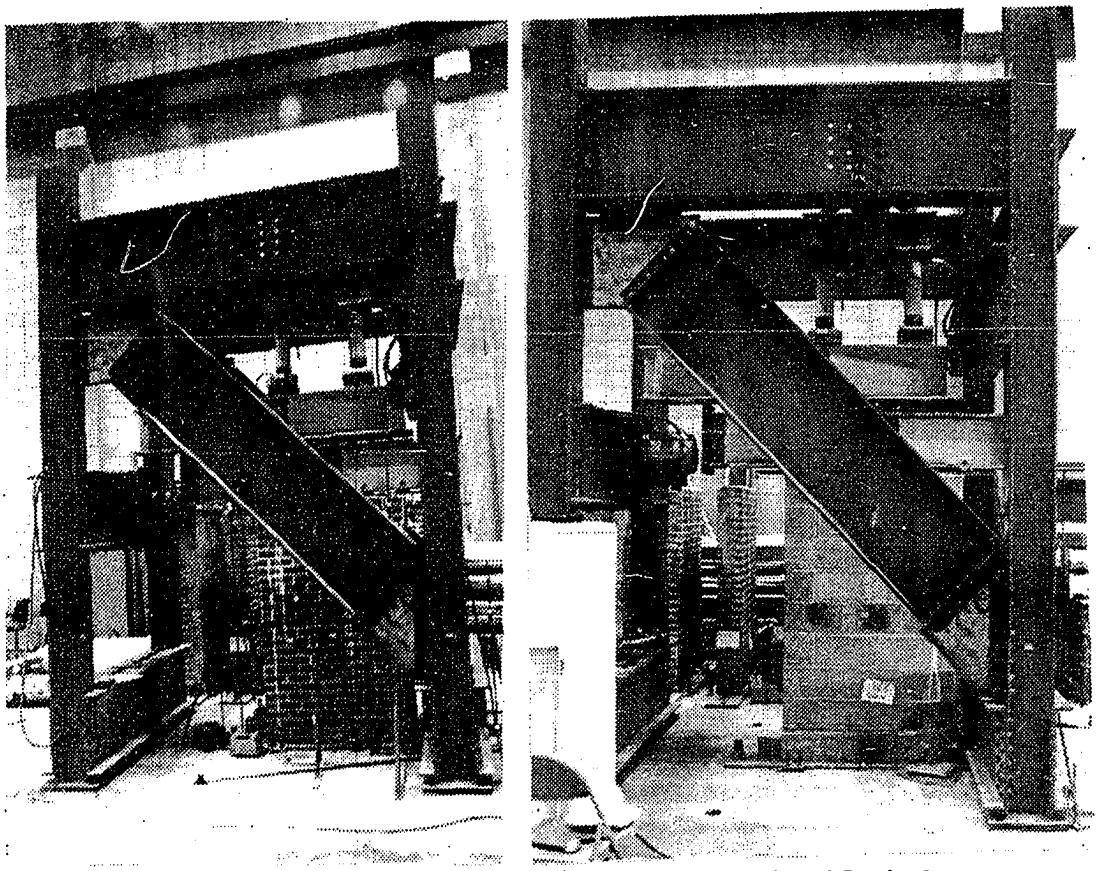

a) Test frame with brick face

b) Test frame with block face

Figure 6. Test frame

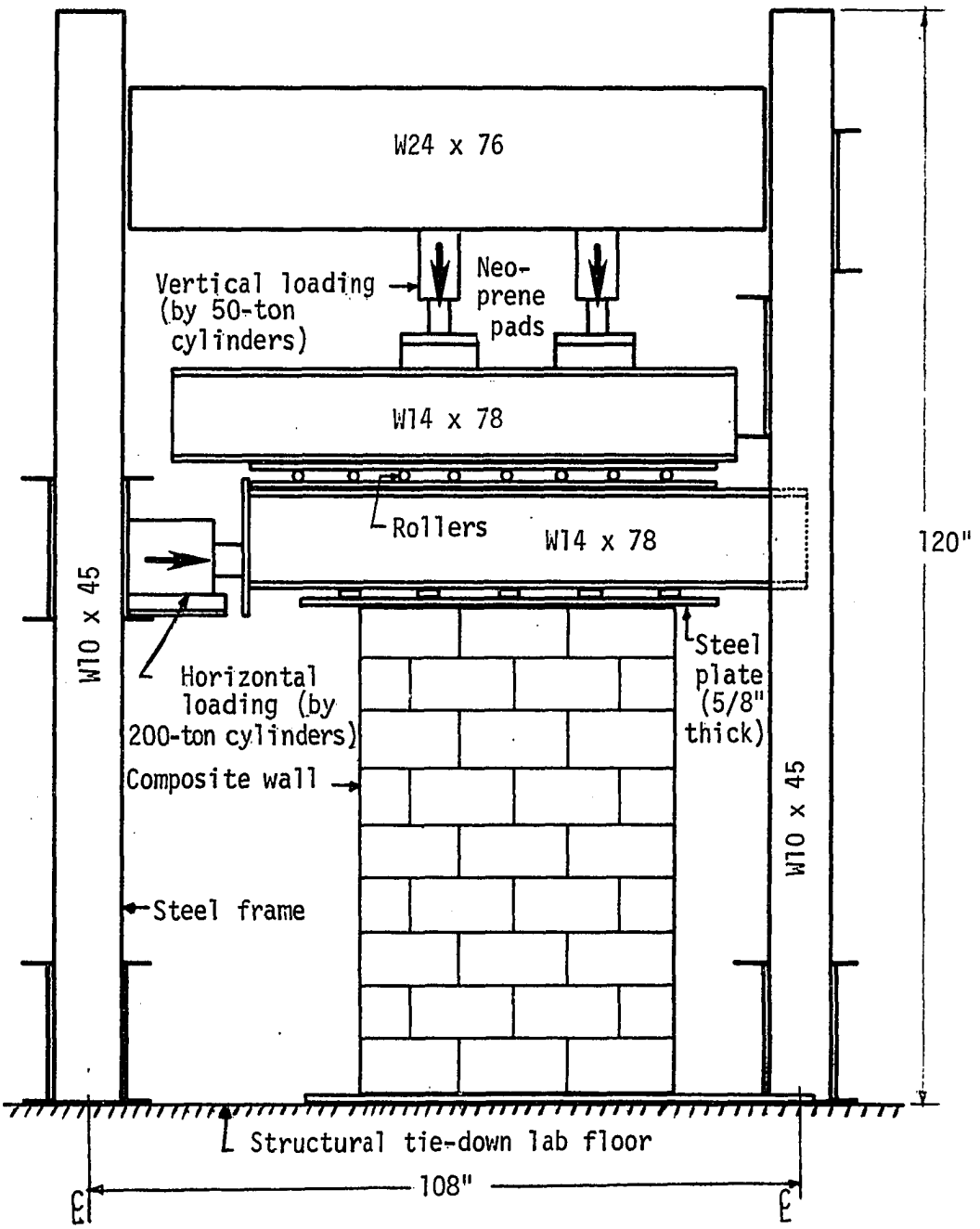

Figure 7. Loading mechanism

Mortar and grout

Type "M" mortar was used as specified in the UBC code [10] for reinforced masonry. The mortar was mixed in accordance with ASTM-C270-73 specifications [9] and proportioned by volume as 1:0.25:3.5 (cement: lime:sand). The cement was Portland cement type "I" (ASTM-C150-78a); the lime was hydrated lime type "S" (ASTM-C207-76); the sand was in accordance with ASTM-C144-76 [9].

Grout mixed in accordance with ASTM-C476-71 was used and proportioned by volume as 1:3 (cement:fine aggregate). The cement was Portland cement Type "I" (ASTM-C150-78a); the fine aggregate was in accordance with ASTM-C404-76 [9]. The properties of the sand and the aggregate are shown in Table 1.

Table 1. Sand and aggregate properties

Sand used for	Percent passing through sieve #								Fineness modulus
	3/8	4	8	16	30	50	100	200	
Mortar	100	100	99.9	99.1	89.5	26.9	1.6	0	1.83
Grout	100	95.5	81.9	66.8	43.2	3.3	0.08	0	3.09

Two-inch mortar and grout cubes molded from brick units moistened with oil were made from each mix used in building the specimens. Fig. 8 shows the molds used for these cubes. The cubes were cured in accordance with ASTM-E447-74 [9]. Before testing, the mortar and grout cubes were capped with sulfur material in accordance with ASTM-C140-75 [9].

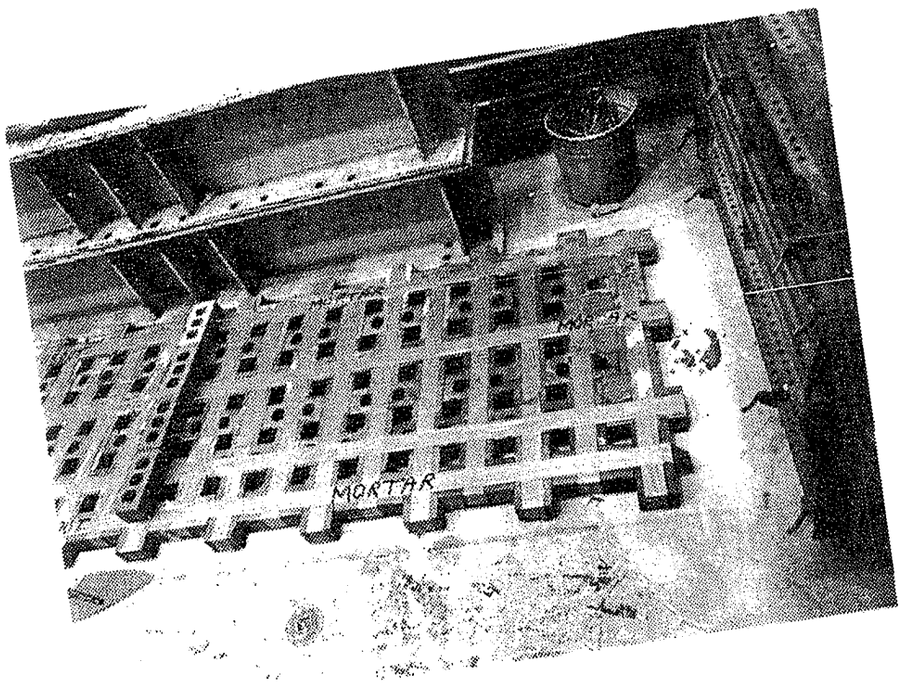

Figure 8. Molds used for mortar and grout cubes

The first group of cubes was tested after 7 and 28 days' curing. The other cube groups were tested after 28 days' curing and also at the average age of full-size walls.

Cubes were tested for each associated grouping of the walls. The results of testing a total of 106 mortar cubes and 83 grout cubes are given in Table 2.

Table 2. Compressive strengths for mortar and grout cubes
a) Compressive strengths for mortar

Age of cubes (days)	Compressive strength f'_m (psi)					
	Group I		Group II		Group III	
	f'_m	c.o.v.	f'_m	c.o.v.	f'_m	c.o.v.
7	2400	9.5	--	--	--	--
28	2748	15	2029	20	2341	16
37	--	--	--	--	2350	11.2
85	--	--	2033	15.8	--	--

b) Compressive strengths for grout cubes

Age of cubes (days)	Compressive strength f'_m (psi)					
	Group I		Group II		Group III	
	f'_m	c.o.v.	f'_m	c.o.v.	f'_m	c.o.v.
7	3412	17	--	--	--	--
28	3880	13.5	4012	20.6	4112	13
37	--	--	--	--	4120	15.5
85	--	--	4020	18.6	--	--

Brick units and prisms

The brick units were made of 3-hole clay brick, having a nominal size of 2 1/4x3 5/8x7 5/8 inches with a net area greater than 75% of

the gross. The average dimensions, physical properties and strength properties for the brick units are given in Table 3. These properties were found according to ASTM-C67-78 [9].

Table 3. Material properties for brick

Width in.	Length in.	Height in.	Gross area $in.^2$	Net area $in.^2$	Net area percent %	Absorption percent %	Moisture content %	Weight lb.	Compressive strength (psi)	
									Gross area	Net area
3.55	7.49	2.29	26.56	20.45	77	2.6	16.6	3.70	12480	16260

One-wythe prisms were built of brick materials similar to the walls and cured under the same conditions, in accordance with ASTM-E447-74 [9]. The prisms were tested under compression only with load either perpendicular to or parallel with the bed joint. Average dimensions of the prisms were 15.8-in. high, 7.6-in. wide and 3.5-in. thick. The prisms were loaded using the compression test machine, having a maximum capacity of 400,000 lbs., and stress-strain curves obtained. Typical stress-strain curves are shown in Fig. 9. Prisms were tested at an age equivalent to the average age of the walls. A total of 30 prisms were tested, for which the results are given in Table 4. The average properties of all brick tests were:

For load perpendicular to bed joint: f'_m = 3371 psi; E = 4.23×10^6 psi; ν = 0.21.

For load parallel to bed joint: f'_m = 2521 psi; E = 3.16×10^6 psi; ν = 0.15.

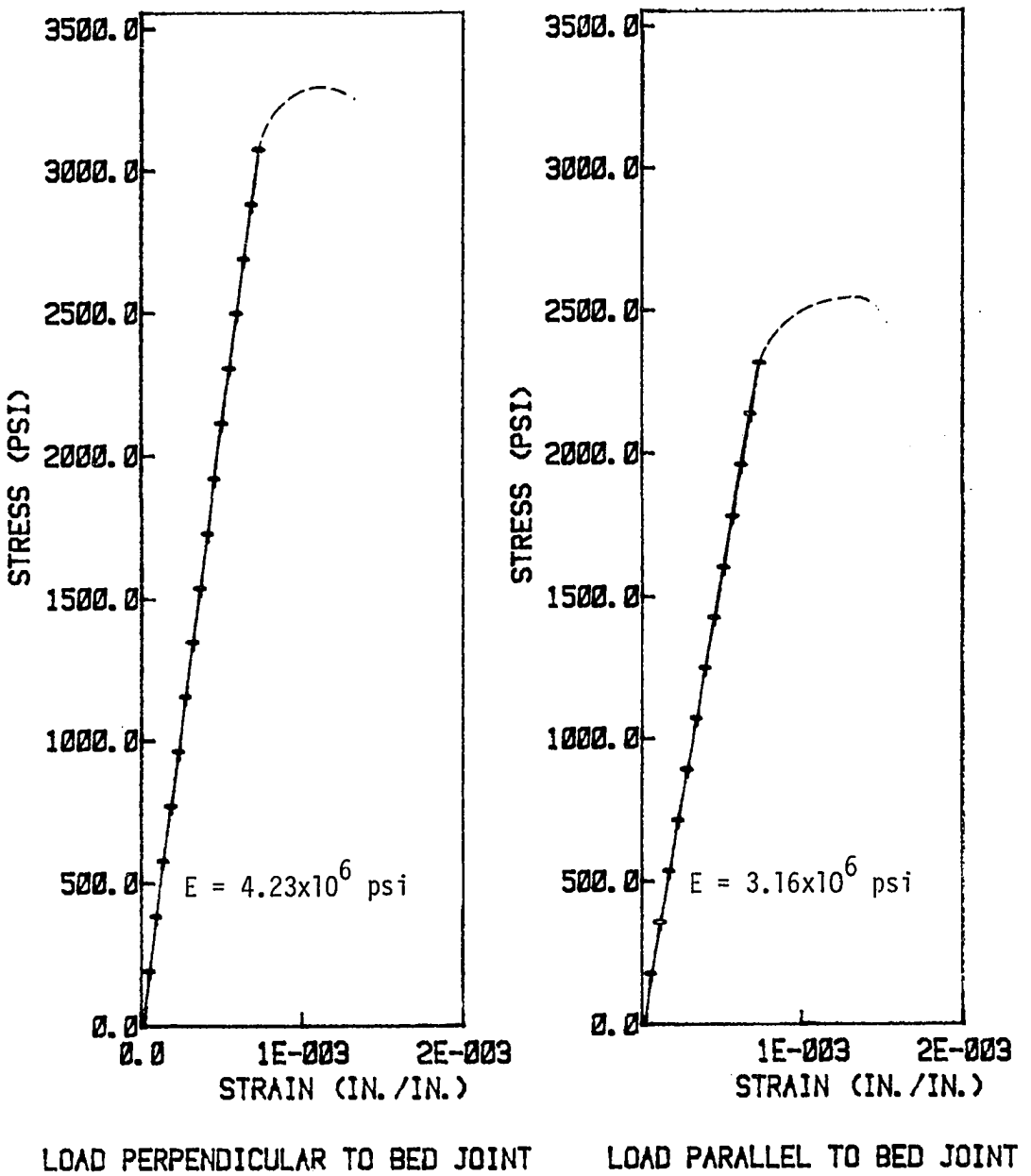

Figure 9. Stress-strain curves for brick prisms

Table 4. Compressive strength for brick prisms

Group	Load perpendicular to bed joints		Load parallel to bed joint	
	f'_m (psi)	c.o.v.	f'_m (psi)	c.o.v.
I	5190	9.2	4010	9.9
II	3301	18	1782	15.7
III	1912	12.7	1580	9.5

Reinforced grout prisms

One-wythe prisms of reinforced grout were built from materials similar to the walls and cured under the same conditions, in accordance to ASTM-E 447-74 [9]. The average prism dimensions were 8.55-in. high, 4.4-in. wide, and 2.2-in. thick. The reinforcement was welded wire fabric (WWF 4x4x4x4). The prisms were tested using the 400,000-lb. compression test machine, with load applied either perpendicular to or parallel with the lines of main reinforcement. The tests took place at an age equivalent to the average age of the walls. A total of 8 prisms were tested, with the following results:

For loads perpendicular to main steel: f'_m = 2590 psi; c.o.v. = 11.6%;

For loads parallel to main steel: f'_m = 3350 psi; c.o.v. = 7.4%.

PART 2A. BEHAVIOR OF REINFORCED BRICK-TO-BLOCK WALLS

Behavior of reinforced brick-to-block walls

M. H. Ahmed, Graduate Research Assistant
M. L. Porter, Professor
A. Wolde-Tinsae, Associate Professor

From the Department of Civil Engineering, Iowa State University, Ames, IA 50011

ABSTRACT

The results of testing six brick-to-block reinforced composite masonry panels subjected to gravity and in-plane shear loads are discussed herein. Each wall contained two wythes with a nominal 2-inch collar joint. In the first 5 walls, this joint was grouted and reinforced with either welded wire fabric or vertical and horizontal bars. For the last wall, vertical bars were placed and grouted in the block openings and the collar joint was not grouted. Instead, the two wythes were connected by a horizontal truss joint reinforcement in the bed mortar. The vertical load was applied first and held constant for all walls, followed by the horizontal (in-plane) load. The loads (either vertical or horizontal) were applied as distributed loads along the top of the wall (which was free to move), with the base fixed. The wall panels were approximately 4 feet wide, 6 feet high, and 9 inches thick. One-wythe and composite prisms were built corresponding to each wall to determine the strength properties. A comparison of strength characteristics of the tested walls is discussed herein.

The literature review and the control tests in Part 1 are to be inserted here for publication submission.

CONCRETE BLOCK UNITS AND PRISMS

The units were made from 3-hole concrete blocks with a nominal size of 3 5/8x7 5/8x15 5/8 inches and a net area greater than 75% of the gross. Physical and strength properties for the block units, as well as average dimensions, are given in Table 5. These properties were found according to ASTM-C140-75 [9].

Table 5. Material properties for concrete block

Width in.	Length in.	Height in.	Gross area $in.^2$	Net area $in.^2$	Net area percent %	Absorption percent %	Moisture content %	Weight lb.	Compressive strength (psi)	
									Gross area	Net area
3.70	15.62	7.59	57.86	43.79	75.7	8.9	20.7	25.7	1900	2510

One-wythe block prisms were built from materials similar to the walls and cured under the same conditions, in accordance with ASTM-E447-74 [9]. Average dimensions were 15.7-in. high, 15.7-in. wide, and 3.65-in. thick. The prisms were tested using the 400,000-lb. compression test machine. The applied load was either perpendicular or parallel to the bed joint. The tests took place at an age equivalent to the average age of the walls and stress-strain curves were obtained. Typical stress-strain curves are shown in Fig. 10. A total of 25 prisms were tested; the average of the results are shown in Table 6. Average properties for all of the tested block prisms were:

For loads perpendicular to bed joint: f_m = 1509 psi; $E_t = 1.52 \times 10^6$

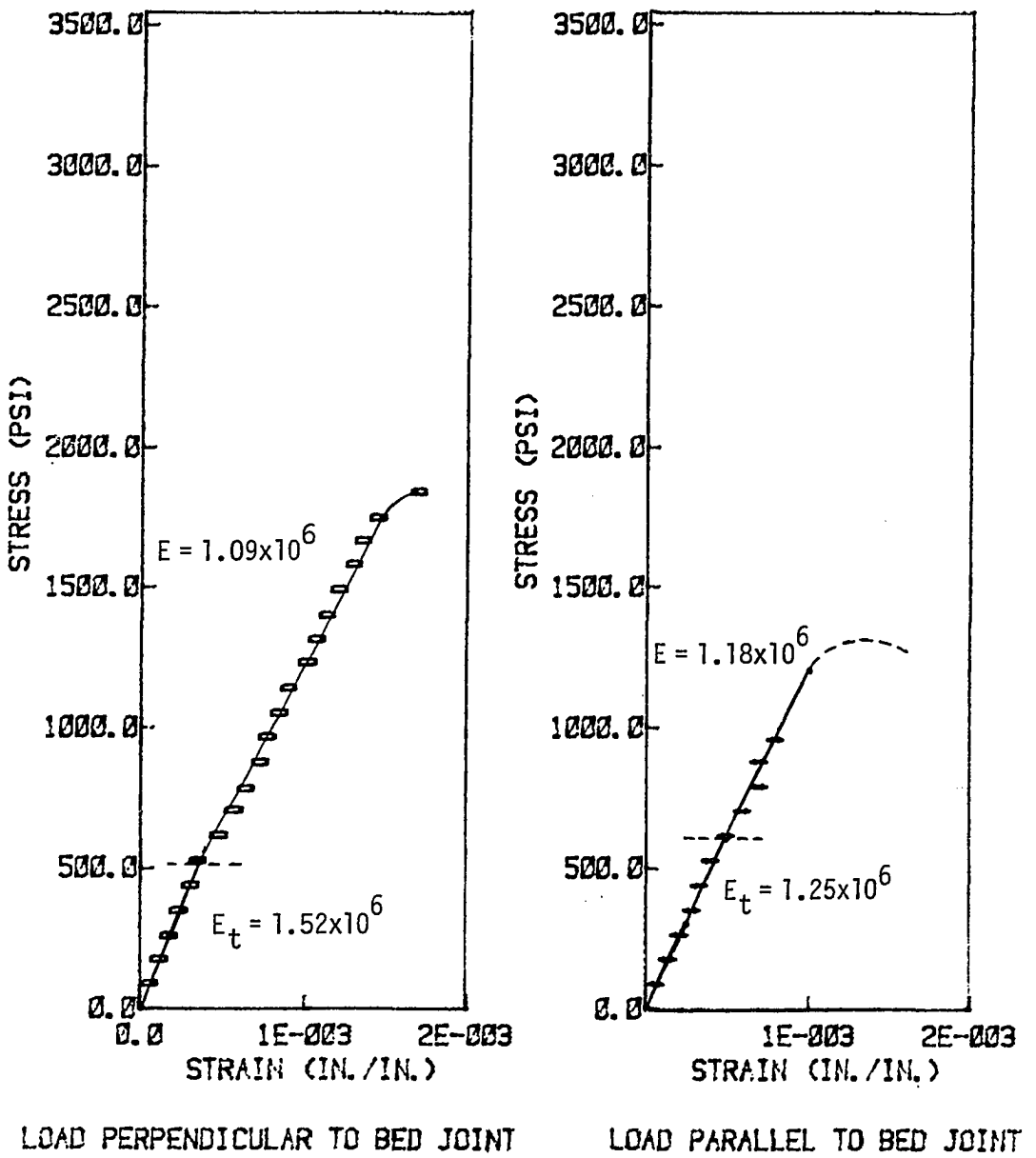

Figure 10. Stress-strain curve for block prisms

psi; ν = 0.22.

For loads parallel to bed joint: f'_m = 1416 psi; $E_t = 1.25 \times 10^6$ psi; ν = 0.267.

Table 6. Compressive strength for block prisms

Group	Load perpendicular to bed joints		Load parallel to bed joints	
	f'_m (psi)	c.o.v.	f'_m (psi)	c.o.v.
I	1940	14.7	1820	7.5
II	1345	23.0	1190	19.0
III	1175	10.6	970	16.6

Fig. 11 shows examples of failures in one-wythe prisms. Fig. 6a shows the failure of a brick prism with the load applied perpendicular to the bed joints. Figs. 6b-6c show typical failures for two block prisms with the load parallel and perpendicular to the bed joint, respectively.

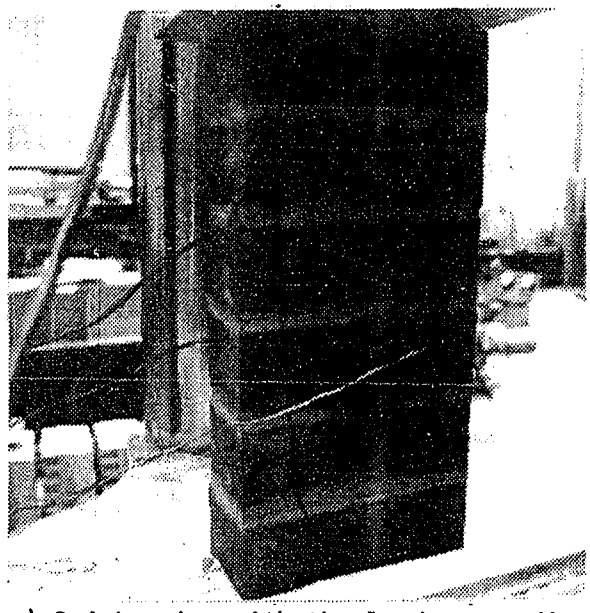

a) Brick prism with the load perpendicular to the bed joints

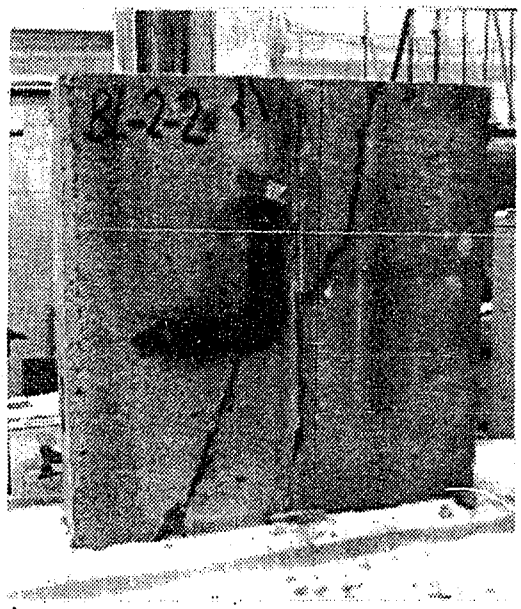

b) Block prism with the load parallel to the bed joint

c) Block prism with the load perpendicular to the bed joint

Figure 11. Failure for brick and block prisms

COMPOSITE WALLS

Six composite brick-to-block walls were built in three different stages. Walls of two wythes, with a nominal 2-in. reinforced collar joint, were tested. All walls were approximately 6-ft. high and 4-ft. wide, were built either on a steel T-section (WT6x32.5) or on a steel plate 1.25 inches thick. Straight coil loops were welded to the steel base and positioned to align with the holes of the masonry. The holes of the first two layers of the brick wythe and those of the first layer of the block wythe were grouted to bond the coil loops to the masonry, after which the walls were cured in accordance with ASTM-E447-74 [9] and tested after at least 28 days. The walls were designated as: W1, W3, W5, W7, W9 and W11. Table 7 indicates the age of each wall and its amount of reinforcement. The procedure used to build the walls is given in Appendix A.

Table 7. Test age and reinforcement details for brick-to-block walls

Wall		Test age days	Reinforcement	
Group	No.		Vertical	Horizontal
I	W1	56	WWF[a] 4x4x4x4	
II	W3	83	WWF 4x4x4x4	
II	W5[b]	98	WWF 4x4x4x4	
III	W7[b]	30	WWF 4x4x4x4	
III	W9[b]	32	1#3 & 2#4 bars	5#3 bars
III	W11[c]	36	1#3 $ 2#4 bars	truss joint

[a]Welded wire fabric consisted of No. 4 gage horizontal and vertical wires.

[b]The vertical reinforcement was welded to the steel base.

[c]The vertical bars were placed in the block holes and grouted. The truss joint reinforcement was 1/8 inch thick, 5 5/8 inches wide, and placed horizontally in the bed joint every 16 inches (6 brick layers or 2 block layers).

Five composite prisms were built, using materials similar to those of each wall. The prisms and walls were cured under the same conditions and tested on the same day. The average dimensions were 15.8-in. high and 15.7-in. wide. Thickness and reinforcement were similar to the corresponding full-sized wall. The prisms were loaded vertically in accordance with ASTM Specifications [9] and failed as follows: Horizontal cracks along the bed joints started in both wythes at about two-thirds of the ultimate load. These cracks were followed by vertical separation between the masonry wythe and the collar joint. Vertical cracks crossing the masonry units of both wythes occurred next, followed by complete failure. Average dimensions of the walls and compressive strengths of composite prisms are given in Table 8.

Table 8. Average dimensions of the walls and compressive strengths of the composite prisms

Wall designation	Width (in.)	Thickness (in.)	Height (in.)	Thickness of collar joint	Gross area ($in.^2$)	f'_m psi	c.o.v. %
W1	47.6	9.10	72.2	1.85	433.16	1680	15.5
W3	47.8	8.92	74.1	1.67	426.11	2365	3.0
W5	47.7	9.18	72.7	1.93	437.52	2170	13.9
W7	47.9	9.28	72.4	2.03	444.7	1816	12.3
W9	47.7	9.39	71.6	2.14	447.9	1722	3.2
W11[a]	47.8	9.45	71.7	2.20	346.55	978	10

[a]Noncomposite: No grouted collar joint.

Measurements

Strains and deflections were measured at different load points. Paper-back strain gages of lengths 0.6, 0.8 and 2.4 inches were used for masonry units. The first two lengths of the strain gages were used for the brick units, and the last one (the long one) was used for the block units. These strain gages were located at five points on each wall as follows: at the center and the two edges of the vertical and horizontal center lines of the wall. Some of these strain gages were destroyed either during building the wall or due to cracks in the units. The results of the strains are given in (Figs. 26 and 27) Appendix B. The deflections were measured using dial gages with 0.001-inch sensitivity.

Test Procedure

Before testing the walls, a preliminary test was carried out to check the capacity and rigidity of the frame. The details of this test are given in Appendix C.

The test procedure for all walls was the same and is described as:

(1) Strain gages and load cell (to give the vertical load readings) were connected to a programmable data acquisition system.

(2) Initial readings were taken after applying the vertical load in three cycles, from zero to 10 kips and back to zero.

(3) Vertical load was applied in increments up to the intended precompression load, then kept approximately constant until the end of the test. The value of the intended vertical load was determined as different ratios (1, 3/4 and 2/3) of the allowable loads. After applying high values of horizontal load, the vertical load changed.

Therefore, it was readjusted for every load point.

(4) Next, horizontal load was applied in increments until the wall failed, i.e. reached its ultimate load-carrying capacity.

(5) At every load point, strains, deflections and loads were recorded. Cracks were recorded, marked and numbered with the same number as the load point.

The walls were oriented so that the horizontal load was always applied from east to west. For all walls except "W9," the block wythe was on the north side.

Composite Wall Test Results

Wall "W1"

Wall "W1" was subjected to a precompression load of 178 kips (close to the allowable load). The first crack (a horizontal tensile bond failure at the bottom of the wall in the first bed joint) occurred at a lateral load of 58 kips. The next major crack across both wythes occurred at the ultimate load (76 kips) (load point 22). These cracks appeared in the west side at the bottom of the wall. The cracks were slightly inclined in the brick wythe and almost vertical in the block wythe. Later progressive cracks (No. 23 in Fig. 12) occurred in the west side of both wythes, and diagonally in the brick wythe, through the brick units only. These cracks were followed by a vertical separation between the masonry and the collar joint. The entire lower quadrant on the west side of the brick was displaced outward (to the south direction). Bearing failure occurred at the bottom of the wall on the west corner, in addition to separation failure in both wythes and diagonal shear in the brick wythe

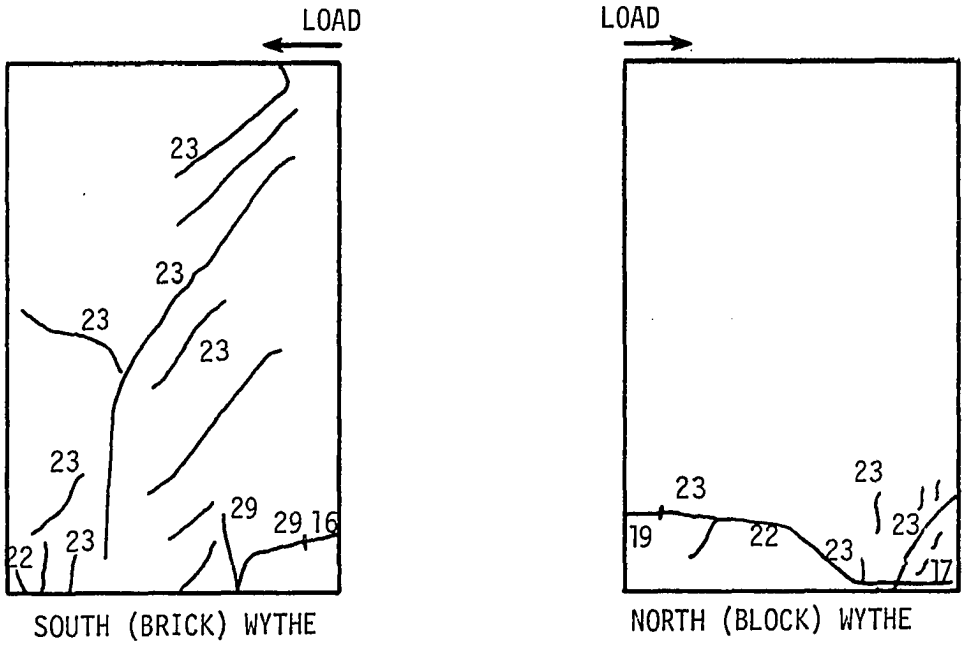

Load point	1	2	3	4	5	6	7	8	9	10	11	12	13	14	15	16	17	18	19	20	21	22	23
Vertical load (k)	0	50	100	100	140	178	178	178	178	178	178	178	178	178	178	178	178	178	178	178	178	178	178
Horizontal load (k)	0	0	0	0	0	0	4	10	16	22	28	36	40	46	52	58	64	58	64	70	76	76	70

Figure 12. Crack pattern for wall "W1"

only, in conjunction with the ultimate horizontal load. The crack pattern at different load points is shown in Fig. 12.

Wall "W3"

Wall "W3" was subjected to a precompression load of 146 kips (3/4 of the allowable load). Before testing, the wall was accidentally lifted from the top by the overhead crane after connection to the floor, so the wall was broken in two through the top of the first block course. No other cracks occurred in the two parts of the wall, so the cracked parts were cleaned, mortared, grouted and cured for 28 days. Six cubes were made from the grout mix and tested with the wall. The average compressive strength was 2660 psi, with a coefficient of variance of 10.9%. When the wall was tested, the first major crack occurred at a lateral load of 42 kips. This crack (in the repaired bed joint) was horizontal. At a lateral load of 64 kips, bearing cracks in both wythes occurred at the bottom west side of the wall. This crack was followed by a separation between the brick wythe and the collar joint. In conjunction with the ultimate load, bearing failure in both wythes occurred; diagonal shear failure, in addition to separation, occurred only in the brick wythe. The crack pattern at different load points is shown in Fig. 13.

Wall "W5"

Wall "W5" was subjected to a precompression load of 135 kips (3/4 of the allowable load). The first visible crack, horizontal at the first bed joint in the brick wythe, occurred at a lateral load of 60 kips. At a lateral load of 84 kips, bearing cracks in both wythes occurred in the

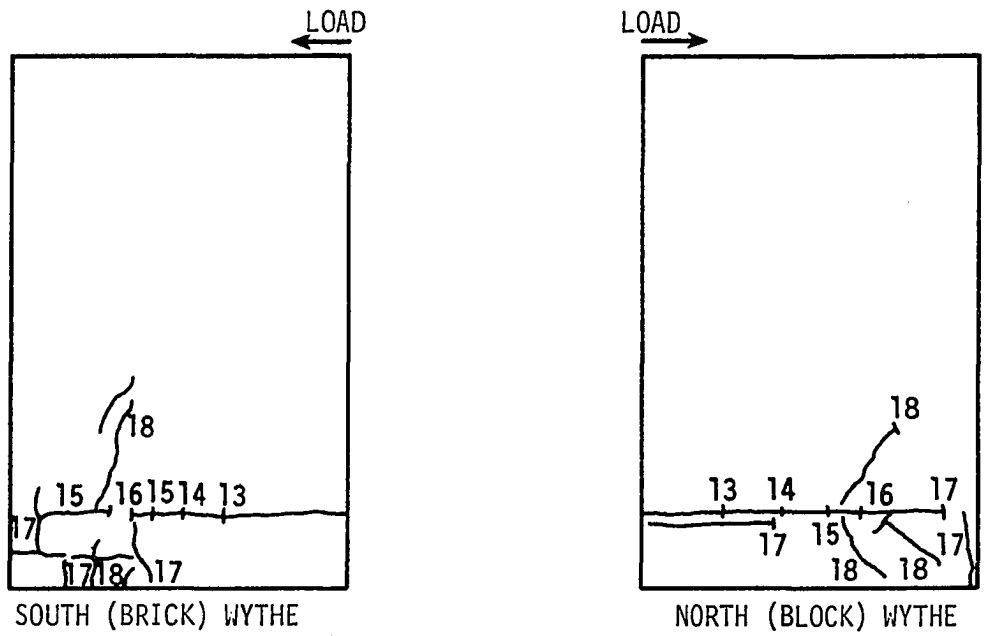

Load point	1	2	3	4	5	6	7	8	9	10	11	12	13	14	15	16	17	18
Vertical load (k)	0	30	60	90	120	146	146	146	146	146	146	146	146	146	146	146	146	146
Horizontal load (k)	0	0	0	0	0	0	6	12	18	24	30	36	42	48	54	60	54	28

Figure 13. Crack pattern for wall "W3"

bottom west corner of the wall. At the ultimate load (89.5 kips), the bottom corner of the west edge of the wall had significant bearing failure. No separation failure occurred in this wall. The crack pattern at the different load points is shown in Fig. 14.

Wall "W7"

Wall "W7" was subjected to a precompression load of 178 kips (close to the allowable load). The first visible crack, horizontal in the brick wythe at the first bed joint of the wall, occurred at a lateral load of 36 kips. At the ultimate load (90 kips), bearing failure occurred in the brick wythe in the bottom-west corner, followed by separation of the brick from the collar joint. These failures were followed by bearing failure in the block wythe and the appearance of a major diagonal crack in the brick wythe. At this stage, the load dropped to 60 kips, at which a stair-step type of cracking appeared. The lateral load dropped to 40 kips, at which load bearing failure progressed in both wythes. The crack pattern at different load points is shown in Fig. 15.

Wall "W9"

A precompression load of 118 kips (2/3 of the allowable load) was applied on wall "W9". At a lateral load of 36 kips, a horizontal crack appeared in the first bed joint of the brick. As the lateral load increased, several more horizontal cracks occurred at the first two bed joints in both wythes. At the ultimate load (78 kips), separation of the brick wythe and collar joint occurred, followed by crushing of the bottom-west corner bearing failure in both wythes. Fig. 16 shows the

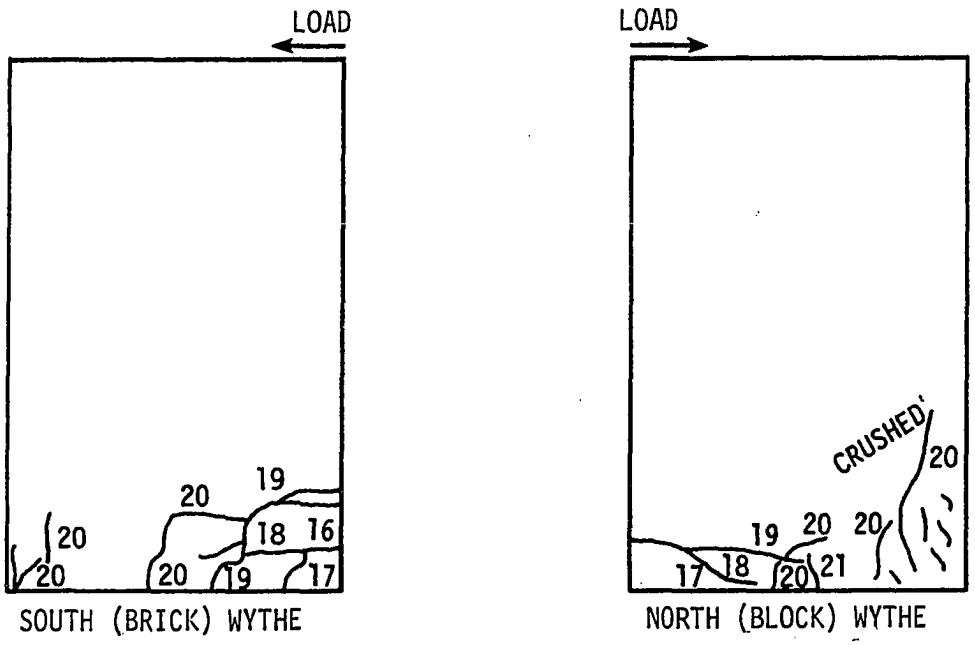

Load point	1	2	3	4	5	6	7	8	9	10	11	12	13	14	15	16	17	18	19	20	21	22	23
Vertical load (k)	0	30	60	90	120	135	135	135	135	135	135	135	135	135	135	135	135	135	135	135	135	135	135
Horizontal load (k)	0	0	0	0	0	0	6	12	18	24	30	36	42	48	54	60	66	72	78	72	84	90	80

Figure 14. Crack pattern for wall "W5"

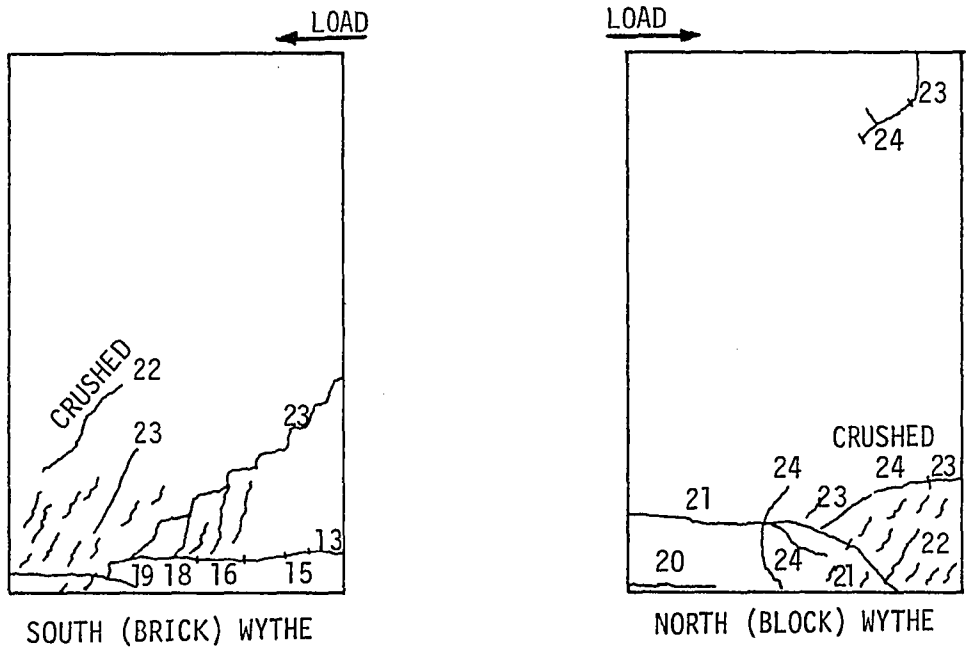

Load point	1	2	3	4	5	6	7	8	9	10	11	12	13	14	15	16	17	18	19	20	21	22	23	24
Vertical load (k)	0	30	60	90	120	150	178	178	178	178	178	178	178	178	178	178	178	178	178	178	178	178	178	178
Lateral load (k)	0	0	0	0	0	0	0	6	12	18	24	30	36	42	48	54	60	66	72	78	84	71	60	40

Figure 15. Crack pattern for wall "W7"

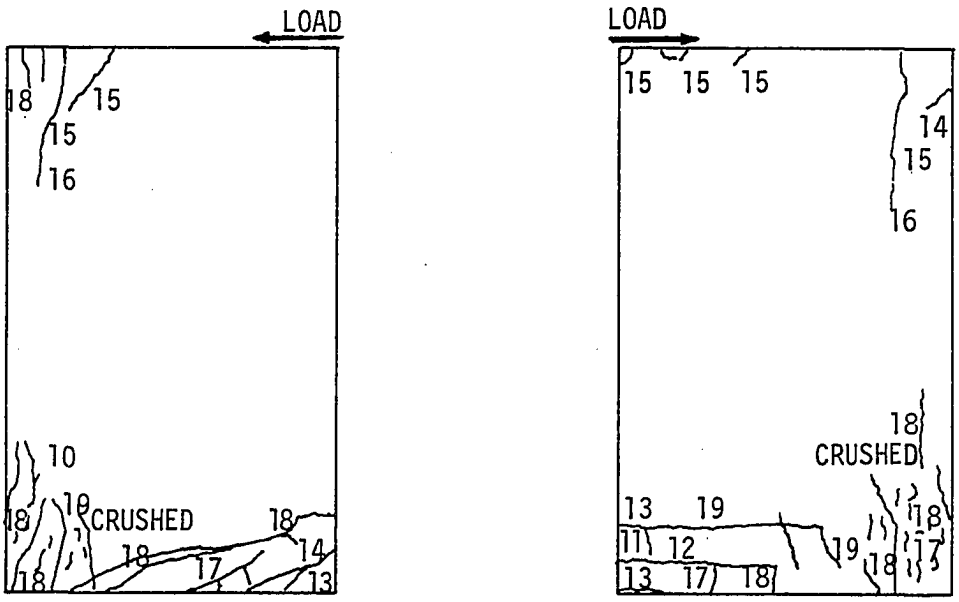

Load point	1	2	3	3	5	6	7	8	9	10	11	12	13	14	15	16	17	18	19
Vertical load (k)	0	30	60	90	118	118	118	118	118	118	118	118	118	118	118	118	118	118	118
Lateral load (k)	0	0	0	0	0	6	12	18	24	30	36	42	48	54	60	66	72	78	48

Figure 16. Crack pattern for wall "W9"

crack pattern at the different load points for both wythes.

Wall "W11"

Wall "W11" was not grouted or reinforced in the collar joint. The block wythe was reinforced through the holes and grouted instead, and truss joing reinforcement was used horizontally in the bed joints connecting the two wythes. The precompression on the wall was 138 kips (similar to "W5"). The first horizontal crack occurred at a lateral load of 42 kips, at the bottom-west corner of the brick wythe. Vertical cracks in the brick side appeared at the top middle of the wall at a lateral load of 48 kips (load point No. 16) and propagated downward as the lateral load increased. At a lateral load of 72 kips, some other cracks occurred in the brick side at the bottom; four major diagonal cracks at the middle of the block wythe also occurred. Several other diagonal and horizontal cracks occurred in both wythes at a lateral load of 78 kips, followed by sudden failure. The failure at the ultimate load can be described as: bearing failure in both wythes at the compressive corner, in addition to the diagonal shear failure in both wythes. Fig. 17 shows the crack pattern at different load points. Figs. 18 through 21 show pictures of different types of failures. Figs. 18 and 19 show examples of bearing failures in the brick and the block wythes, respectively. Fig. 20 shows the diagonal failure in walls W1, W7 and W11. Fig. 21 shows examples of the vertical separation between the masonry wythe and the collar joint.

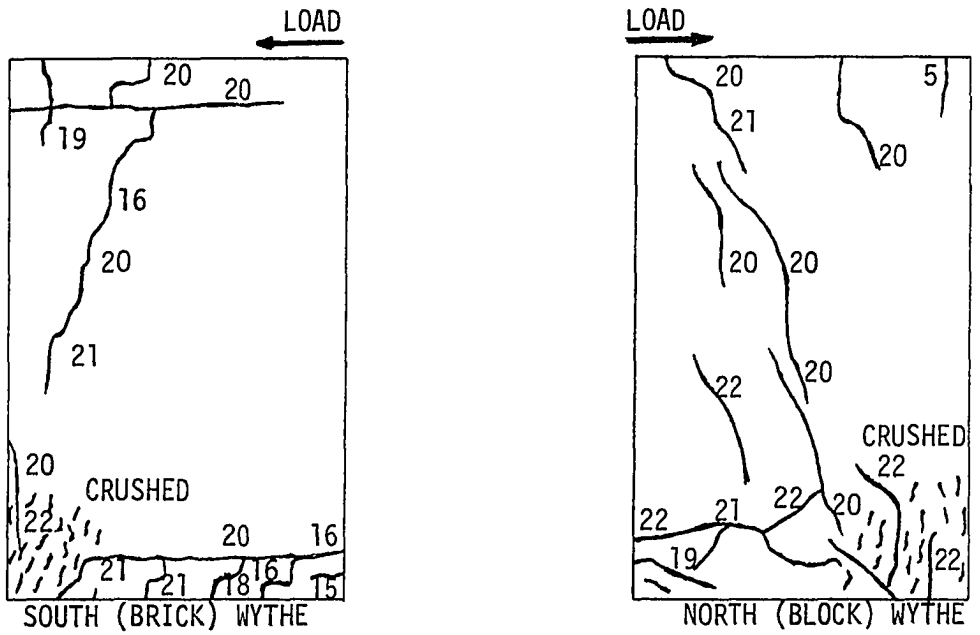

Load point	1	2	3	4	5	6	7	8	9	10	11	12	13	14	15	16	17	18	19	20	21	22
Vertical load (k)	0	30	60	90	120	138	138	138	138	138	138	138	138	138	138	138	138	138	138	138	138	138
Lateral load (k)	0	0	0	0	0	0	4	8	12	16	20	24	30	36	42	48	54	60	66	72	78	75

Figure 17. Crack pattern for wall "W11"

a) Bearing failure in wall W3 (brick side)

b) Bearing failure in wall W7 (brick side)

Figure 18. Examples of bearing failure in the brick wythe

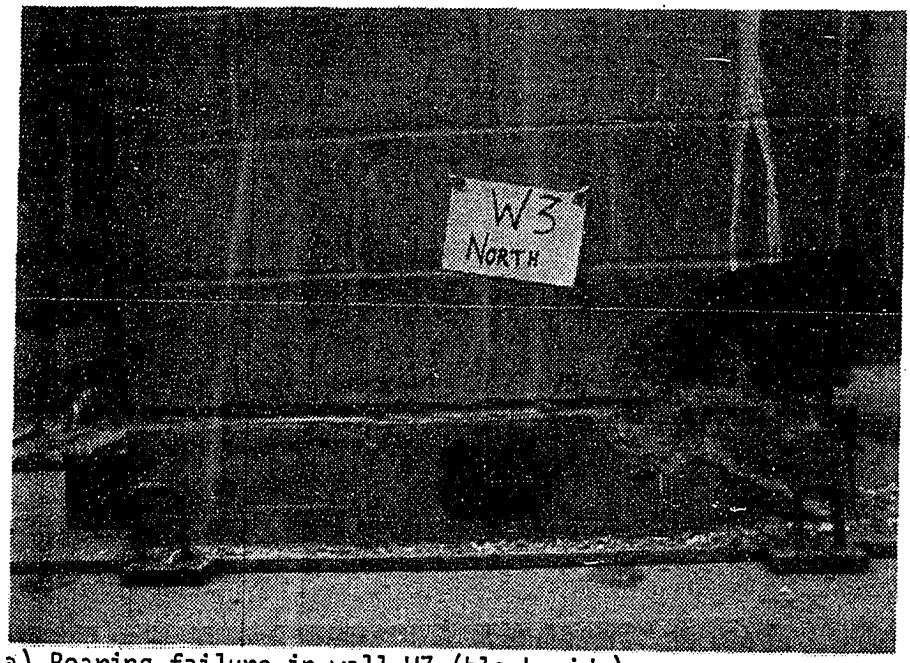

a) Bearing failure in wall W7 (block side)

b) Bearing failure in wall W5 (block side)

Figure 19. Examples of bearing failure in the block wythe

a) Diagonal crack in the brick b) Stair-step crack

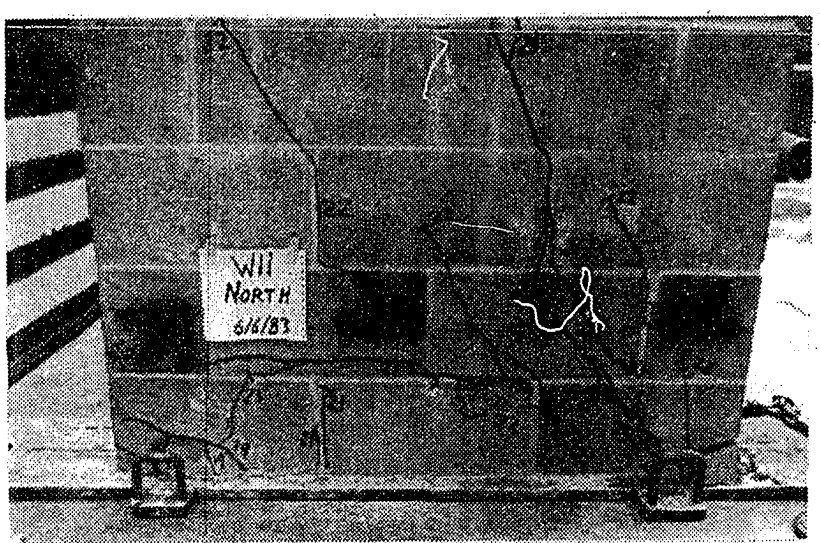

c) Diagonal crack in the block

Figure 20. Examples of diagonal failure

a) Vertical separation in W1 b) Vertical separation in W9

Figure 21. Examples of separation between masonry and the collar joint

Discussion of Walls Behavior

The modes of failure for the tested brick-to-block walls can be summarized as one or a combination of the following: bearing failure at the compressive corner at the bottom of the wall; bond failure between the brick wythe (or in both wythes) and the collar joint; or diagonal shear failure in one wythe, as in the block wythe for "W11", or in the brick wythe for "W1" and "W7". The vertical separation between the brick and collar joint occurred after the brick wythe failure had caused an increase of the interfacial bond stresses on reaching ultimate shear load. Summaries of these modes of failure and the maximum measured loads for all walls are given in Table 9. Load-deflection curves are shown in Figs. 22 through 24. Each figure contains curves for walls having the same intended precompression load (Nu). For each wall, the first portion of the load-deflection curve was a straight line (to about one-third of the ultimate load). The stiffness of the walls, based on the straight-line portion, is given in Table 10 (stiffness is defined as the force required to produce a unit deflection). The steel did not yield in any of the tested walls (as evidenced by measured strains and as shown in Appendix B).

Fig. 22 shows that for walls "W1" and "W7," the load-deflection curves were very close to each other, although there are some differences as follows:

(1) Initial stiffness for wall "W1" was slightly greater than that of "W7"; however, at higher loads, "W7" proved stiffer.

(2) Ultimate shear force increased by 18%, which may be due in part to

Table 9. Maximum loads and modes of failure for the brick-to-block walls

Wall designation	Intended precompression load (kips)	Measured[a] precompression load (kips)	Ultimate lateral load (kips)	First crack load		Separation load		Mode of failure	
				Brick	Block	Brick	Block	Brick	Block
W1	178	179.9	76	58	64	76	76	Diagonal shear failure & bond failure	Bearing failure & bond failure
W3	146	159.7	64.2	42	42	64	--	Bearing failure & diagonal shear crack start & bond failure	Bearing failure
W5	135	166	89.5	60	66	--	--	Bearing failure	Bearing failure
W7	178	182.3	90	36	78	90	--	Stair-step & bearing & partial of diagonal failure & bond failure	Bearing failure
W9	118	146.4	78	36	48	78	--	Bearing failure & bond failure	Bearing failure
W11	138	153.3	78	42	66	--	--	Bearing failure & diagonal shear failure	

[a]The precompression load increased during test and was readjusted at every load point. This value is the measured one at the ultimate lateral load point (at failure).

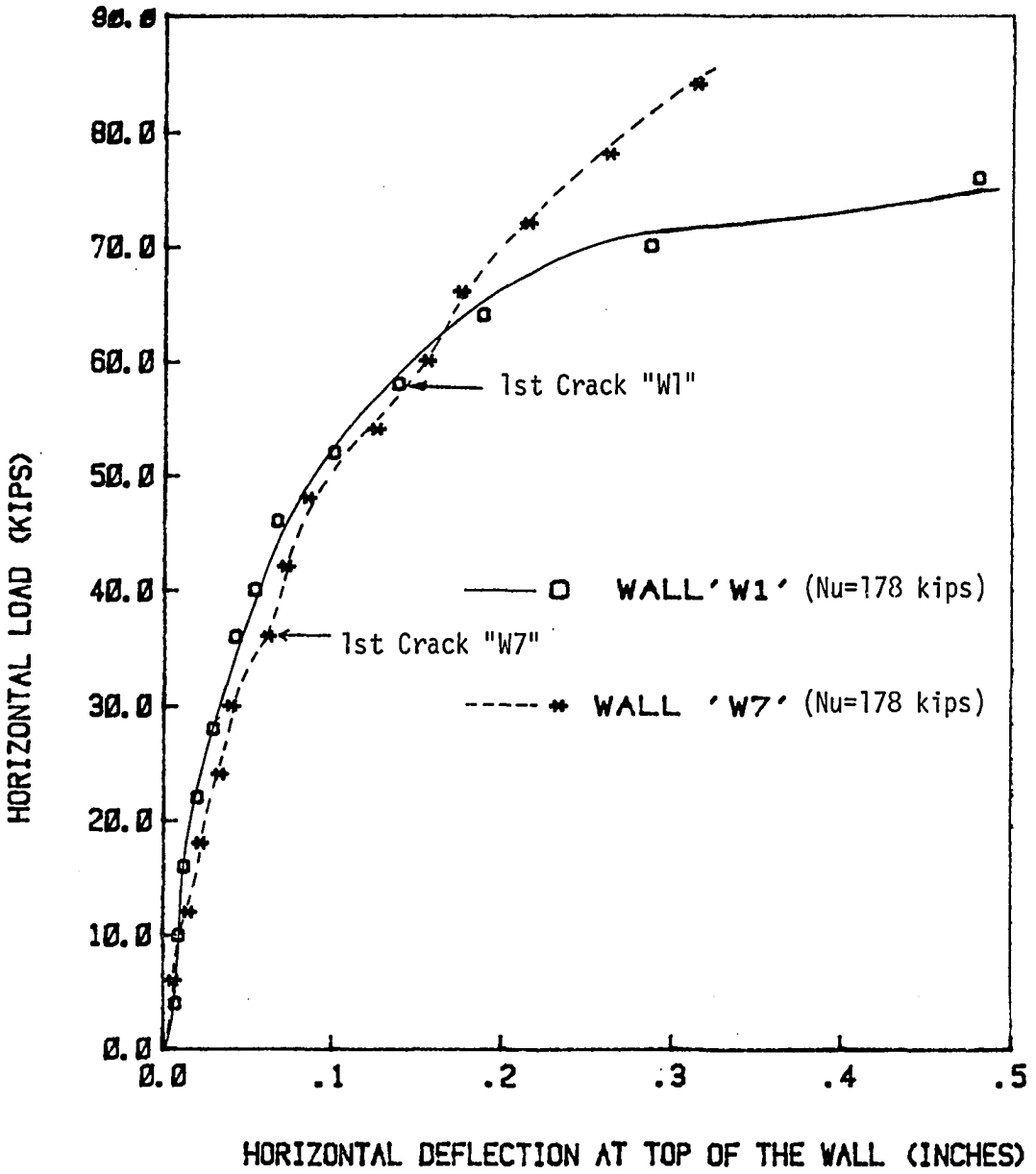

Figure 22. Load-deflection curves for walls "W1" and "W7"

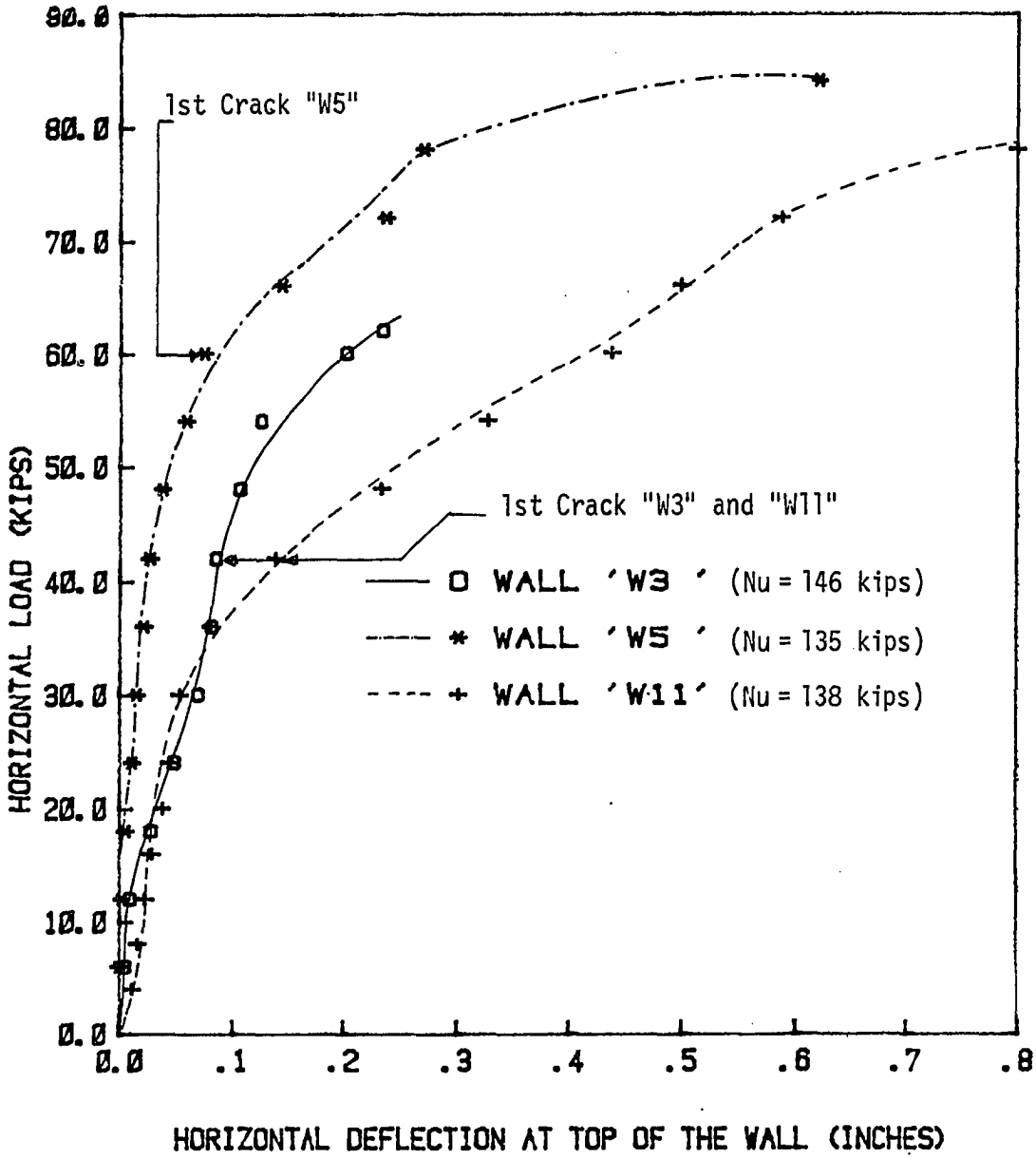

Figure 23. Load-deflection curves for walls "W3", "W5" and "W11"

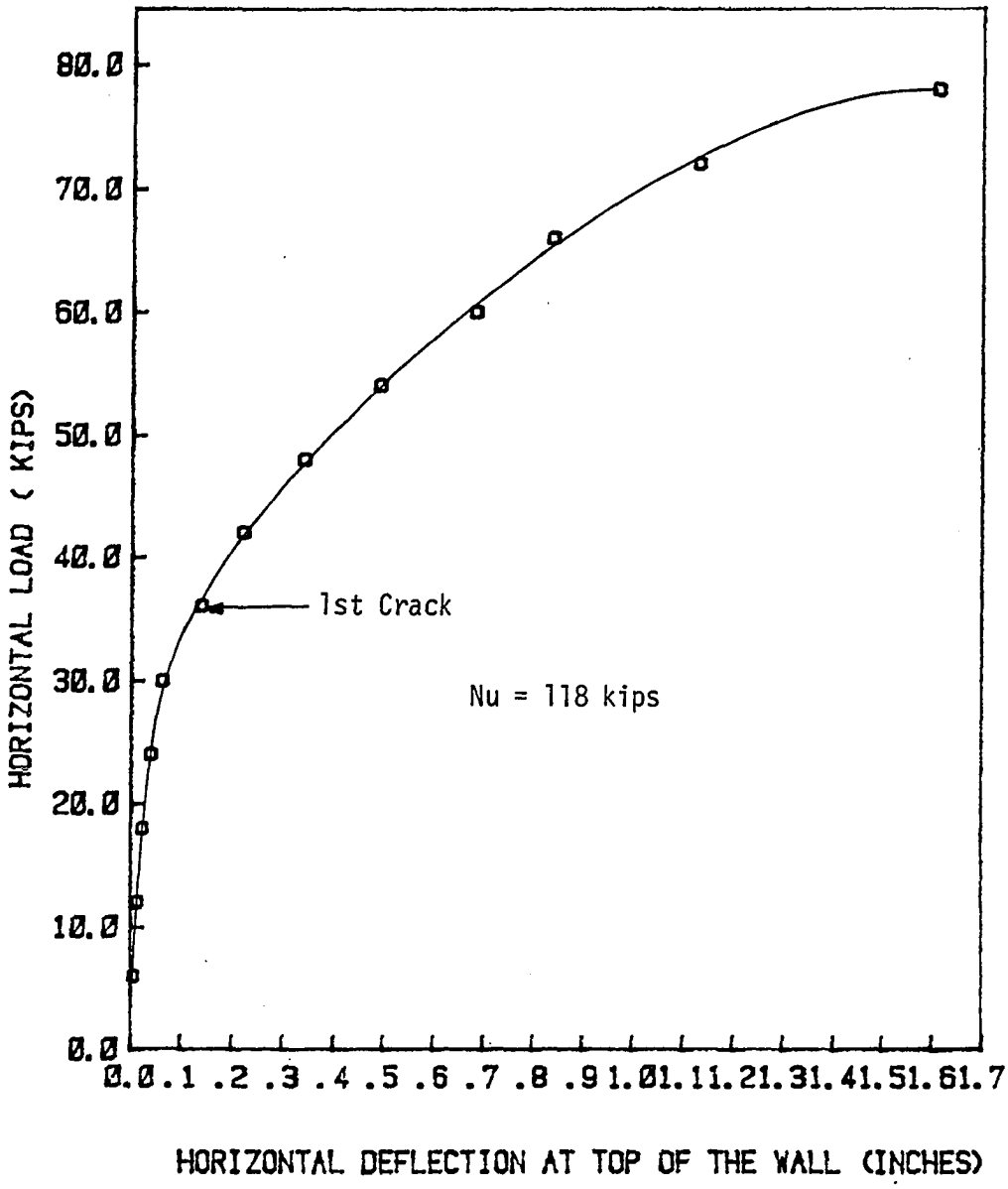

Figure 24. Load-deflection curve for wall "W9"

Table 10. Stiffness values for brick-to-block walls

Wall designation	W1	W3	W5	W7	W9	W11
Stiffness[a] (k/in.)	1600	1600	2200	800	933	590

[a]Stiffness is calculated by measuring the slope of the straight-line portion in the load deflection curve.

transmission of tensile stresses as a result of welding the mesh to the base.

(3) All block wythes failed identically but all brick wythes failed differently, i.e., bearing failure only occurred in the block wythes while diagonal shear and/or bearing failure occurred in the brick wythes.

(4) For "W7", the separation load of the brick wythe increased by 18.4%, compared to that of "W1".

These walls were identical except that "W7" used mesh welded to the steel base, simulating continuity in reinforcement.

Fig. 23 shows load-deflection curves for "W3", "W5" and "W11." "W11" was the noncomposite wall. These walls had similar precompression loads. "W3" and "W5" were identical, except that "W3" broke and was repaired before testing commenced. The load-deflection curve for "W3" is different than that for "W5", probably because the repaired joint was weaker and thicker than the regular one. Therefore, the following comparison is primarily between walls "W5" and "W11," from which one may conclude:

(1) grouting the collar joint increases wall stiffness by at least three times (about 370%) and also increases ultimate shear force by 15%;

(2) the initial straight-line portion of both load-deflection curves, i.e., to the load where the first crack appeared, exhibited the wall's elastic behavior during that stage; and

(3) the load at first crack for "W5" was about 43% greater than that for "W11".

Fig. 24 shows the load-deflection curve for "W9", the wall having the lowest precompression load. This curve indicates that "W9" was the most ductile wall, indicating that ductility may increase as the precompression load decreases.

The load-deflection curve given by Meli [5] is similar to the load-deflection curves obtained for the tested walls. More walls should be tested to obtain values for the contants of the curve and the effect of the different parameters on these constants.

The relationship between shear strength, $v_{ult.}$, and precompressive stress may be written generally as:

$$v_{ult.} = V_{SB} + \mu\sigma_c \qquad (2)$$

where: V_{SB} = the ultimate shear bond strength

μ = the coefficient of friction

σ_c = the precompression stress.

A comparison of the constants of Equation 2 with those suggested by previous research for a single wythe is given in Table 11. The comparison shows that the single wythe Equation 2 cannot predict the shear strength for the composite wall.

Table 12 shows the relationship between experimental ultimate bond stresses causing separation and those obtained from Equation 1. The

Table 11. Comparison between the constants of Equation 2 as given by previous research for one wythe

Ref.	Type of wall	Constants		W1		W3		W5		W7		W9	
		V_{SB} psi	μ	$v^{c}_{ult.}$[a]	$v^{m}_{ult.}$[b]	$v^{c}_{ult.}$	$v^{m}_{ult.}$	$v^{c}_{ult.}$	$v^{m}_{ult.}$	$v^{c}_{ult.}$	$v^{m}_{ult.}$	$v^{c}_{ult.}$	$v^{m}_{ult.}$
12	Ungrouted block	67	1.1	519	175.5	444	150.7	406	204.6	507	202.4	357	174.1
12	Grouted block	110→150	1.2		175.5		150.7		204.6		202.4		174.1
13	Ungrouted block	32	0.9	402	175.5	340	150.7	310	204.6	392	202.4	269	174.1
13	Grouted block	180	1.0	591	175.5	523	150.7	489	204.6	580.3	202.4	443.5	174.1
2	Brick	220	1.1	672	175.5	597	150.7	559	204.6	660	202.4	510	174.1
14	Brick	15	0.167	84	175.5	72	150.7	67	204.6	82	202.4	59	174.1

[a] $v^{c}_{ult.}$ is the calculated ultimate shear value for the precompression stress for the wall.

[b] $v^{m}_{ult.}$ is the actual ultimate shear value for the composite wall.

Table 12. The bond stresses using Equation 1 compared to test data

Wall	W1	W3	W5	W7	W9
f'_m	1680	2365	2170	1816	1722
V_{SB}	56.2	63.3	61.3	57.6	56.6
Ultimate measured bond stress V_{SB}	175.5	150.2	--[a]	202.4	174.1
Factor of safety	3.1	2.37		3.5	3.08

[a]The separation failure did not take place in this wall.

table indicates that actual bond stresses were more than 100 psi, as suggested in Ref. 10. Table 12 also indicates that these walls had an average safety factor of 3, which is a reasonable value for masonry. Therefore, Equation 1 can be recommended to determine the allowable bond stresses for composite masonry walls.

The allowable shear strength, v, as given by the ACI Code [14] for walls with height-to-width ratio of more than one, is:

$$v = 1.5 \sqrt{f'_m} \qquad (3)$$

Table 13 shows the ultimate shear stresses for the tested walls based on the gross area. A comparison of these values with the allowable ones is shown in Fig. 25, which indicates that the precompression

Table 13. Ultimate lateral stresses and the precompression stresses for brick-to-block walls

Wall designation	W1	W3	W5	W7	W9	W11[a]
Intended precompression stresses (psi)	410.9	342.6	308.6	400.3	263.5	398.2
Ultimate lateral stresses (psi)	175.5	150.7	204.6	202.4	174.1	225.1
Measured precompression stresses (psi)	415.3	374.8	379.4	409.9	326.9	442.4

[a]The area for this wall is considered as the masonry area neglecting the collar joint area.

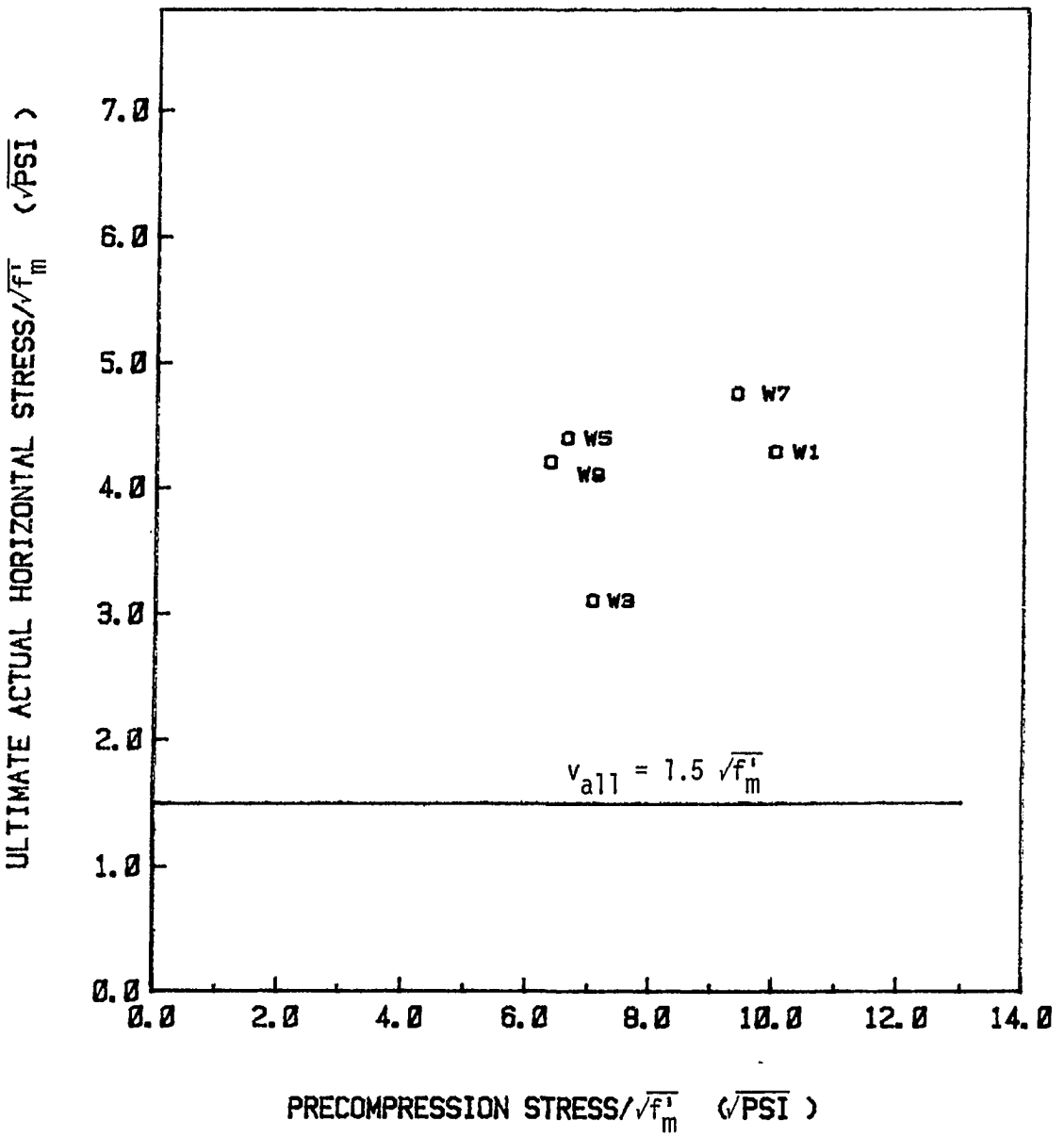

Figure 25. Comparison of ACI Code equation and experiments of the brick-to-block walls

stresses had small effect on ultimate shear stresses. This is probably due to the small range of precompression stresses in these tests. The average value of the safety factor is 2.9 (if the results of "W3" are ignored). Therefore, the allowable shear stresses given by the Code are reasonable for composite masonry walls.

CONCLUSIONS AND RECOMMENDATIONS

Based on the six brick-to-block composite walls tested, the following conclusions can be drawn:

(1) Using a composite masonry wall with grouting and reinforcing the collar joint versus the block wythe increases the ultimate shear load by 15%; the initial stiffness by more than 300%; and the first crack load by 43%.

(2) Precompression stress has little effect on ultimate shear stress. Therefore, wider ranges of precompression stresses should be considered in the future.

(3) The equation proposed by Williams and Geschwindner [7] for the allowable bond stresses can be recommended for composite walls having a safety factor of 3.0.

(4) Ductility decreases as precompression stress increases.

(5) The steel did not yield in any wall, even though the minimum amount allowed by code was used. Therefore, further study should be done using less steel.

(6) Ultimate shear load and stiffness increased by about 18% after welding mesh to the base, which simulated the continuity of steel.

(7) The load-deflection curve can be approximated as a trilinear relationship, as proposed by Meli [5]. More tests should be conducted considering different parameters to find constants which define this curve.

(8) The ultimate shear strength for the composite wall cannot be

predicted using the single wythe method as given in Equation 2.

(9) The assumption of composite action for the wall was valid based on the strain and the behavioral results.

(10) Ultimate shear stresses for the tested walls ranged from 150.7 psi to 204.6 psi.

(11) The failure modes for brick-to-block walls were mainly bearing failure in both wythes, in addition to separation failure involving either one or both wythes and the collar joint for walls W1, W3, W7, and W9 and diagonal shear failure in one wythe, as in the block wythe for "W11", or in the brick wythe for "W1" and "W7".

ACKNOWLEDGMENTS

The authors express their thanks to the Masonry Institute of Iowa and to the Masons Union of Iowa for providing material and labor for building the specimens. Thanks are also due to the Civil Engineering Department and Engineering Research Institute at Iowa State University. The assistance of Mr. Doug Wood is appreciated.

REFERENCES

1. J. C. Grogan. "Miscellaneous reinforced brick masonry structures." Proc. Second International Brick Masonry Conference, Stoke-on-Trent, England, (April 1970), 327-330.

2. J. R. Benjamin and H. A. Williams. "The behavior of one-story brick shear walls." Proc. ASCE, Journal of the Structural Division, ST-4-84 (1958), 1-29.

3. R. R. Schneider. "Lateral load tests on reinforced grouted masonry shear walls." State of California, Department of Public Works, Division of Architecture, Sacramento, California, 1959.

4. I. H. E. Nilsson and A. Losberg. "The strength of horizontally loaded prefabricated brick panel walls." Proc. Second International Brick Masonry Conference, Stoke-on-Trent, England, (April 1970), 191-196.

5. R. Meli. "Behavior of masonry walls under lateral loads." Proc. Fifth World Conference on Earthquake Engineering, v. 1, Rome, (1974), 853-862.

6. M. Hatzinikolas; J. Longworth and J. Warwaruk. "The effect of joint reinforcement on vertical load carrying capacity of hollow concrete block masonry." Proc. of the North American Masonry Conference, University of Colorado, Boulder, Colorado, 1978.

7. R. T. Williams and L. F. Geschwindner. "Shear stress across collar joints in composite masonry walls." Proc. 2nd North American Masonry Conference, University of Maryland, College Park, Maryland, August, 1982.

8. J. C. Scrivener. "Shear tests on reinforced brick masonry walls." British Ceramic Research Association LTD, Technical Note No. 342, Heavy Clay Division, Melbourne, Australia, October 1982.

9. Masonry Institute of America. "1979 Masonry codes and specification." Masonry Institute of America, Los Angeles, California, 1979.

10. J. E. Amrhein. "Reinforced masonry engineering handbook." Clay and Concrete Masonry, Masonry Institute of America, Los Angeles, California, 1983.

11. A. A. Hamid; R. G. Drysdale and A. C. Heiderbrecht. "Shear strength of concrete masonry joints." Proc. ASCE, Journal of the structural division, ST-7-105 (1979), 1227-1240.

12. G. A. Hegemier; S. K. Arya; G. Krishnamoorthy; W. Nachbar and R. Fugerson. "On the behavior of joints in concrete masonry." Proc. of the North American Masonry Conference, University of Colorado, Boulder, Colorado, 1978.

13. U. C. Kalita and A. W. Hendry. "An experimental and theoretical investigation of the stresses and deflection in model cross-wall structures." Proc. Second International Brick Masonry Conference, Stoke-on-Trent, England, April, (1970), 209-214.

14. American Concrete Institute. "Building code requirements for concrete masonry structures and commentary." ACI Standard 531-79 and ACI Report 531R-79, Detroit, Michigan, June, 1979.

APPENDIX A. PROCEDURE FOR BUILDING AND TESTING THE COMPOSITE WALLS

Each wall was built in three days, as follows:

(1) One of the wythes (and one-half of the other one) was built first;

(2) Except in the case of steel bars welded to the base, reinforcement was placed and one-half of the wall was grouted. The second wythe was then completed; and

(3) The remaining part of the wall was grouted.

The walls were then tested in the load frame. The vertical load was applied using two hydraulic cylinders attached to a steel beam (W14x78). The load was transferred to another steel beam (W14x78) through 9-rollers on which the horizontal load was applied directly. The loads were transferred from the latter beam to the wall through straight coil loops grouted in the top of all wythes. These loops were anchored to a steel plate at the top and bolted to the loaded beam. The total shear capacity of the loops was designed to be higher than the expected ultimate shear capacity of the walls.

APPENDIX B. STRAIN RESULTS

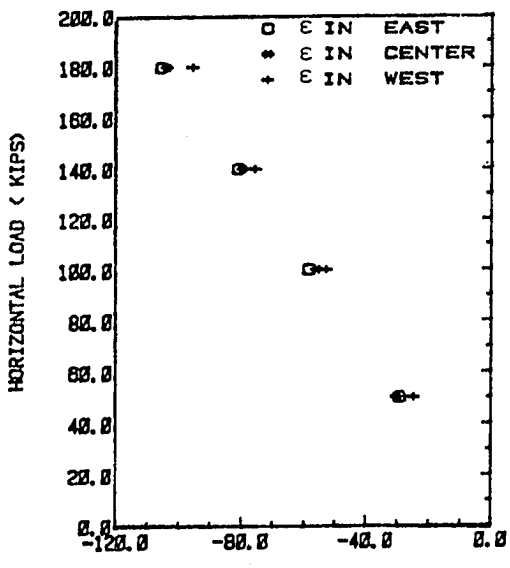

VERTICAL STRAINS AT THE HORIZONTAL AXIS THROUGH THE CENTER OF THE WALL 'W1' (με)

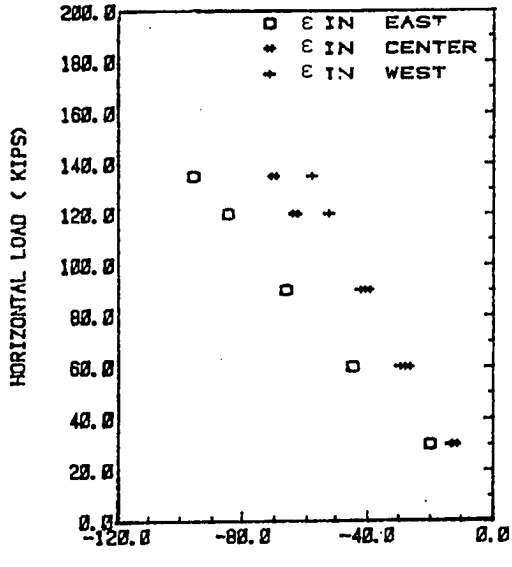

VERTICAL STRAINS AT THE HORIZONTAL AXIS THROUGH THE CENTER OF THE WALL 'W5' (με)

Figure 26. Vertical strain at the horizontal axis at the middle of the wall

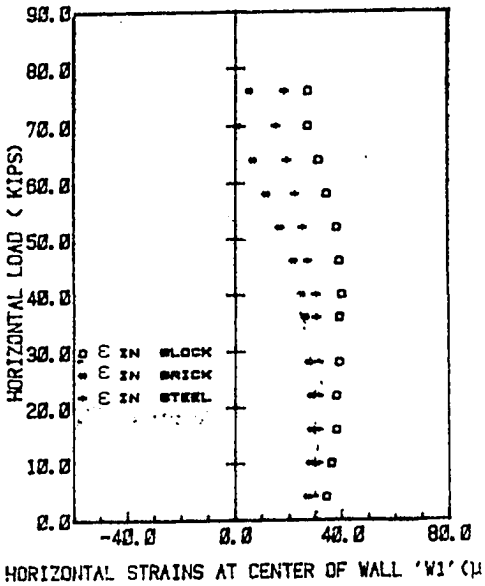

HORIZONTAL STRAINS AT CENTER OF WALL 'W1'(με)

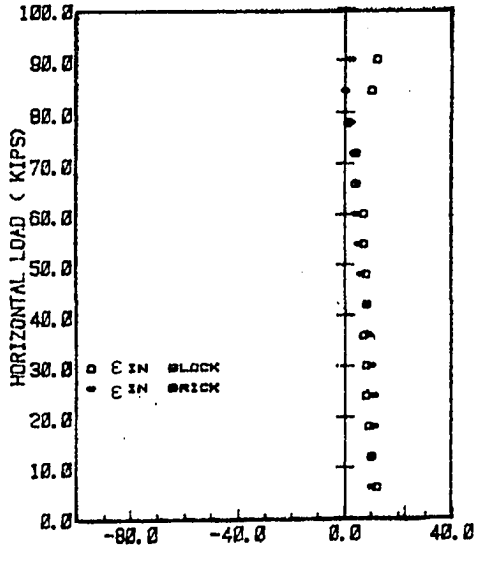

HORIZONTAL STRAINS AT CENTER OF WALL 'W5'(με)

Figure 27. Horizontal strain at center of the wall

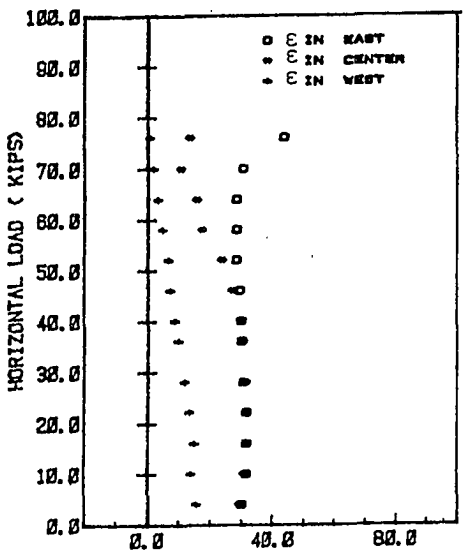

HORIZONTAL STRAINS AT THE HORIZONTAL AXIS THROUGH THE CENTER OF THE WALL 'W1' (με)

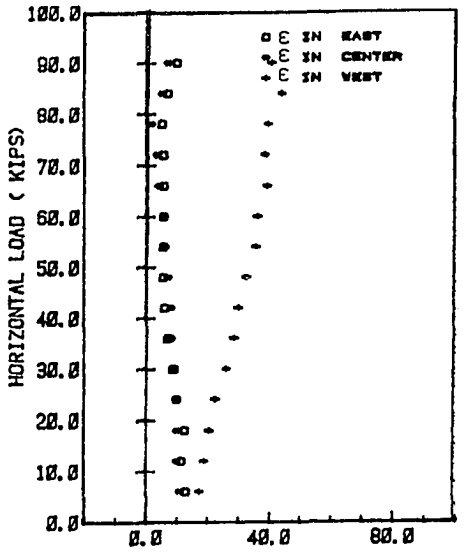

HORIZONTAL STRAINS AT THE HORIZONTAL AXIS THROUGH THE CENTER OF THE WALL 'W5' (με)

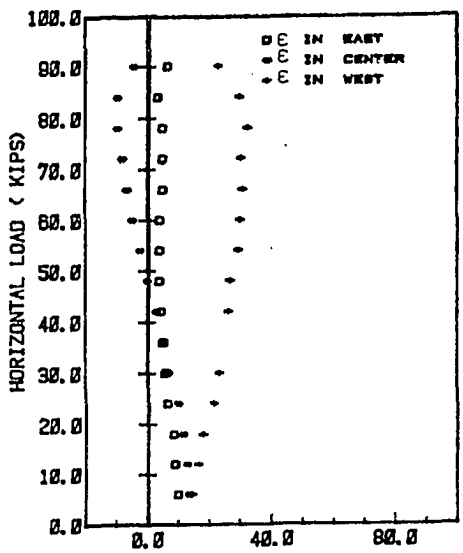

HORIZONTAL STRAINS AT THE HORIZONTAL AXIS THROUGH THE CENTER OF THE WALL 'W5' (με)

Figure 28. Horizontal strain at the horizontal axis at the middle of the wall

APPENDIX C. PRELIMINARY TEST FOR THE LOAD FRAME

A preliminary test was carried out to assess the capacity and the rigidity of the load frame. A steel beam connected to the lab floor, fixed at the bottom and free to move at the top, was used as a cantilever beam. Only a horizontal load was applied, at about 96 inches from the fixed end. Two strain gages were placed on the horizontal beam at which the horizontal cylinder was attached; two more strain gages were placed at the bottom of the fixed end of the cantilever beam. The applied load reached a value of about 120 kips, showing a maximum measured deflection of 0.001 inches without significant strain.

PART 2B. BEHAVIOR OF REINFORCED BRICK-TO-BRICK WALLS

Behavior of reinforced brick-to-brick walls

M. H. Ahmed, Graduate Research Assistant
M. L. Porter, Professor
A. Wolde-Tinsae, Associate Professor

From the Department of Civil Engineering, Iowa State University, Ames, IA 50011

ABSTRACT

The results of testing five brick-to-brick reinforced composite masonry panels subjected to gravity and in-plane shear loads are discussed herein. Each wall contained two wythes with a nominal 2-inch collar joint. This joint was grouted and reinforced with either welded wire fabric or vertical and horizontal bars. The vertical load was applied first and held constant for all walls, followed by the horizontal (in-plane) load. The loads (either vertical or horizontal) were applied as distributed loads along the top of the wall (which was free to move), with the base fixed. The wall panels were approximately 4 feet wide, 6 feet high and 9 inches thick. One-wythe and composite prisms were built corresponding to each wall to determine the strength properties. A comparison of strength characteristics of the tested walls is discussed herein.

The literature review and the control tests in Part 1 are to be inserted here for publication submission.

COMPOSITE WALLS

Five composite brick-to-brick walls were built in three different stages. Walls of two wythes, with a nominal 2-in. reinforced collar joint, were tested. All walls were approximately 6-ft. high and 4-ft. wide, were built either on a steel T-section (WT6x32.5) or on a steel plate 1.25 inches thick. Straight coil loops were welded to the steel base and positioned to align with the holes of the masonry. The holes of the first two layers of the brick wythe and those of the first layer of the block wythe were grouted to bond the coil loops to the masonry, after which the walls were cured in accordance with ASTM-E447-74 [9] and tested after at least 28 days. The walls were designated as: W2, W4, W6, W8 and W10. Table 5 indicates the age of each wall and its amount of reinforcement. The procedure used to build the walls is given in Appendix A.

Table 5. Test age and reinforcement details for brick-to-brick walls

Wall		Test age	Reinforcement	
Group	No.	days	Vertical	Horizontal
I	W2	80		WWF[a] 4x4x4x4
II	W4	66		WWF 4x4x4x4
II	W6	76		WWF 4x4x4x4
III	W8	37	1#3 & 2#4 bars[b]	5#3 bars
III	W10	38	1#3 & 2#4 bars	4#3 bars & truss joint[c]

[a]Welded wire fabric consisted of No. 4 gage horizontal and vertical wires.

[b]The vertical reinforcement was welded to the steel base.

[c]The truss joint was 1/8 inch thick, 5 5/8 inches wide and placed horizontally in the bed joint every 16 inches (6 brick layers). For all other walls, the reinforcement was placed in the collar joint.

Five composite prisms were built, using materials similar to those of each wall. The prisms and walls were cured under the same conditions and tested on the same day. The average dimensions were 15.8-in. high and 15.7-in. wide for the first wall only; for the other walls, these dimensions were 15.8-in. high and 7.6-in. wide. Thickness and reinforcement were similar to the corresponding full-size wall. The prisms were loaded vertically in accordance with ASTM specifications [9] and failed as follows: Horizontal cracks along the bed joints started in both wythes at about two-thirds of the ultimate load. These cracks were followed by vertical separation between the masonry wythe and the collar joint. Vertical cracks crossing the masonry units of both wythes occurred next, followed by complete failure. Average dimensions of the walls and compressive strengths of composite prisms are given in Table 6. Typical failure of the composite prisms is shown in Fig. 10.

Measurements

Strains and deflections were measured at different load points. Paper-back strain gages of lengths of 0.6, 0.8 and 2.4 inches were used for masonry units. The first two lengths of the strain gages were used for the brick units and the last one (the long one) was used for the block units). These strain gages were located at five points on each wall as follows: at the center and the two edges of the vertical and horizontal center lines of the wall. Some of these strain gages were destroyed either during building the wall or due to cracks in the units. The results of the strains are given in (Fig. 22) Appendix B. The deflections were measured using dial gages with 0.001-inch sensitivity.

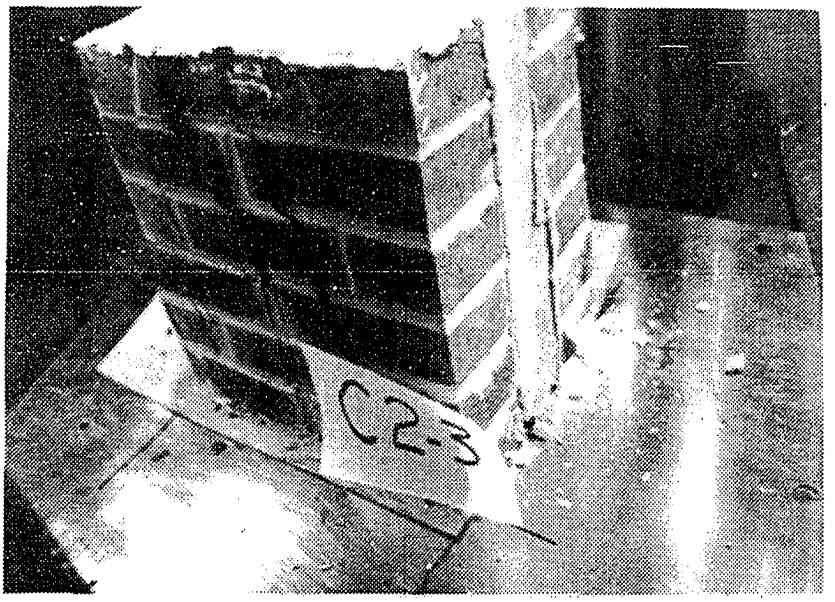

Figure 10. Typical failure in composite prism

Test Procedures

Before testing the walls, a preliminary test was carried out to check the capacity and rigidity of the frame. The details of this test are given in Appendix C.

Table 6. Average dimensions of the walls and compressive strengths of the composite prisms

Wall designation	Width (in.)	Thickness (in.)	Height (in.)	Thickness of collar joint	Area ($in.^2$)	f'_m psi	c.o.v. %
W2	48.5	8.73	72.1	1.63	423.41	3020	21.0
W4	47.7	8.94	72.1	1.84	426.6	2890	13.6
W6	47.5	9.13	72.3	2.03	433.44	2452	8.8
W8	47.5	9.45	71.6	2.35	448.5	2088	6.2
W10	47.6	9.08	71.8	1.98	432.5	2136	13.1

The test procedure for all walls was the same and can be described as:

(1) Strain gages and load cell (to give the vertical load readings) were connected to a programmable data acquisition system.

(2) Initial readings were taken after applying the vertical load in three cycles, from zero to 10 kips and back to zero.

(3) Vertical load was applied in increments up to the intended precompression load, then kept approximately constant until the end of the test. The value of the intended vertical load was determined as different ratios (1, 0.9, 0.75 and 0.5) of the allowable load. After applying high values of horizontal load, the vertical load changed. Therefore, it was readjusted for every load point.

(4) Next, the horizontal load was applied in increments until the wall

failed, i.e., reached its ultimate load-carrying capacity.

(5) At every load point, strains, deflections and loads were recorded. Cracks were recorded, marked and numbered with the same number as the load point.

The walls were oriented so that the horizontal load was always applied from east to west. Fig. 11 shows the joint reinforcement and the composite wall under construction.

Composite Wall Test Results

Wall "W2"

Wall "W2" was subjected to a precompression load of 160 kips (0.9 of the allowable load). The first crack occurred at a lateral load of 48 kips at the first bed joint from the bottom of the wall in both wythes. This crack was horizontal, indicating tensile bond failure. Several vertical cracks occurred at the bottom-west corner of the south wythe, followed by a separation crack between the south wythe and the collar joint at a lateral load of 88 kips. After a drop in the horizontal load, bearing failure in both wythes propagated toward the east and a diagonal crack propagated from the bottom of the south wythe at a lateral load of 83.3 kips. Bearing failure in both wythes occurred in conjunction with the ultimate load of 90 kips in addition to separation failure and diagonal shear failure in the south wythe only. The crack pattern at different load points is shown in Fig. 12.

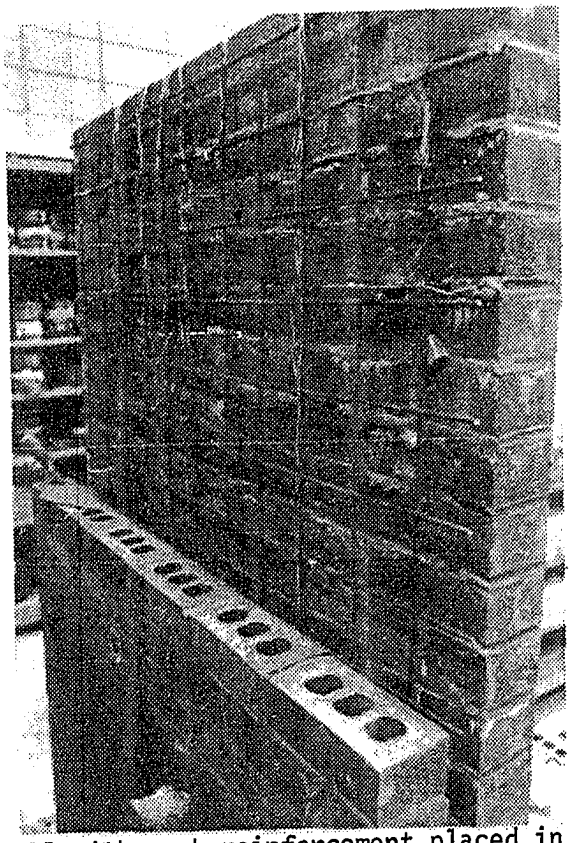

a) The composite wall with mesh reinforcement placed in collar joint

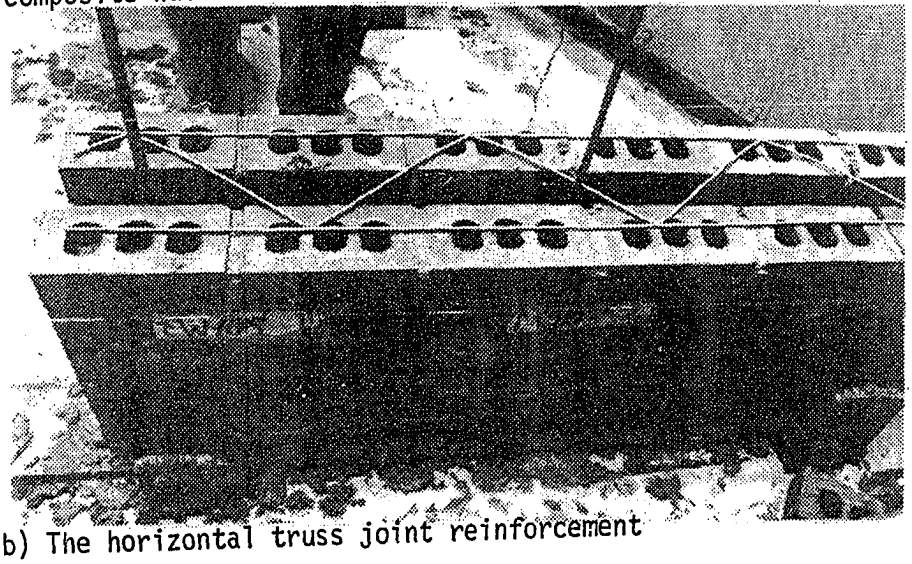

b) The horizontal truss joint reinforcement

Figure 11. Composite wall under construction and the joint reinforcement

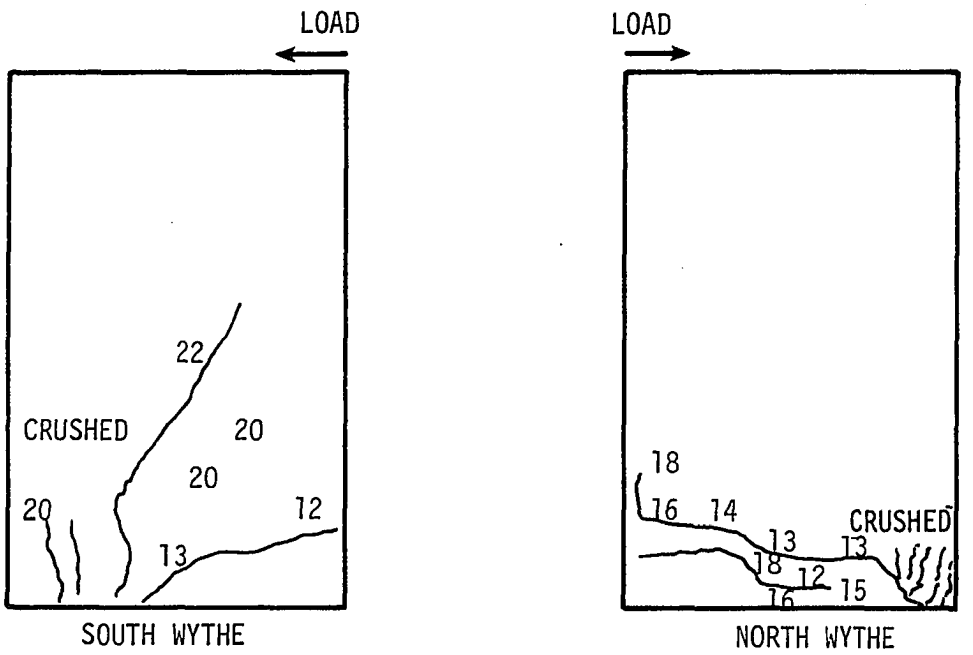

Load point	1	2	3	4	5	6	7	8	9	10	11	12	13	14	15	16	17	18	19	20	21	22
Vertical load (k)	0	50	100	160	160	160	160	160	160	160	160	160	160	160	160	160	160	160	160	160	160	160
Horizontal load (k)	0	0	0	0	6	12	18	24	30	36	42	48	54	60	66	72	78	84	90	88	84	83.3

Figure 12. Crack pattern for wall "W2"

Wall "W4"

Wall "W4" was subjected to a precompression load of 90 kips (0.5 of the allowable load). A horizontal crack occurred at a lateral load of 24 kips. This crack was at the second bed joint in both wythes. At a lateral load of 66 kips, a diagonal crack in the bottom-west corner occurred through the brick units in the north wythe. At this stage, the lateral load was released because the precompression load was decided to be raised to 180 kips. This lateral load was reapplied until the wall failed. The first crack occurred in the same place as in the first test, but at higher load (i.e., at a lateral load of 40 kips, compared to first crack's appearance at 24 kips in the first test). The bearing failure increased and the welds connecting the plate to which the hydraulic cylinder was fixed broke at a lateral load of 72 kips. The test was then terminated, and was repeated after fixing the plate. No cracks occurred other than those previously recorded when the load was reapplied. However, a double separation between the two wythes and the collar joint occurred at the ultimate load of 94.4 kips in addition to the bearing failure in both wythes. The crack pattern at the different load points is shown in Fig. 13.

Wall "W6"

Wall "W6" was subjected to a precompression load of 135 kips (0.75 of the allowable load). The first crack occurred horizontally at the first bed joint at the bottom of the wall in both wythes at a lateral load of 18 kips. Several horizontal cracks occurred at the bottom of both wythes at a lateral load of 48 kips. Some vertical bearing type

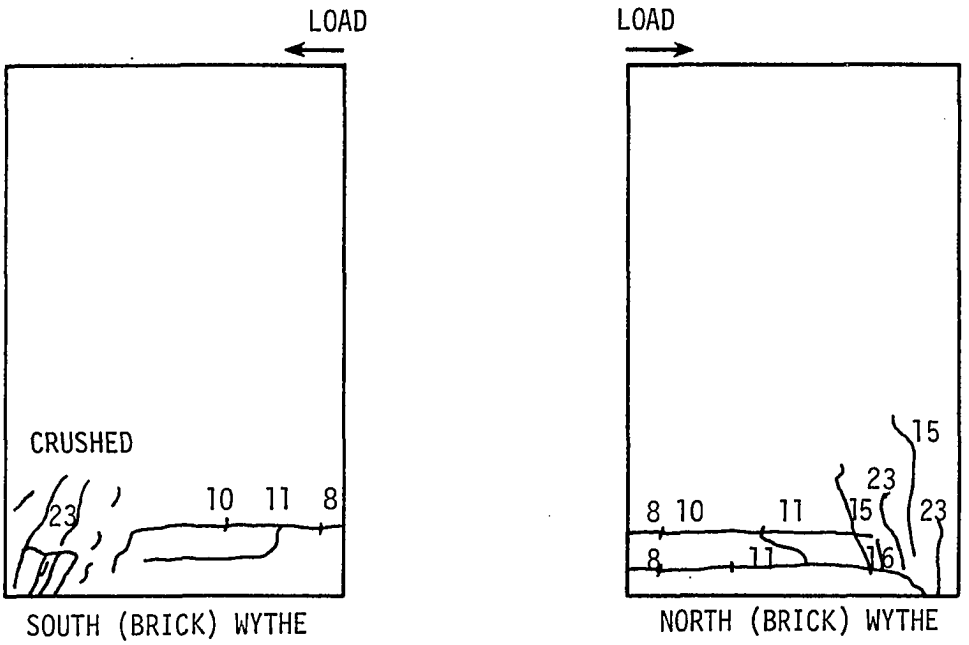

Load point	1	2	3	4	5	6	7	8	9	10	11	12	13	14	15	16	17	18	19	20	21	22	23	24	25	26	27
Vertical load (k)	0	30	60	90	90	90	90	90	90	90	90	90	90	90	90	90	0	180	180	180	180	180	80	180	180	180	180
Lateral load (k)	0	0	0	0	6	12	18	24	30	36	42	48	54	60	66	72	0	0	20	40	60	70	71	82	90	80	68

Figure 13. Crack pattern for wall "W4"

cracking also occurred at the bottom-west corner of both wythes, followed by complete bearing failure of that corner, at the ultimate load of 85.3 kips. In addition, vertical and diagonal cracks appeared at the south wythe only. The crack pattern at the different load points is shown in Fig. 14.

Wall "W8"

The precompression load on wall "W8" was 157 kips (0.9 of the allowable load). The first crack was vertical and occurred at the bottom-west corner of the north wythe at a lateral load of 36 kips. Horizontal cracks in the first bed joint of the south wythe occurred at a lateral load of 48 kips. Similar cracks occurred in the north wythe at a lateral load of 66 kips. The bottom-west corner in the north wythe was crushed, followed by a vertical separation between the north wythe and the collar joint, at an ultimate load of 96 kips. Another vertical separation between the south wythe and the collar joint in the west side occurred, but only after the first vertical separation. The crack pattern at the different load points is shown in Fig. 15.

Wall "W10"

Wall "W10" was subjected to a precompression load of 157 kips (0.9 of the allowable load). The first crack occurred horizontally at the second bed joint in the south wythe at a lateral load of 24 kips, and also in the north wythe at a lateral load of 42 kips. Crushing of the bottom-west corner in the north wythe occurred at the ultimate load of 90 kips followed by similar curshing in the south face. Vertical

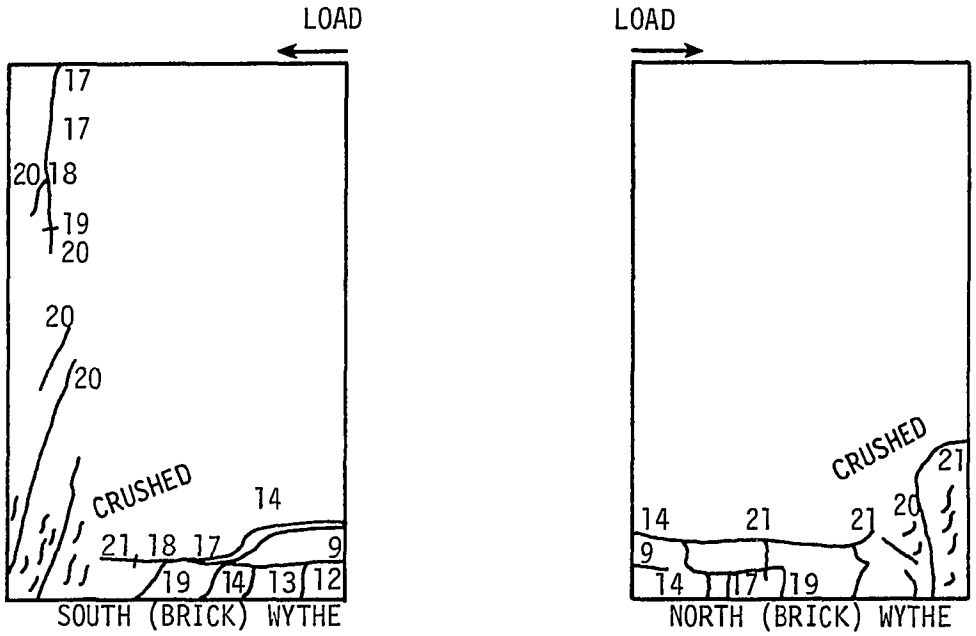

Load point	1	2	3	4	5	6	7	8	9	10	11	12	13	14	15	16	17	18	19	20	21
Vertical load (k)	0	30	60	90	120	135	135	135	135	135	135	135	135	135	135	135	135	135	135	135	135
Horizontal load (k)	*0*	*0*	*0*	*0*	*0*	*0*	*6*	*12*	*18*	*24*	*30*	*36*	*42*	*48*	*54*	*60*	*66*	*72*	*78*	*84*	*81*

Figure 14. Crack pattern for wall "W6"

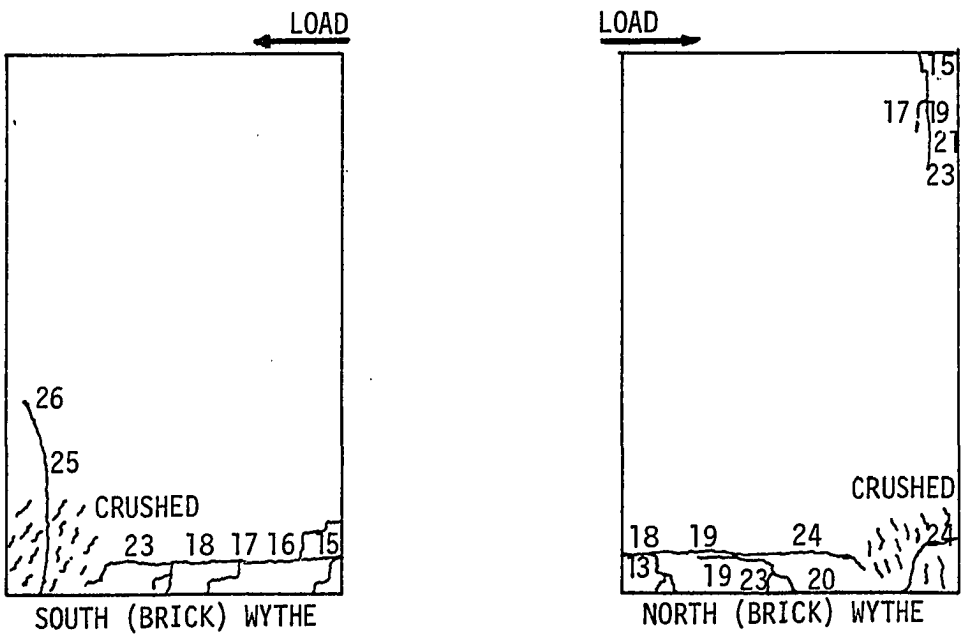

Load point	1	2	3	4	5	6	7	8	9	10	11	12	13	14	15	16	17	18	19	20
Vertical load (k)	0	30	60	90	120	157	157	157	157	157	157	157	157	157	157	157	157	157	157	157
Lateral load (k)	0	0	0	0	0	0	6	12	18	18	24	30	36	42	48	54	60	66	72	77

Load point	21	22	23	24	25	26
Vertical load (k)	157	157	157	157	157	157
Lateral load (k)	78	84	90	96	93	86

Figure 15. Crack pattern for wall "W8"

double separation between the two masonry wythes and the collar joint occurred following the crushing of the bottom-west corner. The crack pattern at the different load points is shown in Fig. 16. Figs. 17 and 18 show photographs for different types of cracks. Fig. 17 shows examples of bearing failure in walls "W2" and "W6". Fig. 18 shows the vertical separation between the masonry and the collar joint and the diagonal failure in walls "W2" and "W8".

Discussion of Walls Behavior

The tested brick-to-brick walls failed in the following ways: bearing failure of the compressive corner at the bottom of the wall, followed by bond failure between the masonry and the collar joint. A summary of these modes of failure and the maximum measured loads for all walls is given in Table 7. The load-deflection curves are shown in Figs. 19 and 20. The initial straight-line portion in these curves occurred for only low loads. No reinforcement yielded in any wall (as evidenced by measured strains and as shown in Appendix B).

Fig. 19 shows the load-deflection curves for "W2", "W8" and "W10". These three walls were subjected to about the same intended precompression load (Nu). These walls differed in type of reinforcement only. They had, however, almost the same area of steel. Comparing the results of these three walls indicates:

(1) Wall "W2" was stiffer at very low loads, but "W10" was stiffer than the other two walls at higher lateral loads.

(2) The joint reinforcement in wall "W10" reduced the ultimate lateral load, but not significantly (about 6%). This agrees with similar

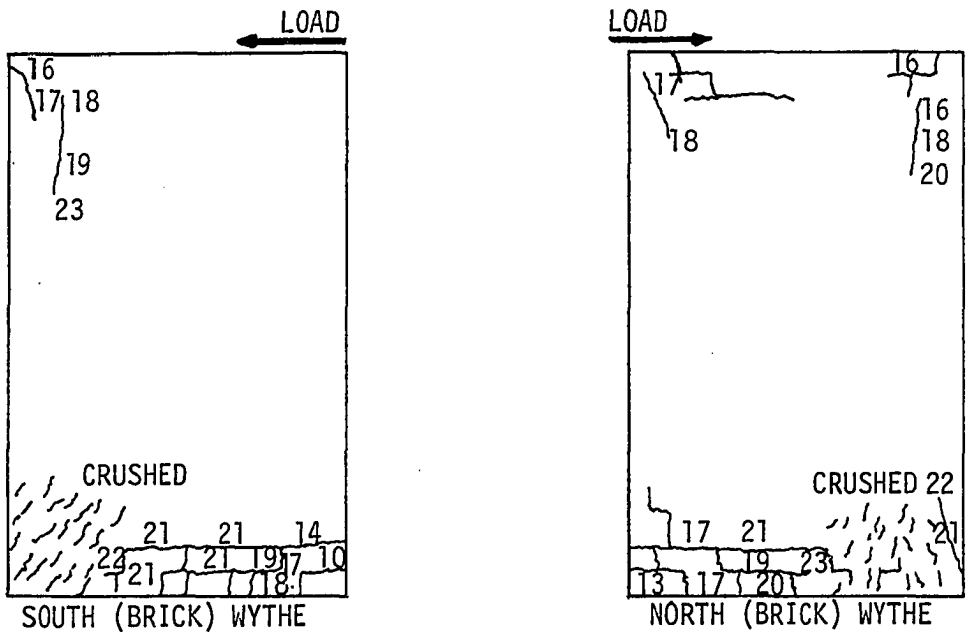

Load point (k)	1	2	3	4	5	6	7	8	9	10	11	12	13	14	15	16	17	18	19	20	21	22	23
Vertical load (k)	0	30	60	90	120	157	157	157	157	157	157	157	157	157	157	157	157	157	157	157	157	157	157
Lateral load (k)	0	0	0	0	0	0	6	12	18	24	30	36	42	48	54	60	66	72	78	83	84	90	85

Figure 16. Crack pattern for wall "W10"

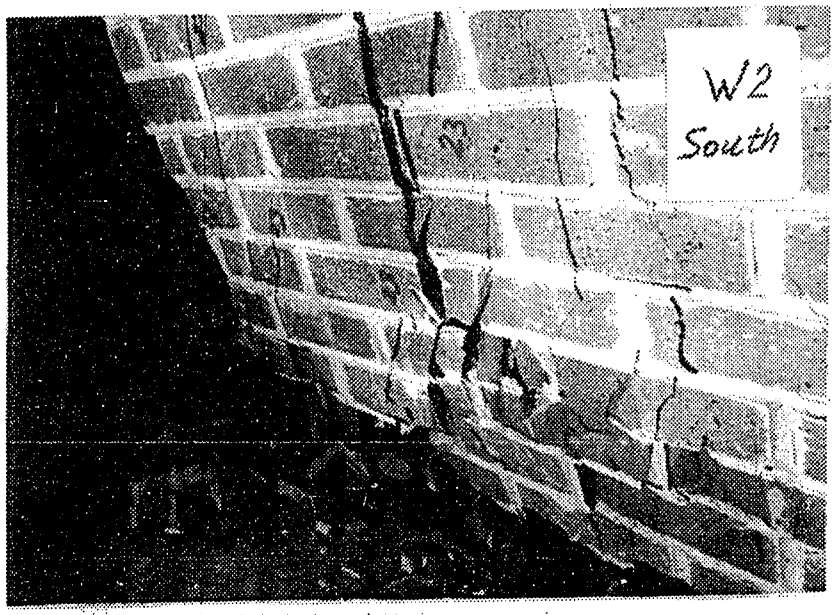

a) Bearing failure in wall "W2"

b) Bearing failure in wall "W6"

Figure 17. Examples of bearing failure

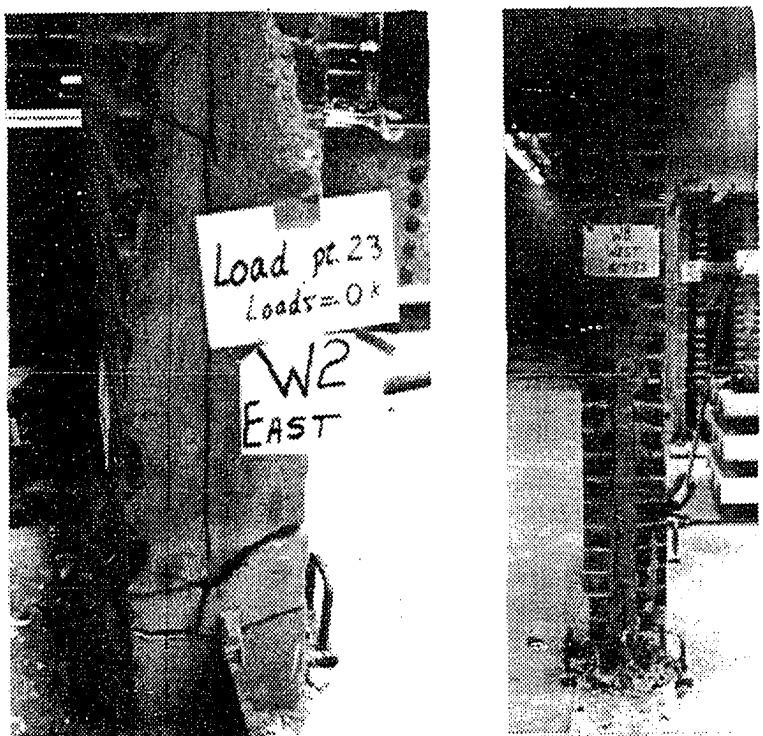

a) Vertical separation between the masonry and the collar joint

b) Diagonal failure in wall "W2"

Figure 18. Examples of diagonal failure and separation between the masonry and the collar joint

Table 7. Maximum loads and modes of failure for the brick-to-brick walls

Wall designation	Intended precompression load (kips)	Measured[a] precompression load (kips)	Ultimate lateral load (kips)	First crack load (kips)		Separation load (kips)		Mode of failure	
				North	South	North	South	North	South
W2	160	196.9	90	48	48	--	88	Bearing failure	Bearing failure & diagonal crack started & bond failure
W4	180	200.4	94.4	40	40	90	90	Bearing failure & bond failure	Bearing failure & bond failure
W6	135	172.3	85.3	18	18	--	--	Bearing failure	Bearing failure & vertical and diagonal failure
W8	157	174.8	96	36	48	96	96	Bearing failure & bond failure	Bearing failure & bond failure
W10	157	173.8	90	24	42	90	90	Bearing failure & bond failure	Bearing failure & bond failure

[a]The precompression load increased during test and was readjusted at every load point. This value is the measured one at the ultimate lateral load point (at failure).

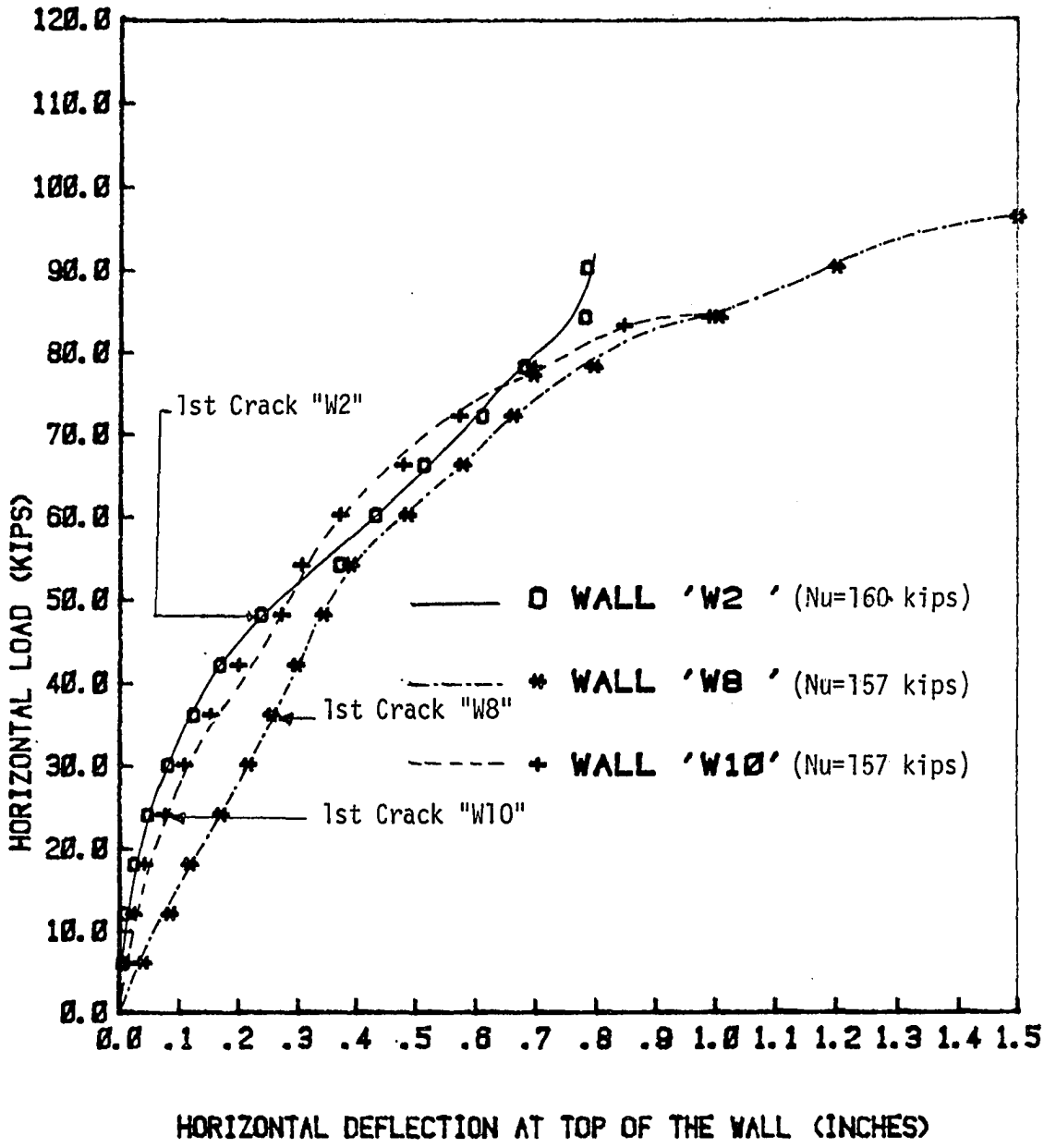

Figure 19. Load-deflection curves for walls "W2", "W8" and "W10"

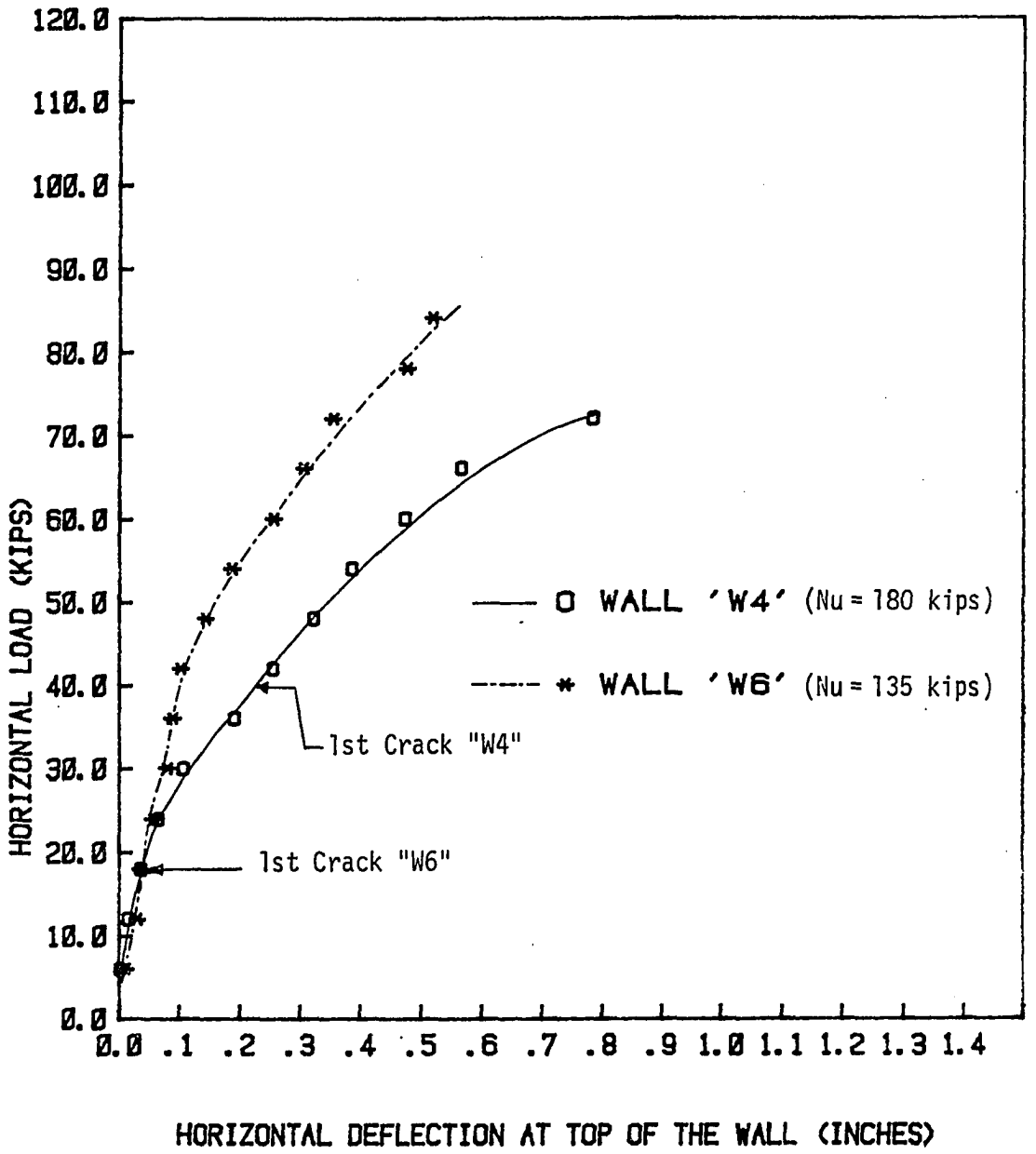

Figure 20. Load-deflection curves for walls "W4" and "W6"

conclusions for load bearing (only) single wythe wall [6].

(3) The modes of failure in the three walls were similar (bearing failure and separation).

(4) The use of mesh reinforcements or truss joint reinforcements each provided the walls with greater ductility than vertical and horizontal bars and allowed the wall to deflect more before failure.

(5) The vertical separation occurred only at the ultimate lateral load. This may indicate that the bond failure was due to the large deflection rather than the high lateral loads.

(6) The first crack in wall "W2" occurred at a higher lateral load than either of walls "W8" or "W10".

Fig. 20 shows the load-deflection curves for walls "W4" and "W6". These were identical, with different intended precompression loads. This figure indicates similar deflections at low lateral loads and at higher loads. Increasing of the precompression load had little effect on the ultimate lateral load (e.g., a 33% increase in the precompression load increased the ultimate lateral force by only 10.7%).

Table 8 shows the ultimate bond stresses that caused the separation, and compares them to the values obtained from the equation given in [7] as

$$V_{SB} = 38.9 + 0.0103\ f'_m \qquad (2)$$

The average safety factor is 3.25, which is reasonable for masonry. The table indicates that the actual bond stresses were more than 100 psi, as suggested in Ref. 10. Therefore, Equation 2 is recommended to determine the allowable bond stresses for composite masonry walls.

The allowable shear strength, v, as given by the ACI Code [11]

Table 8. The bond stresses using the proposed equation [7] and the test data

Wall	W2	W4	W6	W8	W10
f'_m (psi)	3020	2890	2452	2088	2136
V_{SB} (psi)	70	68.7	64.2	60.4	60.9
Ultimate measured bond stresses	207.8	211	--[a]	214.1	208.1
Factor of safety	2.97	3.07		3.54	3.42

[a]The separation failure did not take place in this wall.

for walls with height-to-width ratio of more than one is:

$$v = 1.5 \sqrt{f'_m} \geq 75 \text{ psi} \qquad (3)$$

A comparison between ultimate and allowable shear stresses is shown in Fig. 21. These ultimate values are given in Table 9.

The average value of the safety factor is 2.9 (from Table 9), meaning that the allowable value given in the codes (Equation 3) is applied for composite masonry.

Table 9. Ultimate lateral stresses and the precompression stresses for brick-to-brick walls

Wall	W2	W4	W6	W8	W10
Intended precompression stresses (psi)	377.9	421.9	311.5	350.1	363
Ultimate lateral stresses (psi)	212.6	221.3	196.8	214.1	208.1
Measured precompression stresses (psi)	465	469.8	397.5	389.7	401.8
Allowable lateral stresses (psi) (Equation 3)	75	75	74.3	68.5	69.3
Safety factor	2.83	2.95	2.65	3.13	3

The relationship between ultimate shear strength and precompression stress can be written in the general form of:

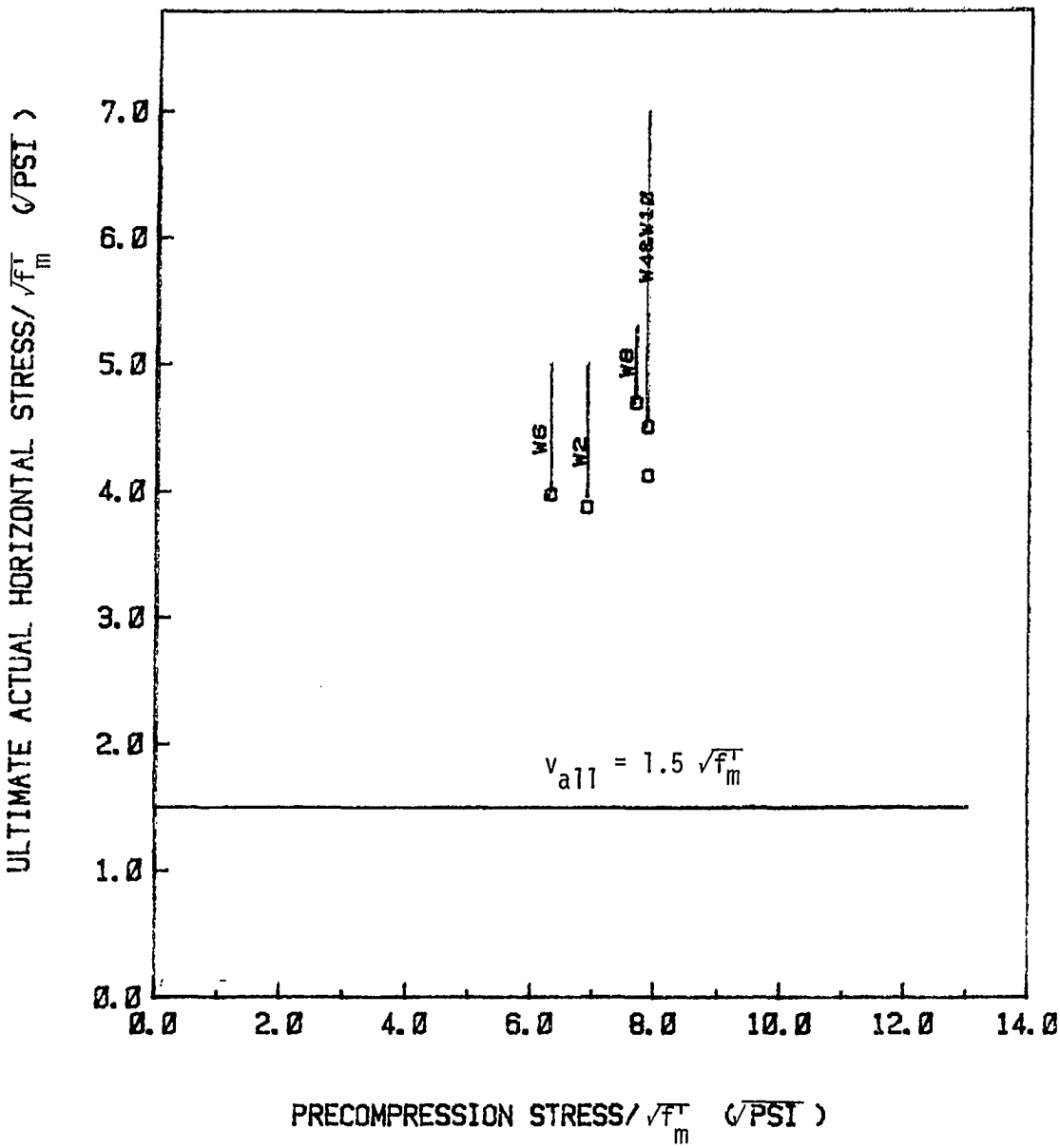

Figure 21. Comparison between the allowable shear strength and the experimental results of brick-to-brick walls

$$v_{ult.} = V_{SB} + \mu\sigma_c \quad (4)$$

where: $v_{ult.}$ = the ultimate shear stress

V_{SB} = the ultimate shear bond strength

μ = the coefficient of friction

σ_c = the precompression stress.

The values of V_{SB} and μ for single brick wythe are given by the research investigations indicated in Table 10. The proposed constants for composite walls are also shown in the table. Therefore, Equation 4 can be written in the form:

$$v_{ult.} = 141 + 0.19\ \sigma \quad (5)$$

The comparison shows that the proposed equation is valid for all tested composite walls.

Table 10. Comparison between the constants of Equation 4, as given by previous research, for one wythe and proposed constants for composite walls

Ref.	Constants		W2		W4		W6		W8		W10	
	V_{SB}	μ	$v^c_{ult.}$	$v^m_{ult.}$	$v^c_{ult.}$	$v^m_{ult.}$	$v^c_{ult.}$	$v^m_{ult.}$	$v^c_{ult.}$	$v^m_{ult.}$	$v^c_{ult.}$	$v^m_{ult.}$
2	220	1.1	672	212.6	597	221.3	559	196.8	660	214.1	510	208.1
12	15	0.167	84	212.6	72	221.3	67	196.8	82	214.1	59	208.1
Proposed	141	0.19	212.8	212.6	221.2	221.3	200.2	196.8	207.5	214.1	210	208.1

CONCLUSIONS AND RECOMMENDATIONS

The following conclusions can be made for brick-to-brick walls:

(1) The failure modes for brick-to-brick walls were mainly bearing failure in both wythes, in addition to separation failure involving either one or both wythes and the collar joint.

(2) The precompression load has only a small effect on the ultimate shear stress. However, a wider range of precompression loads should be considered in the future.

(3) Williams and Geschwindner's proposed equation for the bond stresses [7] can be used for these composite walls with a safety factor of 3.25.

(4) Joint reinforcement reduces the ultimate shear load, but not significantly ($\simeq$ 6%). This reduction agrees with similar conclusions [6] for load bearing single wythe walls. However, additional tests are needed to substantiate this conclusion.

(5) Although the minimum amount of steel required by the ACI Code was used, the steel did not yield. Therefore, further studies should be done using less steel.

(6) Ultimate shear stresses range from 196.8 psi to 221.3 psi.

(7) The load deflection curve can be approximated as a trilinear relationship, as proposed by Meli [5]. More tests should be conducted considering different parameters to find the constants which define this curve.

(8) Ultimate shear strength can be predicted using Equation 5. The allowable shear stress can then be calculated using a safety factor

of 3 as follows: $v_{all} = 47 + 0.0625\ \sigma_c$.

(9) The allowable value (Equation 3) of shear stresses as given in the ACI Codes can be applied for composite walls.

ACKNOWLEDGMENTS

The authors express their thanks to the Masonry Institute of Iowa and to the Masons Union of Iowa for providing material and labor for building the specimens. Thanks are also due to the Civil Engineering Department and Engineering Research Institute at Iowa State University. The assistance of Mr. Doug Wood is appreciated.

REFERENCES

1. J. C. Grogan. "Miscellaneous reinforced brick masonry structures." Proc. Second International Brick Masonry Conference, Stoke-on-Trent, England, (April 1970), 327-330.

2. J. R. Benjamin and H. A. Williams. "The behavior of one-story brick shear walls." Proc. ASCE, Journal of the Structural Division, ST-4-84 (1958), 1-29.

3. R. R. Schneider. "Lateral load tests on reinforced grouted masonry shear walls." State of California, Department of Public Works, Division of Architecture, Sacramento, California, 1959.

4. I. H. E. Nilsson and A. Losberg. "The strength of horizontally loaded prefabricated brick panel walls." Proc. Second International Brick Masonry Conference, Stoke-on-Trent, England, (April 1970), 191-196.

5. R. Meli. "Behavior of masonry walls under lateral loads." Proc. Fifth World Conference on Earthquake Engineering, v. 1, Rome, (1974), 853-862.

6. M. Hatzinikolas; J. Longworth and J. Warwaruk. "The effect of joint reinforcement on vertical load carrying capacity of hollow concrete block masonry." Proc. of the North American Masonry Conference, University of Colorado, Boulder, Colorado, 1978.

7. R. T. Williams and L. F. Geschwindner. "Shear stress across collar joints in composite masonry walls." Proc. 2nd North American Masonry Conference, University of Maryland, College Park, Maryland, August, 1982.

8. J. C. Scrivener. "Shear tests on reinforced brick masonry walls." British Ceramic Research Association Ltd., Technical Note No. 342, Heavy Clay Division, Melbourne, Australia, October 1982.

9. Masonry Institute of America. "1979 Masonry codes and specification." Masonry Institute of America, Los Angeles, California, 1979.

10. J. E. Amrhein. "Reinforced masonry engineering handbook." Clay and Concrete Masonry, Published by Masonry Institute of America, Los Angeles, California, 1983.

11. American Concrete Institute. "Building code requirements for concrete masonry structures and commentary." ACI Standard 531-79 and ACI Report 531R-79, Detroit, Michigan, June, 1979.

12. U. C. Kalita and A. W. Hendry. "An experimental and theoretical investigation of the stresses and deflection in model cross-wall structures." Proc. Second International Brick Masonry Conference, Stoke-on-Trent, England, (April 1970), 209-214.

APPENDIX A. PROCEDURE FOR BUILDING AND TESTING THE COMPOSITE WALLS

Each wall was built in three days, as follows:

(1) One of the wythes (and one-half of the other one) was built first;

(2) Except in the case of steel bars welded to the base, reinforcement was placed and one-half of the wall was grouted. The second wythe was then completed; and

(3) The remaining part of the wall was grouted.

The walls were then tested in the test frame. The vertical load was applied using two hydraulic cylinders attached to a steel beam (W14x 78). The load was transferred to another steel beam (W14x78) through 9-rollers on which the horizontal load was applied directly. The loads were transferred from the latter beam to the wall through straight coil loops grouted in the top of all wythes. These loops were anchored to a steel plate at the top and bolted to the loaded beam. The total shear capacity of the loops was designed to be higher than the expected ultimate shear capacity of the walls.

APPENDIX B. STRAIN RESULTS

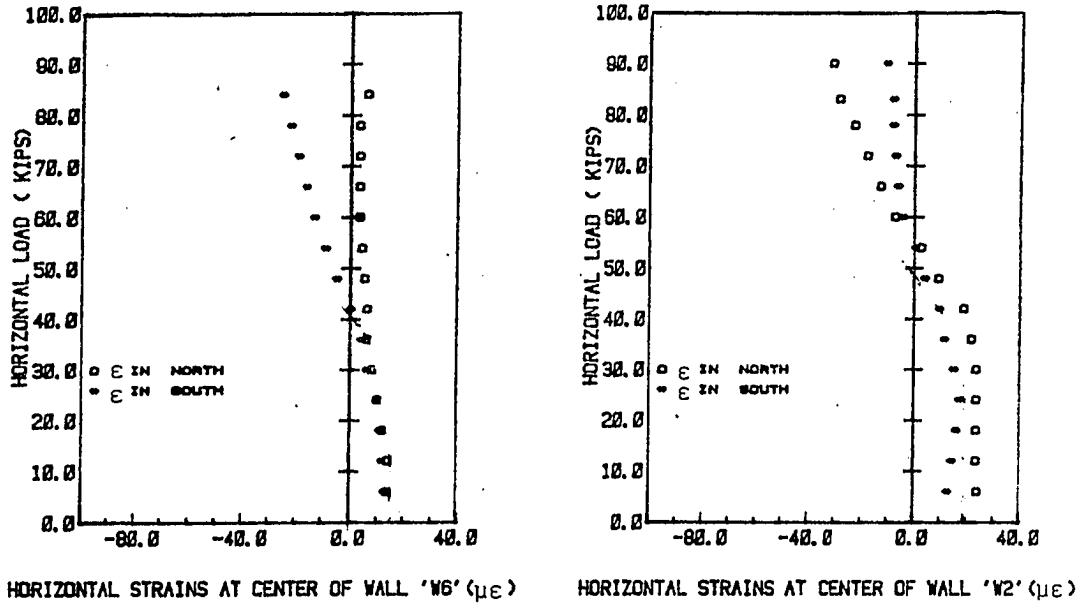

Figure 22. Horizontal strains at center of the wall

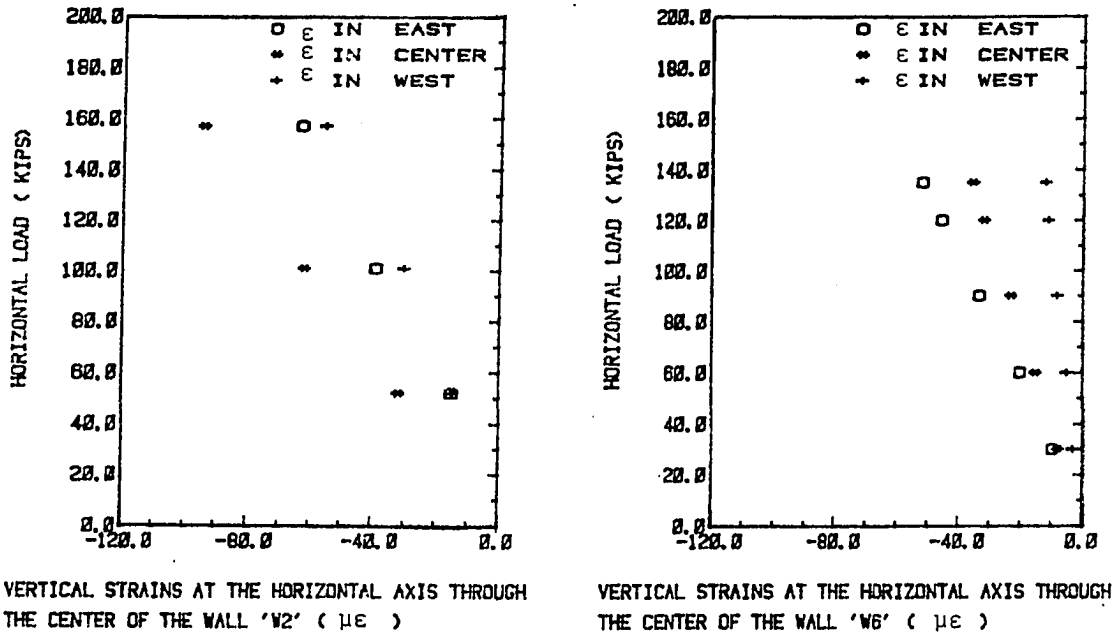

Figure 23. Vertical strains at the Horizontal axis at the middle of the wall

APPENDIX C. PRELIMINARY TEST FOR THE LOAD FRAME

A preliminary test was carried out to assess the capacity and the rigidity of the load frame. A steel beam connected to the lab floor, fixed at the bottom and free to move at the top, was used as a cantilever beam. Only a horizontal load was applied, at about 96 inches from the fixed end. Two strain gages were placed on the horizontal beam at which the horizontal cylinder was attached; two more strain gages were placed at the bottom of the fixed end of the cantilever beam. The applied load reached a value of about 120 kips, showing a maximum measured deflection of 0.001 inches without significant strain.

PART 3. ANALYSIS OF COMPOSITE MASONRY WALLS: PART I

Analysis of composite masonry walls: Part I

M. H. Ahmed, Graduate Research Assistant
A. Wolde-Tinsae, Associate Professor
M. L. Porter, Professor

From the Department of Civil Engineering, Iowa State University, Ames, IA 50011

ABSTRACT

The finite element technique was used to analyze composite masonry walls herein. The composite walls considered were either brick-to-block or brick-to-brick, with a reinforced collar joint between the two wythes. The walls were 6-ft. high, 4-ft. wide, and 9-in. thick. Load-deflection curves and ultimate shear loads were predicted on the basis of the finite element method and on the theory for flexural strength. In the uncracked case, the wall was treated as a cantilever beam fixed at the base and free at the top. In the cracked case, a portion of the bottom of the wall was freed, based on tensile stresses in the mortar which exceeded the mortar's ultimate tensile strength. A proposed load-deflection curve based on finite element results is also discussed herein. The theoretical results were compared with experimental ones.

INTRODUCTION

The design and analysis of reinforced masonry are based on the elastic theory of working stress design. Most of the formulas based on working stress design are similar to those used for reinforced concrete, except that the ultimate strength of the masonry, f'_m, and the allowable stresses are modified to reflect the properties of masonry instead of concrete. Other methods of analyzing masonry walls are not yet recognized in the ACI and UBC Codes. These include the finite element technique, which is widely studied and used.

LITERATURE REVIEW

Cerny and Baldridge [1] compared different methods of distributing lateral in-plane force in multi-story masonry shear walls, then compared their results with more accurate computer analysis submitted there. The methods compared were:

(1) Considering the wall as a beam fixed at both ends, loaded at the top;

(2) Considering the wall as a cantilever beam loaded by uniformly distributed loads along its entire height;

(3) Considering the relative rigidities of the walls as proportioned to the moment of inertia in wall cross section;

(4) Considering the wall as a beam fixed at both ends, and using the simple beam equation to calculate relative rigidity;

(5) Considering the wall as a cantilever element fixed at the base and loaded with a concentrated load at the top.

The computer analysis conducted by Cerny and Baldridge assumed a one-story building with two shear walls treated as beam elements connected in one plane by a very rigid truss element, representing the rigid roof diaphragm. They concluded that method (5) most consistently agreed with their computer analysis.

Kalita and Hendry [2] (1970) reported an investigation of the applicability of shear wall theories to multi-story brickwork buildings. A finite element analysis was conducted and a simplified comparison theory developed from the experimental results. The tested structure

was a five-story building (one-sixth-scale), using one-sixth-scale model bricks for the walls with precast reinforced concrete slabs for the floors. The structure was loaded to produce in-plane lateral loads, in addition to precompression of the walls. Loads were applied by hydraulic cylinders located at the floor levels. Different precompression loads were applied on each floor. For preliminary tests, loads were kept below one-fifth to one-quarter of the expected ultimate load. The tested structure and its load-deflection curves are shown in Figs. 1 and 2. The values of the shear modulus, G, were calculated from the equation:

$$\Delta = \frac{Vh^3}{12\ EI} + \frac{1.2\ Vh}{AG} \qquad (1)$$

where:

Δ = the measured deflection from the straight-line portion of the experimental load-deflection curve;

V = the lateral (in-plane) force;

h = the height of the wall;

E = the elastic stiffness of the wall cross section;

A = the cross sectional area for the wall;

G = the modulus of rigidity; and

I = moment of inertia of wall cross section.

Kalita and Hendry concluded that:

(1) Failure occurred in the first story due to the breakdown of bond and frictional resistance at the brick/mortar interface;

(2) The rigidity and stresses in a brickwork structure can be calculated reasonably by analytical solutions. These solutions include

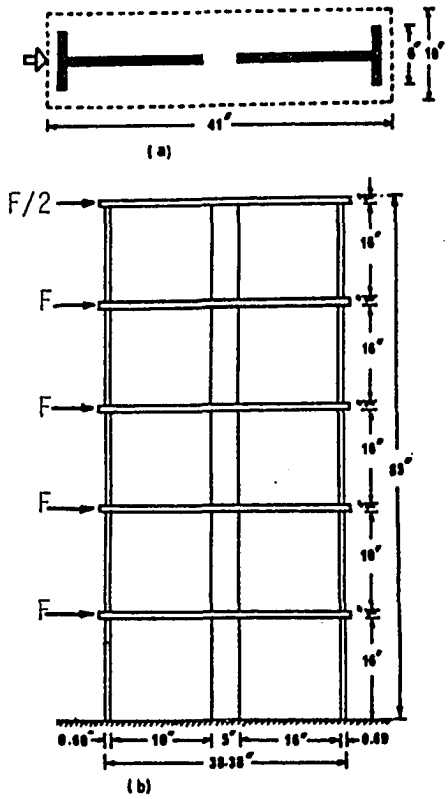

a) Plan and b) elevation of model structure

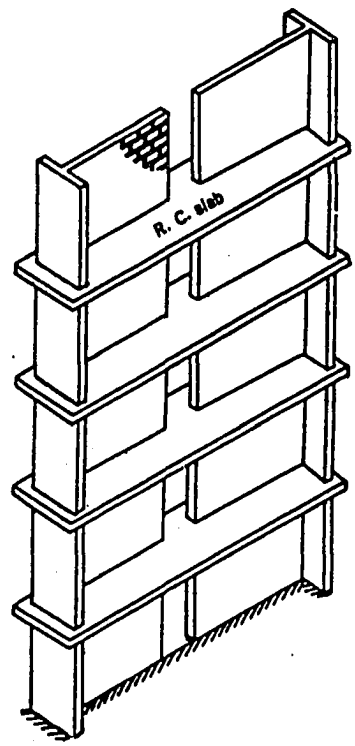

c) Typical construction of brickwork structure

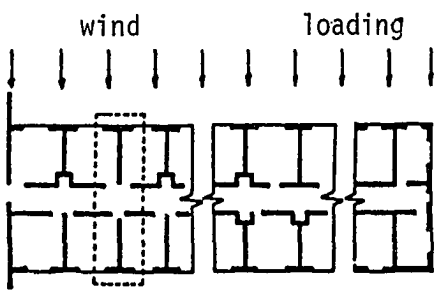

Figure 1. The loaded structure [2]

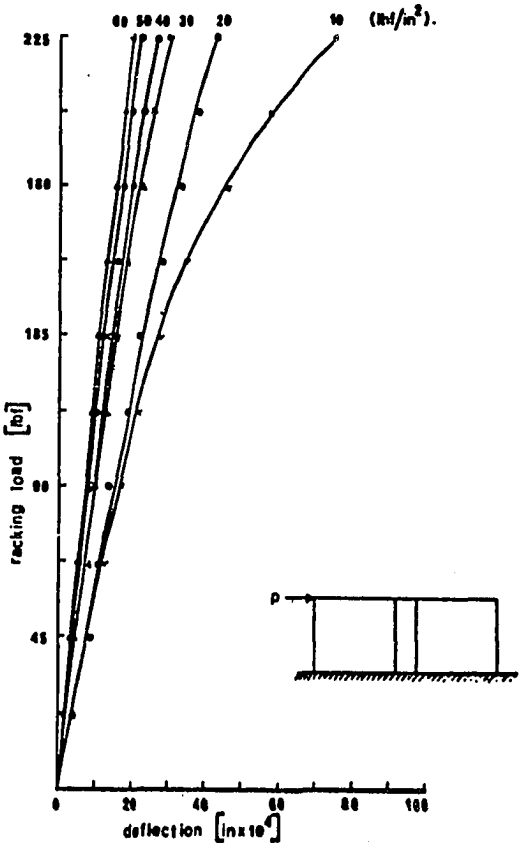

Figure 2. Load/deflection curves at different precompression [2]

the finite element method.

Page [3, 4] reported a nonlinear analysis of masonry walls by the finite element technique. Only in-plane loading was considered; however, the wall was assumed to be a continuum of isotropic elastic bricks acting in conjunction with mortar joints. Both the inelastic mortar properties and progressive joint failure produced the nonlinear response. The finite element subdivision is shown in Fig. 3. The brickwork was modeled using nonlinear characteristics [3]. In the nonlinear model, progressive joint failure was simulated as the load was increased. A comparative finite element analysis which assumed the brickwork to be an isotropic, linear elastic continuum with average properties was conducted. Page concluded that the finite element model yielded results congruent with other tests, even for higher loads, and that the model offered a realistic analysis on the basis of isotropic, elastic behavior.

Anand and Young [5] and Anand et al. [6] applied the finite element technique to inter-laminar shearing stresses in the collar joint of a nonreinforced composite wall. These stresses were caused by in-plane loads applied as one wythe only. The study considered only a two-dimensional element and assumed the materials to behave linearly. The following assumptions were considered:

(1) That all materials were homogeneous;

(2) That displacements bewteen nodal points varied linearly to insure continuity of displacement between elements;

(3) That out-of-plane bending effects were neglected in model development.

(4) That the collar joint, as well as the two wythes, were unreinforced.

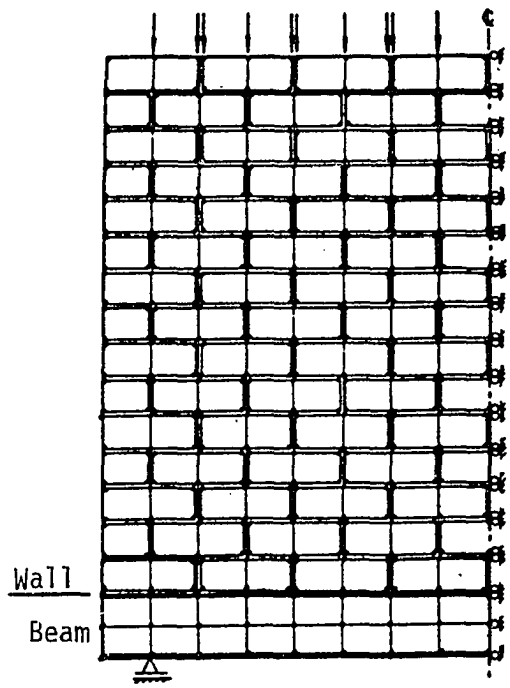

Figure 3. Composite beam test: finite element subdivision [4]

Anand and Young considered longitudinal and transverse models in their study, as shown in Fig. 4. The longitudinal model was considered through the wall length and the transverse model was considered through the wall cross section. They concluded that application of the longitudinal model could obtain results for collar joint shearing stresses which compared with those of the transverse model. However, the longitudinal model did not allow transverse deformation, either due to Poisson's effect or due to bending.

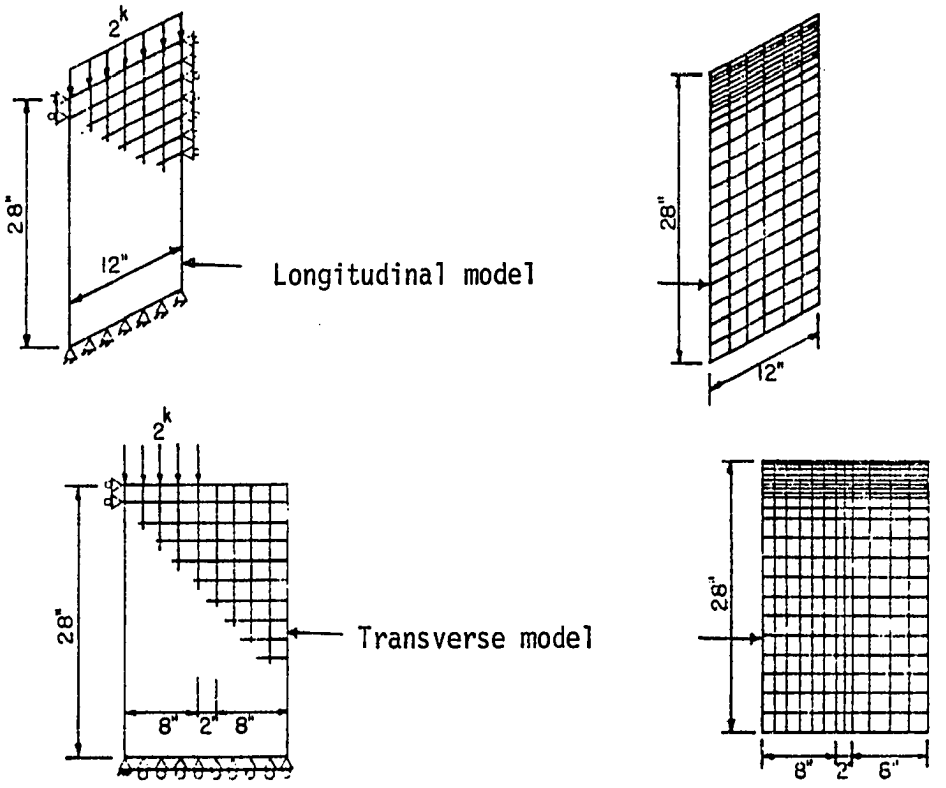

Figure 4. Models and mesh for composite masonry wall [6]

THEORY

The finite element technique is well-known [7, 8] and widely used. The ANSYS [9] computer program used to analyze the composite wall is a large-scale general purpose computer program. The composite wall was considered as a cantilever beam, supported at the bottom and free at the top. The elements were treated as two-dimensional plane stress elements. The following assumptions were made:

(1) all materials are homogeneous;

(2) plane sections through the thickness before loading remain plane after loading;

(3) all displacements vary linearly between the nodal points of the model;

(4) the out-of-plane effects are neglected;

(5) strains are not a function of the thickness;

(6) the tensile force is carried only by the reinforcement after the masonry element cracks;

(7) the loads (both vertically and horizontally) were applied to the wall in proportion of the stiffness of each wythe; and

(8) no interfacial bond stresses are transferred between wythes.

The chosen element in the ANSYS program is a two-dimensional isoparametric solid element with four nodal points.

Elastic Stiffness Matrix

The stiffness matrix of the composite wall was calculated on the basis of the stiffness matrix of each wythe. The total cross section of the composite wall can be written as:

$$A^{1} = b\,[t_{br} + t_{b\ell} + t_{cj}] = b \sum_{i=1}^{3} t_i = bT \qquad (2)$$

The applied force $F = A\,\sigma_{comp.}$ (3)

but $$\sigma_{comp.} = (E_j)_{comp.}\,\varepsilon \qquad (4)$$

Also, $$F = b[(\sigma t)_{br} + (\sigma t)_{b\ell} + (\sigma t)_{cj}] \qquad (5)$$

where: A = cross sectional area for the composite wall;

t_{br}, $t_{b\ell}$, t_{cj} = thickness of brick, block and collar joint wythes;

b = width of the composite wall;

T = total thickness of the composite wall;

F = total force carried by the wall;

$\sigma_{comp.}$ = stress for composite section;

$(E_j)_{comp.}$ = elastic modulus for composite wall; and

ε = strain.

Since the strain was assumed to be constant through thickness, and since plane sections through the thickness remain plane, then

$$\sigma_j = E_j \varepsilon$$

where j can be x, y or z direction.

For the study conducted, E_j was taken as the initial tangent modulus.

Equations 2 through 5 lead to

$$(E_j)_{comp.} = \frac{1}{T}\,[(E_j t)_{br} + (E_j t)_{b\ell} + (E_j t)_{cj}] \qquad (6)$$

The last equation is based on uniaxial stresses. In the general form, Equation 6 can be converted to the matrix format as follows:

$$[E_{comp.}] = \frac{1}{T}\,[t_{br}[E]_{br} + t_{b\ell}[E]_{b\ell} + t_{cj}[E]_{cj}] \qquad (7)$$

---

[1]Refer to the notation section given at the end of this paper.

The stiffness matrix of the composite wall was taken as the average of those values given in [10, 11], for walls 6-ft. high, 4-ft. wide and 9-in. thick. These matrices are given in the Appendix.

Mesh Size

Four sizes of mesh were used, i.e., 6, 24, 40 and 96 grid units. In addition to the masonry elements, the steel elements were treated as bar elements fixed at the bottom. The masonry elements were squares of the same size for all cases except for the mesh of 40 elements. The results obtained with these sizes were compared. The difference in results for the last three sizes proved negligible. The 40-element mesh was chosen as shown in Fig. 5.

Boundary Conditions

The wall was treated as a cantilever beam fixed at the base and free at the top. Since the wall was loaded with vertical and horizontal forces, the stress distribution at the base for the elastic stage is as shown in Fig. 6. The maximum tensile stresses due to the turning moment caused by the lateral load are at the base of the wall. The wall cracks when the tensile stress reaches a value greater than the ultimate value of the weakest element in the wall. The weakest element in tension is the mortar joint, so the wall was treated accordingly in two cases:

(1) Uncracked case: If the tensile stresses at the base were less than ultime tensile stresses for mortar, the wall was assumed uncracked. Therefore, the wall was analyzed by the finite element method, using boundary conditions as previously discussed.

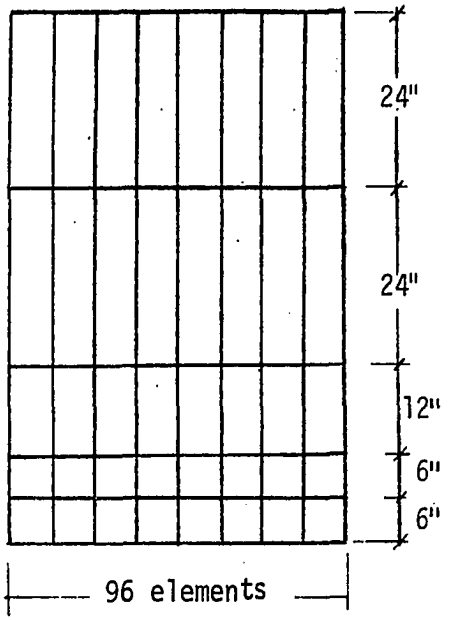

Figure 5. Mesh elements for composite wall

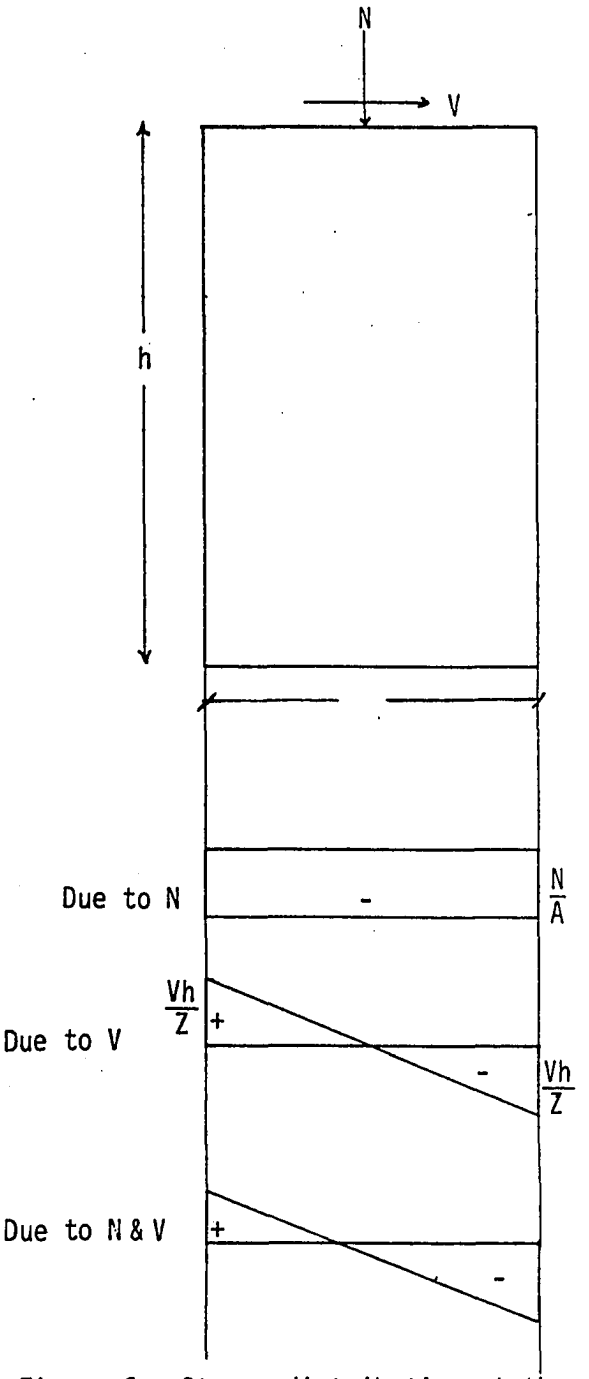

Figure 6. Stress distribution at the base of the wall

(2) Cracked case: Part of the cross section cracks, due to increase of tensile stress beyond the ultimate tensile capacity of the mortar. The cracked portion was freed at the base, keeping the remainder of the wall and the reinforcement as fixed. Stresses were then calculated for the uncracked section and compared with the ultimate tensile capacity to calculate the length of the cracked part. If the tensile stress exceeded the ultimate one established for the first element, the element was freed and considered as cracked. The stresses were then recalculated and the same procedure was repeated until the tensile stress in the next element was less than the ultimate one. For the reinforcement, ANSYS program has the capability of calculating the stresses for a nonlinear material with a specified plasticity ratio. The iterative procedure for obtaining this solution and the resulting plasticity ratio is illustrated in Fig. 7. Two plasticity ratios of 0.01 and 0.1 were compared, resulting in a difference of the maximum deflection of the wall of less than 0.5%. A plasticity ratio of 0.1 is selected.

An example of free nodes in one wall and the resulting shape distortion caused by lateral and vertical loads, see Figs. 8, 9 and 10. In the next horizontal load step, stresses were calculated on the basis of results from the previous cracked portion and the procedure was repeated.

Calculation of stresses

Constant strains at a point through the thickness were assumed for calculation purposes. The finite element output by ANSYS gives the stresses in the wall as one material. The strains were then calculated from these stresses. Next, the stresses in each wythe were calculated

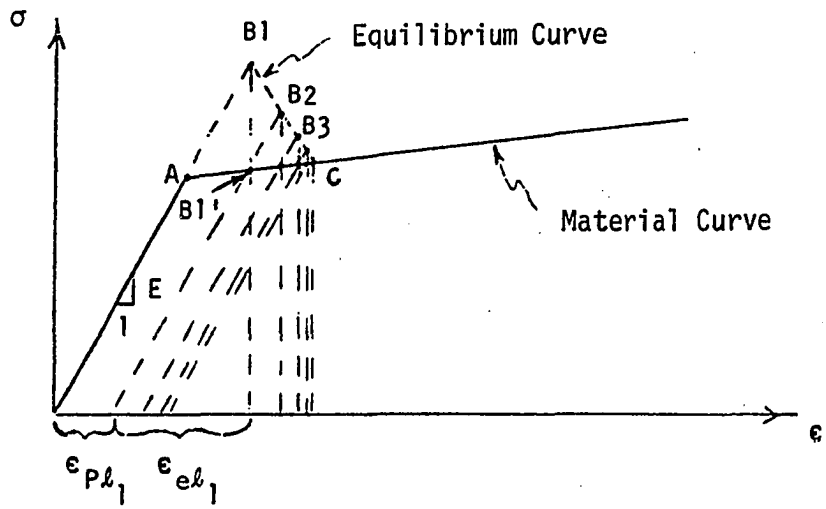

Figure 7. Plasticity convergence [9]

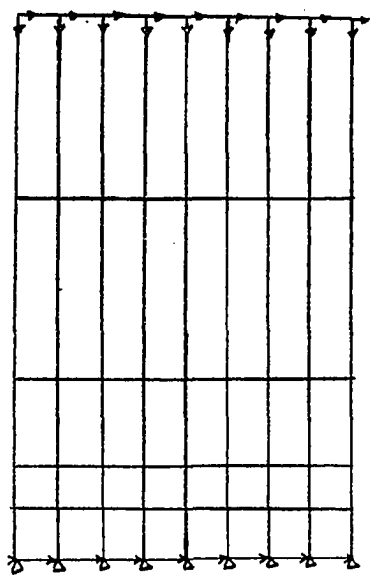

Figure 8. Composite wall with the boundary conditions (uncracked section)

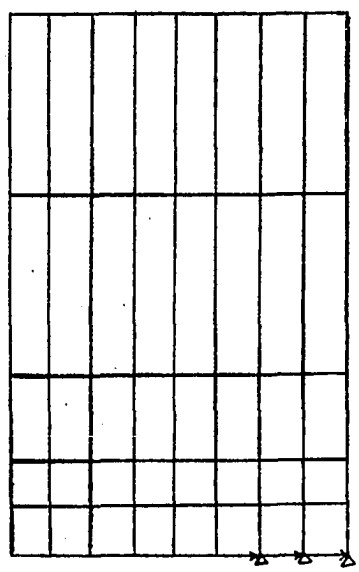

Figure 9. Cracked section for composite wall (6 free nodes)

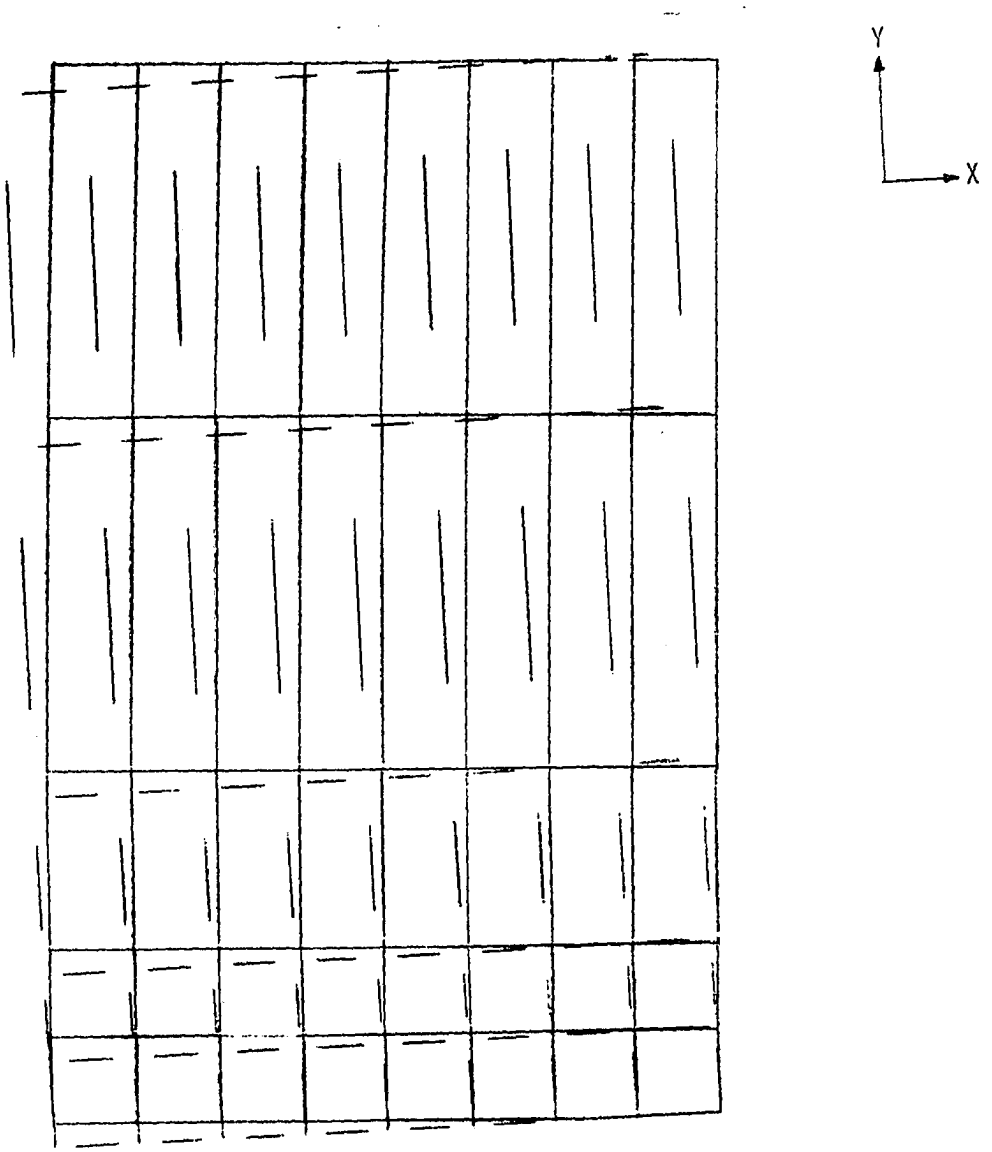

Figure 10. Distorted shape for composite wall with 7 free nodes

with another computer program (written by the author).

Tensile strength of mortar

The tensile strength of mortar varies with the direction of applied force. When a tensile load is applied normal to the bonded faces of the masonry, a strength value is developed. When a shear load is applied parallel to the bonded faces of the masonry, the second strength value is developed. The different parameters affecting tensile strength have been investigated by several experimental programs.

Davison [12] (1961) found that the bond strength between the mortar joint and the upper brick was less than that between the mortar joint and the lower brick. Benjamin and Williams [13] reported the results of compressive and tensile strength of the different mortars. Table 1 summarizes these values. The mortar used in tested composite walls [10, 11] was close to the one tested by Ditto, having properties of 1C:0.25L:3.5S, with compressive strengths of 2748, 2029, and 2341 psi and an overall average compressive strength of 2277 psi.

Table 1. Compressive and tensile strengths for different types of mortar [13]

Mortar properties by volume	28-day compressive strength (psi)	28-day tensile strength (psi)	Reference
1C:0.25FC:3S	3260	402	Stanford Shear wall project
1C:0.25L:3S	3050	300	Ditto
1C:0.50L;4.5S	1200	145	V.P.I. tests
1C:1L:6S	500	55	Ditto
1C:0.25L:3S	2500	225	Ditto

The mortar's ultimate tensile strengths for grouted units according to the ACI Code [14], using a safety factor of 3.5 [15], are as follows:

For loads normal to bed joint = 140 psi

For loads parallel to bed joint = 280 psi.

On the basis of the mesh used, the results of the cracked section will not be affected for a difference in ultimate tensile strength of 10-20%. Therefore, the values used in determining the cracked section were the code values, although these may be lower than actual ones.

DISCUSSION OF RESULTS

Load-Deflection Curve

The finite element method was used with procedures developed for cracked and uncracked wall sections to calculate the deflections of the different nodes. The results, based on the tested walls conducted in [10, 11], are shown in Figs. 11-16.

The walls contained in each figure (Figs. 11-16) were based on the same precompression load. Slight differences in other parameters, such as dimensions, reinforcement or ultimate strength, did not significantly affect the results. The first three figures (Figs. 11-13) compare the load-deflection curves as calculated by the finite element method to the experimental results for the brick-to-block walls. The other figures (Figs. 14-16) show the comparison between the finite element results and the experimental ones for the brick-to-brick walls. These figures indicate good agreement between the experimental load-deflection curves and those calculated by the finite element using the cracked-uncracked case concept for brick-to-block walls. Therefore, the finite element method with the cracked-uncracked case concept can be used to reasonably predict the load-deflection curve for the composite brick-to-block masonry walls. More investigation is needed for brick-to-brick walls.

Ultimate Shear Load

The ultimate shear load was assumed to correspond to an ultimate compression strain of 0.003 at highest point similar to the ultimate shear load for concrete [14, 15]. The strain corresponding to the

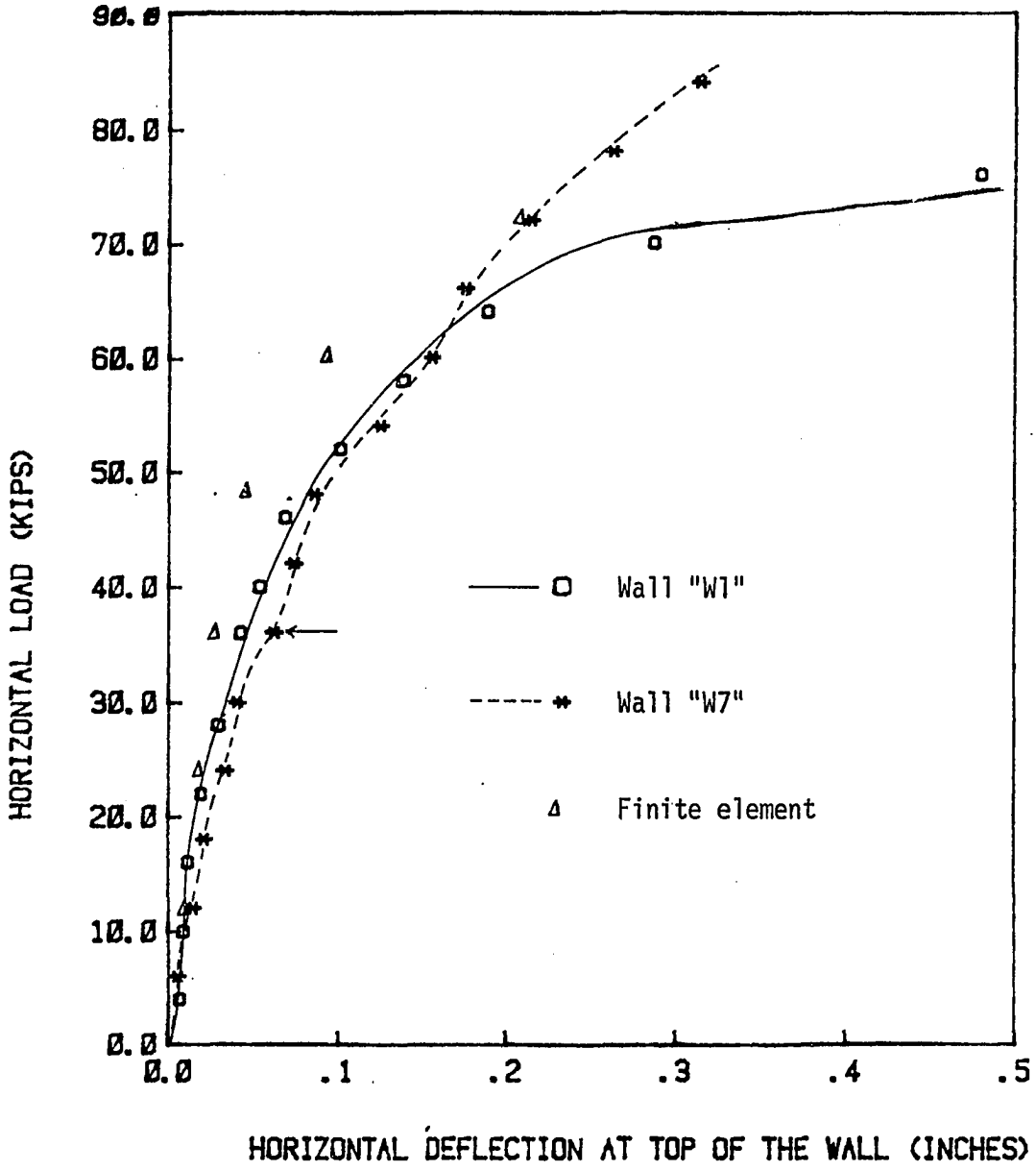

Figure 11. Load-deflection curve for brick-to-block walls "W1" and "W7"

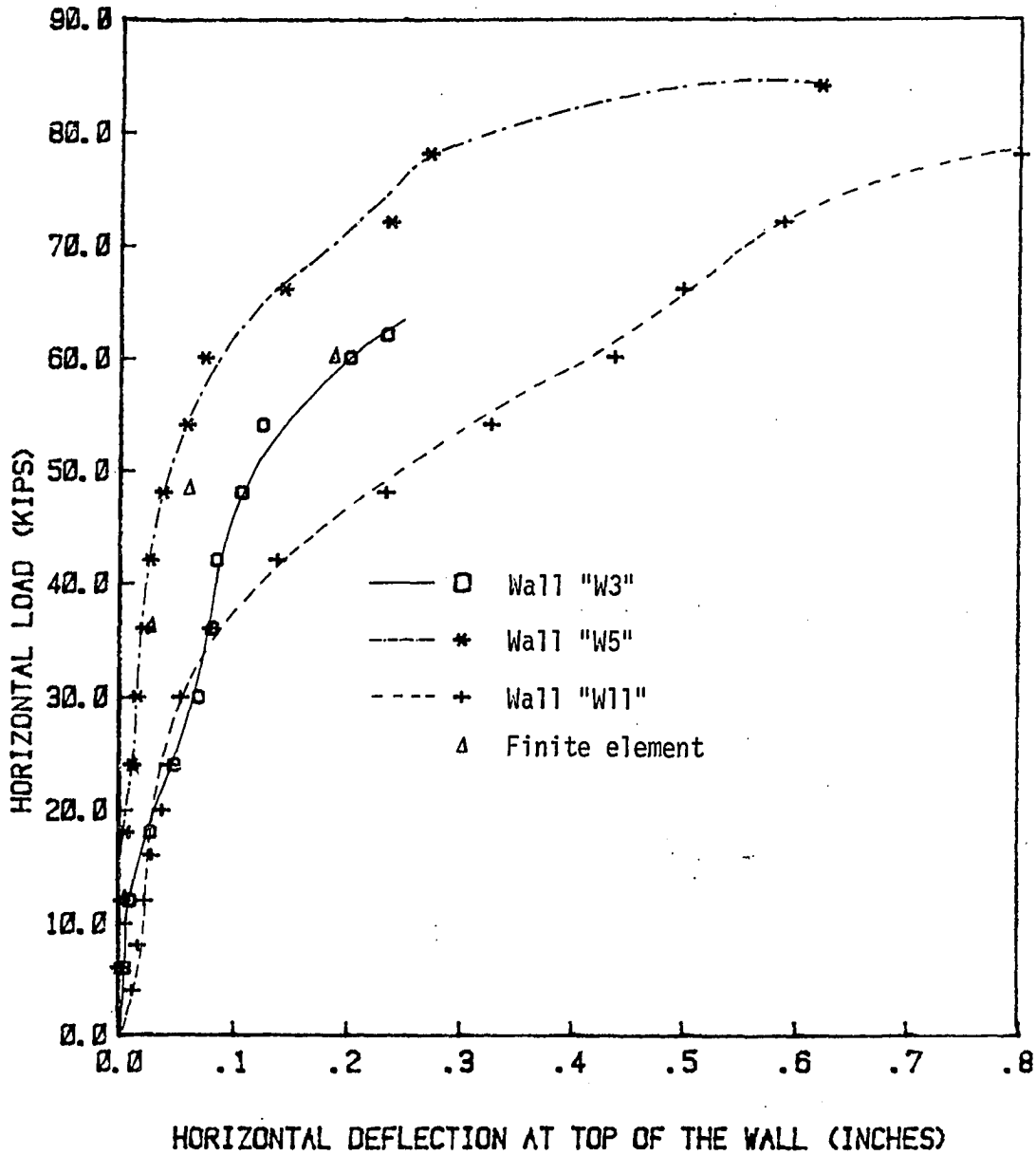

Figure 12. Load-deflection curve for brick-to-block walls "W3", "W5" and "W11"

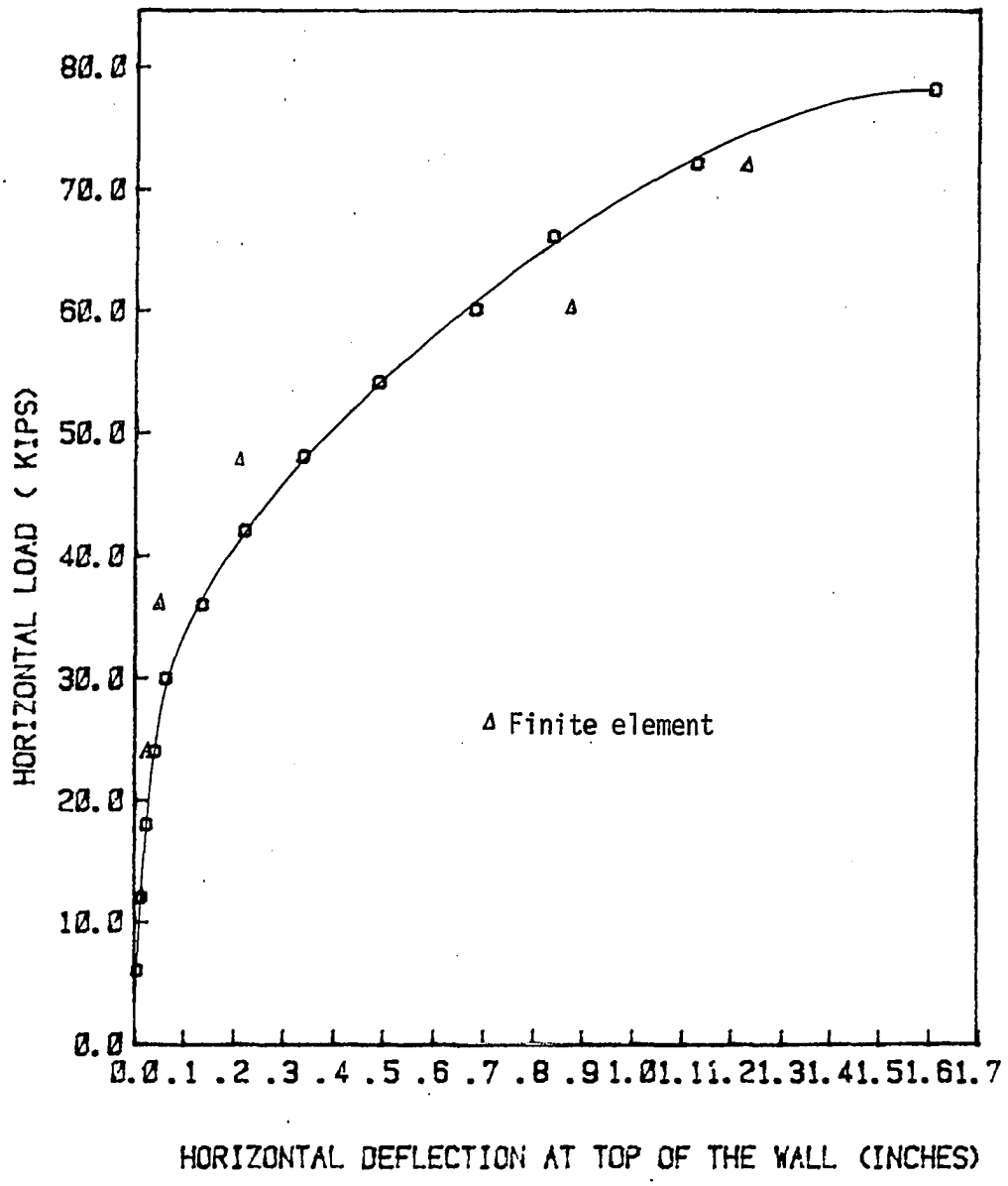

Figure 13. Load-deflection curve for brick-to-block wall "W9"

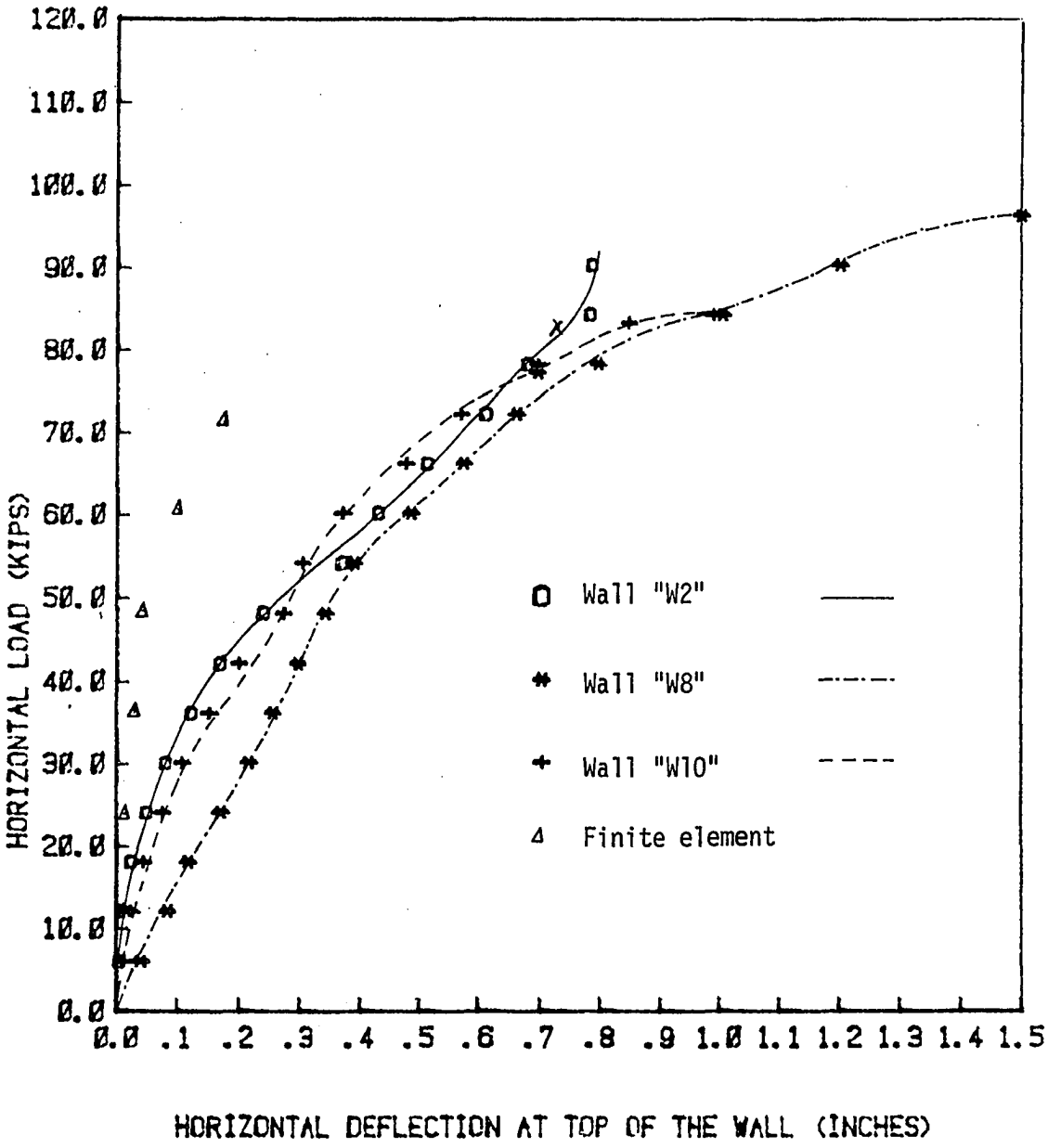

Figure 14. Load-deflection curve for brick-to-brick walls "W2", "W8" and "W10"

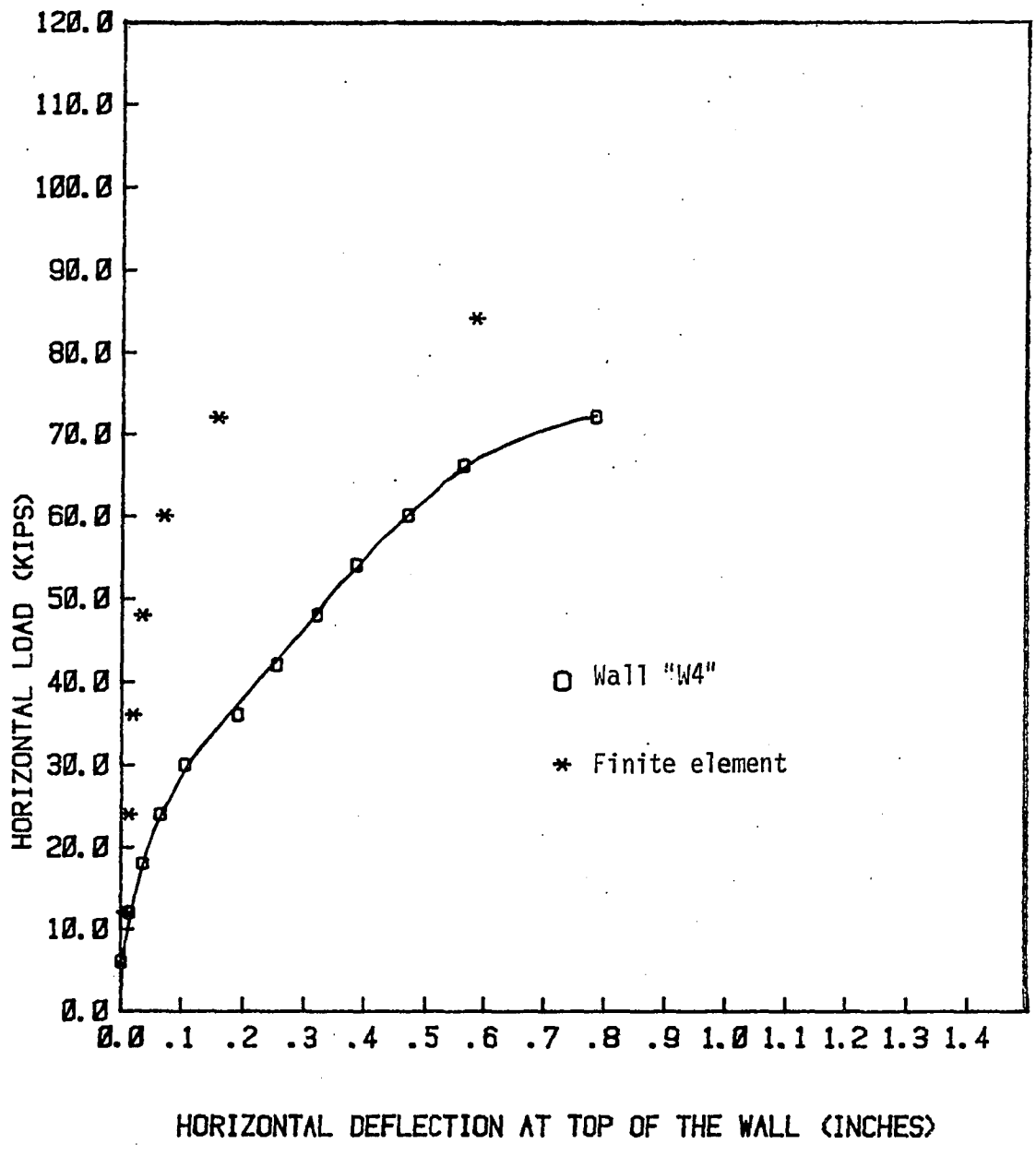

Figure 15. Load-deflection curve for brick-to-brick walls "W4"

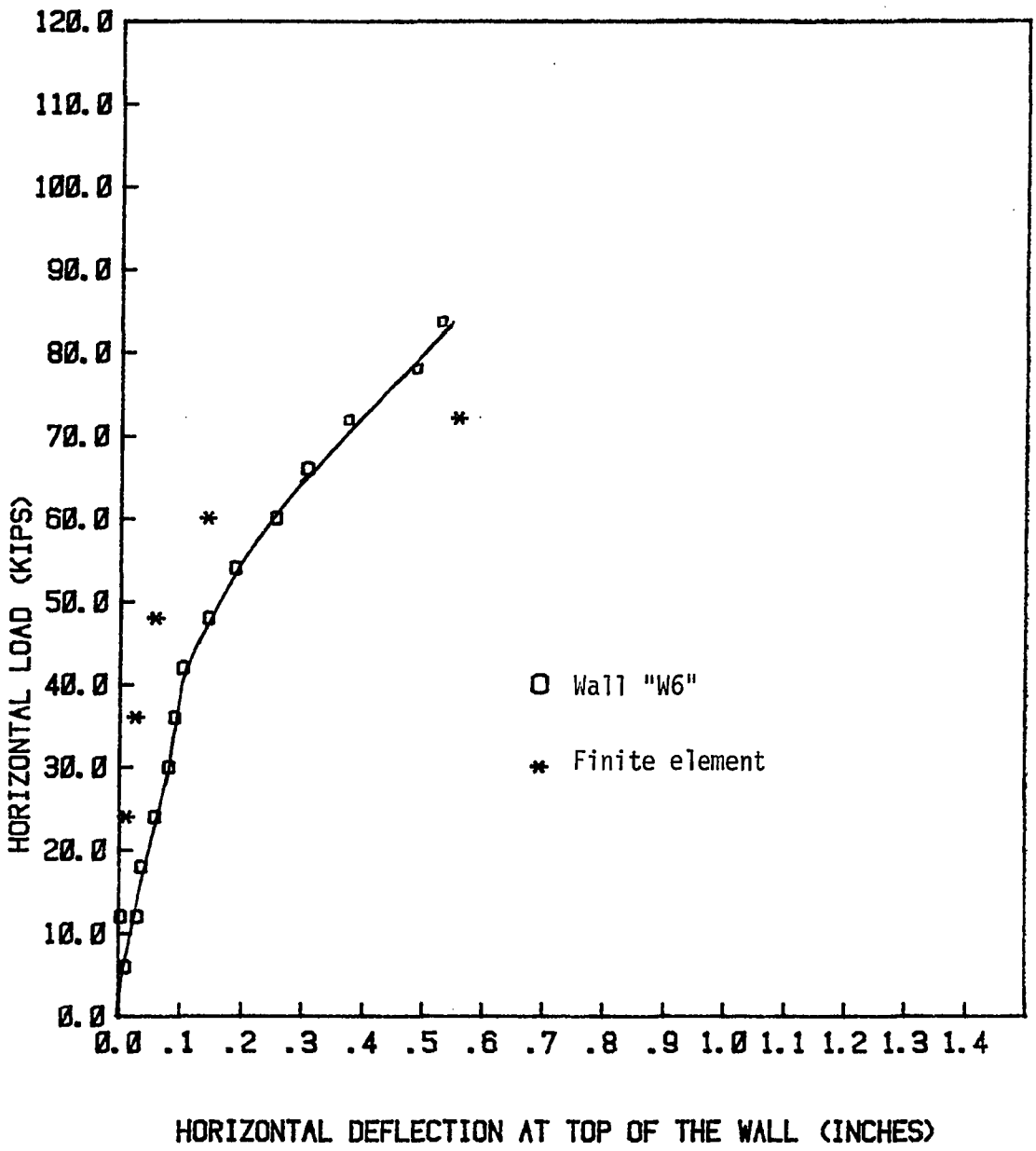

Figure 16. Load-deflection curve for brick-to-brick walls "W6"

ultimate stress of the individual masonry wythe was similar to the behavior of concrete [10, 11, 15]. Therefore, the ultimate strain was assumed to be 0.003, similar to concrete behavior. The stress-strain curves for a single wythe as given in [16, 17, 18] indicate that these curves are similar to concrete, which justifies this assumption. Table 2 shows a comparison of the ultimate shear load by both experiments and finite element method.

Table 2. Comparison between the estimated and measured ultimate shear loads

Brick-to-block walls			Brick-to-brick walls		
Wall No.	Measured V_u	Estimated V_u	Wall No.	Measured V_u	Estimated V_u
W1	76	96	W2	90	102
W3	64.2	96	W4	94.4	112
W5	89.5	96	W6	85.3	100
W7	90	96	W8	96	102
W9	78	83	W10	90	102

Strains on the tested composite walls were measured at different locations to assess the validity of the assumptions that "strain through thickness is constant." Fig. 17 shows examples of these results and indicates the horizontal strains due to the lateral loads in the three wythes (masonry and the grout). This figure indicates that horizontal strains do not vary significantly through thickness. The figure also shows the finite element results compared to the experimental. Both the experimental and the analytical results indicate the strain values to be small.

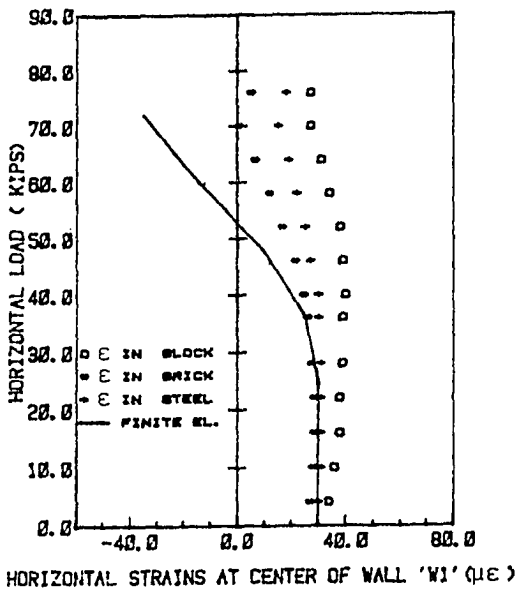

HORIZONTAL STRAINS AT CENTER OF WALL 'W1' (με)

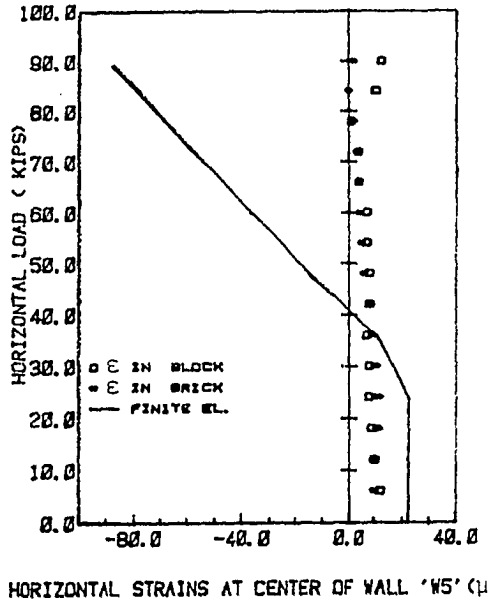

HORIZONTAL STRAINS AT CENTER OF WALL 'W5' (με)

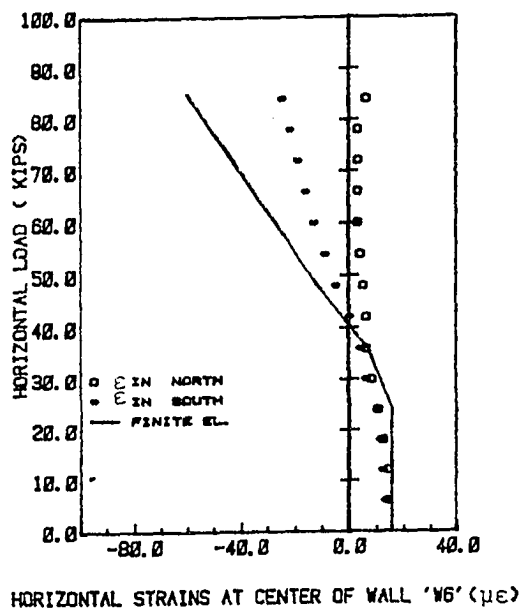

HORIZONTAL STRAINS AT CENTER OF WALL 'W6' (με)

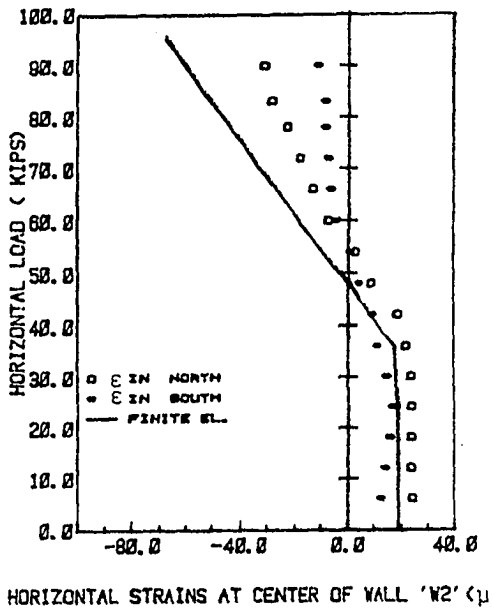

HORIZONTAL STRAINS AT CENTER OF WALL 'W2' (με)

Figure 17. Horizontal strains at center of walls

CONCLUSIONS AND RECOMMENDATIONS

The following conclusions can be made:

(1) The finite element technique with the cracked-uncracked case concept can be used to predict the shear capacity and load-deflection curve for composite brick-to-block walls.

(2) The ultimate shear load can be estimated approximately based on ultimate strains of 0.003 for composite masonry walls using the finite element technique with the cracked-uncracked case concept.

(3) Within the range of loads considered, the effect of the precompression load is not significant on either the load-deflection curve or on the ultimate shear load.

(4) For brick-to-brick walls, more investigation is needed to predict the load-deflection curve.

(5) The strain distribution for the walls validates the assumptions.

ACKNOWLEDGMENTS

The authors express their thanks to the Masonry Institute of Iowa and to the Masons Union of Iowa for providing material and labor for building the specimens. Thanks are also due to the Civil Engineering Department and Engineering Research Institute at Iowa State University. The assistance of Mr. Doug Wood is appreciated.

REFERENCES

1. L. Cerny and C. Baldridge. "Distribution of lateral forces in multistory masonry shear wall systems." TMS Journal, (July-December, 1981), T1-T11.

2. U. C. Kalita and A. W. Hendry. "An experimental and theoretical investigation of the stresses and deflection in model cross-wall structures." Proc. of the Second International Brick Masonry Conference, Stoke-on-Trent, England, (April 1970), 209-214.

3. A. W. Page. "Finite element model for masonry." Proc. ASCE, Journal of the Structural Division, ST-8-104, (August 1978), 1267-1285.

4. A. W. Page. "A non-linear analysis of the composite action of masonry walls." The Institution of Civil Engineers. Part 2, Research and Theory, v. 67, (March 1979), 93-110.

5. S. C. Anand and D. T. Young. "A finite element model for composite masonry." ASCE Convention Exposition, Florida, October, 1980.

6. S. C. Anand; D. T. Young and D. T. Stevens. "A model to predict shearing stresses between wythes in composite masonry walls due to differential movement." Proc. 2nd North American Masonry Conference, University of Maryland, College Park, Maryland, August, 1982.

7. O. C. Zeinkiewicz. "The finite element method." McGraw-Hill book company (UK) Limited, London, England, 1977.

8. R. H. Gallagher. "The finite element analysis fundamentals." Prentice-Hall, Inc., Englewood Cliffs, New Jersey, 1975.

9. Swanson Analysis System, Inc. "ANSYS engineering analysis system user's manual." Swanson Analysis System, Inc., Houston, Pennsylvania, 1981.

10. M. H. Ahmed; M. L. Porter and A. Wolde-Tinsae. "Behavior of reinforced brick-to-block walls." Part 2A of unpublished Ph.D. dissertation by M. H. Ahmed, Iowa State University, Ames, Iowa, 1983.

11. M. H. Ahmed; M. L. Porter and A. Wolde-Tinsae. "Behavior of reinforced brick-to-brick walls." Part 2B of unpublished Ph.D. dissertation by M. H. Ahmed, Iowa State University, Ames, Iowa, 1983.

12. J. I. Davison. "Loss of moisture from fresh mortars to bricks." ASTM Materials Research and Standards, ASTM 1, (5), 1961.

13. J. R. Benjamin and H. A. Williams. "The behavior of one-story brick shear walls." Proc. ASCE, Journal of the Structural Division, ST-4-84, (1958), 1723-1729.

14. American Concrete Institute. "Building code requirements for reinforced concrete." ACI Standard 318-77, Detroit, Michigan, 1977.

15. R. Park and T. Paulay. "Reinforced concrete structures." John Wiley & Sons Inc., New York, 1975.

16. R. Y. Yokel; R. G. Mathey and R. D. Dikkers. "Strength of masonry walls under compressive and transverse loads." NBS Building Science Series 34, Wasington, D.C., March, 1971.

17. V. Turnsek and F. Cacovic. "Some experimental results on the strength of brick masonry walls." Proc. of the Second International Brick Masonry Conference (SIBMAC Proc.), Stoke-on-Trent, England, April, 1970.

18. S. G. Fattal and L. E. Cattaneo. "Structural performance of masonry walls under compression and flexure." NBS Building Science Series 73, Washington, D.C., June, 1976.

NOTATIONS

A Cross sectional area for the composite wall.

b Width of the composite wall

E_j, $(E_j)_{comp}$ Elastic modulus of elasticity for the single wythe and the composite wall

$[E]_{br}$, $[E]_{b\ell}$ and $[E]_{cj}$ Stiffness matrices for brick, block and collar joint

$[E_{comp.}]$ Stiffness matrix for composite wall.

F Total force carried by the wall.

G Modulus of rigidity of the composite wall.

h Wall height.

I Moment of inertia about the strong axis.

j Direction of stress (x, y or z)

N Vertical precompression load.

t_{br}, $t_{b\ell}$ and t_{cj} Thickness of brick, block and collar joint wythes.

T Total thickness of composite wall.

V Lateral (in-plane) load.

Z Elastic section modulus for the composite wall.

Δ Horizontal deflection at the top of the wall.

ε Strain.

$\sigma_{comp.}$ Stress for the composite section.

APPENDIX. STIFFNESS MATRICES FOR THE COMPOSITE WALLS

Block-Brick Walls

For W1

$t_{b\ell} = 3.7"$, $t_{br} = 3.55"$, $t_{gr} = 1.85"$, $t = 9.1'$

$$[E] = 10^6 \begin{bmatrix} 2.451 & 0.5385 & 0 \\ 0.5385 & 2.795 & 0 \\ 0 & 0 & 1.07 \end{bmatrix}$$

$E_x = 2.347 \times 10^6$ psi

$E_y = 2.676 \times 10^6$ psi

$\nu_{xy} = 0.193$

$\nu_{yx} = 0.220$

$G_{xy} = 1.025$ psi

For W3

$t_{b\ell} = 3.7"$, $t_{br} = 3.55"$, $t_{gr} = 1.67"$, $t = 8.92"$

$$[E] = 10^6 \begin{bmatrix} 2.43 & 0.535 & 0 \\ 0.535 & 2.797 & 0 \\ 0 & 0 & 1.067 \end{bmatrix}$$

$E_x = 2.328 \times 10^6$ psi

$E_y = 2.679 \times 10^6$ psi

$\nu_{xy} = 0.191$

$\nu_{yx} = 0.220$

$G_{xy} = 1.022 \times 10^6$ psi

For W5

$t_{b\ell} = 3.7"$, $t_{br} = 3.55"$, $t_{gr} = 1.93"$, $t = 9.18"$

$$[E] = 10^6 \begin{bmatrix} 2.461 & 0.54 & 0 \\ 0.54 & 2.794 & 0 \\ 0 & 0 & 1.071 \end{bmatrix}$$

$E_x = 2.357 \times 10^6$ psi

$E_y = 2.676 \times 10^6$ psi

$\nu_{xy} = 0.193$

$\nu_{yx} = 0.219$

$G_{xy} = 1.026 \times 10^6$ psi

For W7

$t_{b\ell} = 3.7"$, $t_{br} = 3.55"$, $t_{gr} = 2.03"$, $t = 9.28"$

$$[E] = 10^6 \begin{bmatrix} 2.472 & 0.542 & 0 \\ 0.542 & 2.792 & 0 \\ 0 & 0 & 1.072 \end{bmatrix}$$

$E_x = 2.367 \times 10^6$ psi

$E_y = 2.673 \times 10^6$ psi

$\nu_{xy} = 0.194$

$\nu_{yx} = 0.219$

$G_{xy} = 1.026 \times 10^6$ psi

For W9

$t_{b\ell} = 3.7"$, $t_{br} = 3.55"$, $t_{gr} = 2.14"$, $t = 9.39"$

$$[E] = 10^6 \begin{bmatrix} 2.485 & 0.544 & 0 \\ 0.544 & 2.791 & 0 \\ 0 & 0 & 1.073 \end{bmatrix}$$

$E_x = 2.379 \times 10^6$ psi

$E_y = 2.672 \times 10^6$ psi

$\nu_{xy} = 0.195$

$\nu_{yx} = 0.219$

$G_{xy} = 1.027 \times 10^6$ psi

Brick-Brick Walls

For W2

$t_{br} = 3.55"$, $t_{gr} = 1.63"$, $t_{br} = 3.55"$, $t = 8.73$

$$[E] = 10^6 \begin{bmatrix} 3.146 & 0.654 & 0 \\ 0.654 & 3.825 & 0 \\ 0 & 0 & 1.479 \end{bmatrix}$$

$E_x = 3.034 \times 10^6$ psi

$E_y = 3.689 \times 10^6$ psi

$\nu_{xy} = 0.171$

$\nu_{yx} = 0.208$

$G_{xy} = 1.426 \times 10^6$ psi

For W4

$t_{br} = 3.55"$, $t_{gr} = 1.84"$, $t_{br} = 3.55"$, $t = 8.94"$

$$[E] = 10^6 \begin{bmatrix} 3.155 & 0.655 & 0 \\ 0.655 & 3.798 & 0 \\ 0 & 0 & 1.472 \end{bmatrix}$$

$E_x = 3.042 \times 10^6$ psi

$E_y = 3.662 \times 10^6$ psi

$\nu_{xy} = 0.172$

$\nu_{yx} = 0.208$

$G_{xy} = 1.419 \times 10^6$ psi

For W6

$t_{br} = 3.55"$, $t_{gr} = 2.03"$, $t_{br} = 3.55"$, $t = 9.1"$

$$[E] = 10^6 \begin{bmatrix} 3.162 & 0.656 & 0 \\ 0.656 & 3.778 & 0 \\ 0 & 0 & 1.467 \end{bmatrix}$$

$E_x = 3.048 \times 10^6$ psi

$E_y = 3.642 \times 10^6$ psi

$\nu_{xy} = 0.174$

$\nu_{yx} = 0.207$

$G_{xy} = 1.414 \times 10_6$

For W8

$t_{br} = 3.55"$, $t_{gr} = 2.35"$, $t_{br} = 3.55"$, $t = 9.45"$

$$[E] = 10^6 \begin{bmatrix} 3.176 & 0.658 & 0 \\ 0.658 & 3.737 & 0 \\ 0 & 0 & 1.456 \end{bmatrix}$$

$E_x = 3.060 \times 10^6$ psi

$E_y = 3.601 \times 10^6$ psi

$\nu_{xy} = 0.176$

$\nu_{yx} = 0.207$

$G_{xy} = 1.403 \times 10^6$ psi

For W10

$t_{br} = 3.55"$, $t_{gr} = 1.98"$, $t_{br} = 3.55"$, $t = 9.08"$

$$[E] = 10^6 \begin{bmatrix} 3.161 & 0.656 & 0 \\ 0.656 & 3.78 & 0 \\ 0 & 0 & 1.468 \end{bmatrix}$$

$E_x = 3.047 \times 10^6$ psi

$E_y = 3.643 \times 10^6$ psi

$\nu_{xy} = 0.174$

$\nu_{yx} = 0.208$

$G_{xy} = 1.415 \times 10^6$ psi

For W11

t_b = 3.7" , t_{br} = 3.55" , no grout , t = 9.45"

$$[E] = 10^6 \begin{bmatrix} 2.174 & 0.496 & 0 \\ 0.496 & 2.826 & 0 \\ 0 & 0 & 1.041 \end{bmatrix}$$

$E_x = 2.087 \times 10^6$ psi

$E_y = 2.713 \times 10^6$ psi

$\nu_{xy} = 0.176$

$\nu_{yx} = 0.228$

$G_{xy} = 0.999 \times 10^6$ psi

PART 4. ANALYSIS OF COMPOSITE MASONRY WALLS: PART II

Analysis of composite masonry walls: Part II

M. H. Ahmed, Graduate Research Assistant
M. L. Porter, Professor
A. Wolde-Tinsae, Associate Professor

From the Department of Civil Engineering, Iowa State University, Ames, IA 50011

ABSTRACT

The results of tests on eleven composite masonry walls are compared with three different methods of analysis and discussed herein. The walls were each two wythes, of either brick-to-brick or brick-to-block, with a 2-in. reinforced collar joint. The analytic methods employed were the theory for flexural strength, the finite element technique with the cracked/uncracked walls concept, and the ACI and UBC Code values. A proposed equation based on the theory for flexural strength is discussed herein.

INTRODUCTION

Design and analysis of reinforced masonry as recognized by the ACI or UBC Codes is based on the theory of working stress design. Other methods, such as the theory for flexural strength or the limit design, have been recognized for reinforced concrete. This study investigates the availability of using the theory for flexural strength and the finite element technique for reinforced composite masonry walls.

THEORETICAL ANALYSIS

Introduction

Three different methods of analysis are discussed. These methods are based on the theory of working stress design, the theory for flexural strength, and the finite element method.

Working Stress Design

Based on the well-known working stress design [1] and analyzing the masonry shear wall as a cantilever beam, fixed at the base and free at the top, the horizontal deflection measured at the top of the wall due to in-plane loads is calculated by equation [2]

$$\Delta^{1} = \frac{Vh^3}{3EI} + \frac{1.2\ Vh}{AG} \qquad (1)$$

where Δ = the measured deflection from the straight-line portion of the experimental load-deflection curve;

V = the lateral (in-plane) force;

h = the height of the wall;

E = the elastic stiffness of the wall cross section;

A = the cross sectional area for the wall;

G = the modulus of rigidity; and

I = moment of inertia of wall cross section.

This equation can be applied only if the wall is in the elastic range and has no cracks. The allowable shear strength of the masonry shear wall according to the UBC Code [2] is based on the ultimate compressive strength, f'_m, for masonry, as follows:

[1]Refer to the notations section given at the end of the paper.

$$f_v = 1.5\sqrt{f'_m} \leq 75 \text{ psi} \qquad \text{for } h/b \geq 1 \tag{2}$$

$$f_v = (2\text{-}0.5\ h/b)\ \sqrt{f'_m} \leq 150 \text{ psi} \qquad \text{for } 0 \leq h/b \leq 1 \tag{3}$$

The allowable shear load, V_{all}, can be calculated as

$$V_{all} = \text{Actual gross area} \times f_v \tag{4}$$

Theory for Flexural Design

Shear wall equation

The shear wall equation [3, 4] was calculated in accordance with ACI Code [5] specifications for a rectangular shear wall subjected to combined axial load, bending and shear. The equation is:

$$M_u = A_s f_y b \left[(1 + \frac{N_u}{A_s f_y})(\tfrac{1}{2} - \frac{\beta_1 c}{2b}) - \frac{c^2}{b^2}(1 + \frac{\beta^2}{3} - \beta_1)\right] \tag{5}$$

where: $\frac{c}{b} = \frac{A_s f_y + N_u}{2A_s f_y + 0.85\beta_1 b t f'_m}$

$\beta = \frac{f_y}{8700}$

Using the simplified equation with $\beta_1 = 0.85$:

$$M_u = 0.5\ A_s f_y b(1 + \frac{N_u}{A_s f_y})(1 - \frac{c}{b}) \tag{6}$$

Since the shear wall is considered as a cantilever beam, then

$$M_u = h \cdot V_u \tag{7}$$

Table 1 shows the dimensions and the ultimate strengths for the composite masonry walls tested [6, 7]. These walls were two-wythe walls with a 2-inch reinforced collar joint. Five of these walls were brick-to-block walls designated as W1, W3, W5, W7 and W9. The other walls were loaded with in-plane loads, in addition to vertical pre-compression loads. Table 2 shows the ultimate shear force as given in

Table 1. Dimensions and ultimate strengths for composite masonry walls [6, 7]

Wall designation	Average dimension b in.	t in.	h in.	A_{s_2} in.^{2}	f'_m psi	N_u kips	V_u kips
			Brick-to-block				
W1	47.6	9.10	72.2	0.48	1680	178	76
W3	47.8	8.92	74.1	0.48	2365	146	64.2
W5	47.7	9.18	72.7	0.48	2170	135	89.5
W7	47.9	9.28	72.4	0.48	1816	178	90
W9	47.7	9.39	71.6	0.51	1722	118	78
			Brick-to-brick				
W2	48.5	8.73	72.1	0.48	3020	160	90
W4	47.7	8.94	72.1	0.48	2890	180	94.4
W6	47.5	9.13	72.3	0.48	2452	135	85.3
W8	47.5	9.45	71.6	0.51	2088	157	96
W10	47.6	9.08	71.8	0.51	2136	157	90

Table 2. Comparison between the shear forces calculated by Equations 6 and 7 and the ones measured for composite walls

Wall designation	Eq. 7 V_{uc}	V_{um}	V_{um}/V_{uc}	Wall designation	Eq. 7 V_{uc}	V_{um}	V_{um}/V_{uc}
W1	44.4	76	1.71	W2	51.8	90	1.74
W3	44.4	64.2	1.45	W4	54.4	94.4	1.74
W5	42.4	89.5	2.11	W6	43.7	85.3	1.95
W7	46.8	90	1.92	W8	46.4	96	2.07
W9	37.6	78	2.07	W10	46.2	90	1.95

Table 1, with the ultimate shear forces calculated from Equations 6 and 7. This comparison shows that the shear wall equation values are much lower than measured ones. Ignoring the results of "W3" due to the misuse of this wall before testing [6], the comparisons in Table 1 indicate that the actual ultimate shear loads were higher than the calculated ones by an average value of 1.95 for brick-to-block walls and 1.89 for brick-to-brick walls.

Proposed equation for masonry walls

The following assumptions were made to calculate the ultimate shear load for composite masonry walls:

(a) a plane section before bending remains plane after bending [8];

(b) the tensile strength of masonry may be neglected [8];

(c) the ultimate strain for composite masonry is 0.003;

(d) the masonry reaches its ultimate strain before yielding of the tension steel;

(e) the concept of equivalent rectangular stresses is applied; and

(f) vertical reinforcement is equally distributed along the entire section.

Fig. 1 shows the strain and stress distribution for the wall cross section. From the figure, the tensile force carried by the ith steel is

$$T_i^1 = A_{si} E \varepsilon_{ti} \tag{8}$$

$$T_i = A_{si} E \frac{d_i}{K_u b} \varepsilon_u \tag{9}$$

---

[1] See notations at the end of this paper.

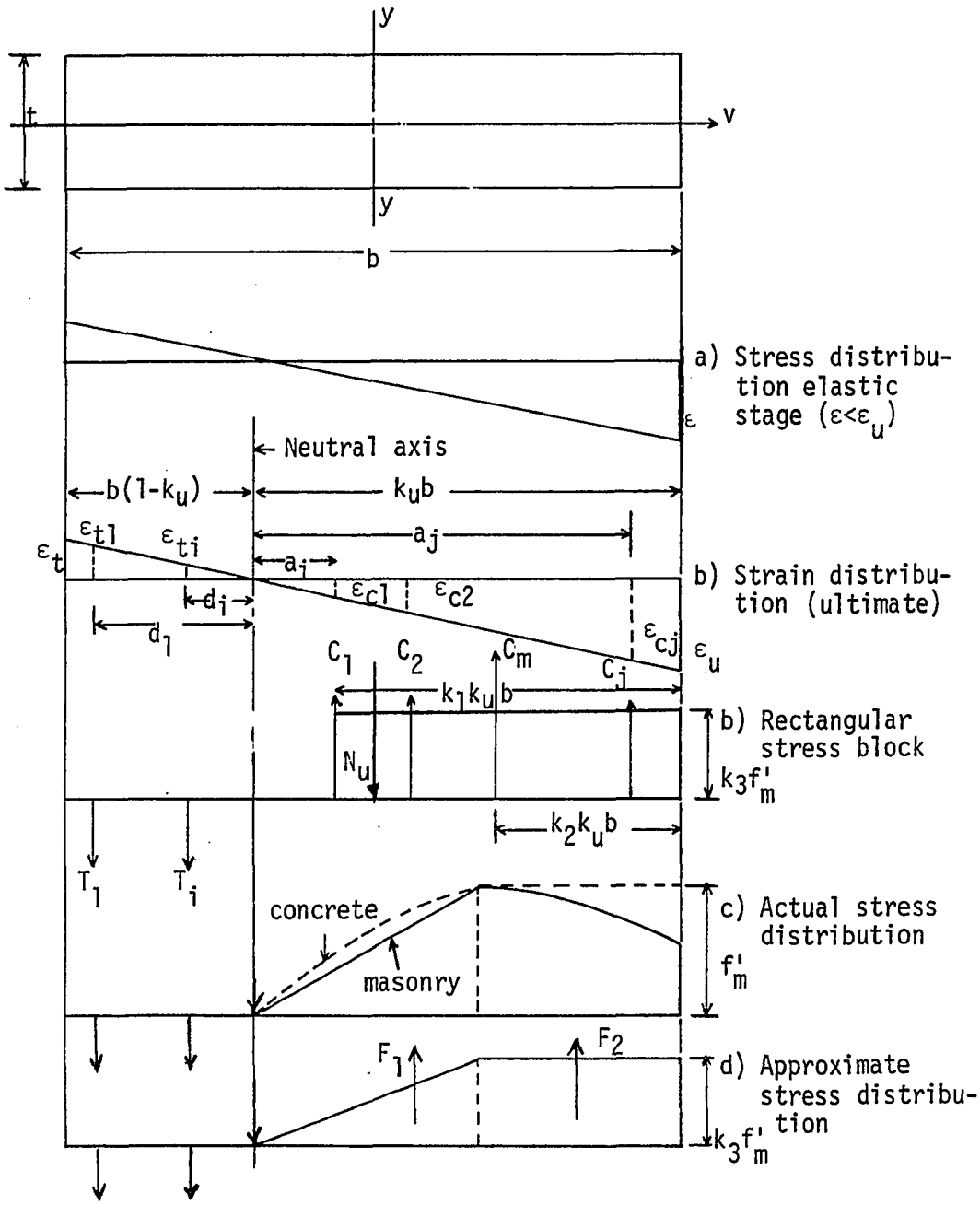

Figure 1. Strain and stress distribution for the wall cross section

Similarly,

$$C_j = A_{sj} E \frac{a_j}{K_u b} \varepsilon_u \tag{10}$$

where:

T_i = tensile force carried by steel at point i;

A_{si}, A_{sj} = area of steel at points i and j;

E = elastic modulus of the composie wall;

ε_{ti} = strains at point i;

d_i = distance of point i from the neutral axis;

K_u = contact;

b = wall width;

ε_u = ultimate strain in masonry;

C_j = compressive force carried by steel at point j; and

a_j = distance of point j from the neutral axis.

Total tensile force $T = \sum T_i$

$$= \frac{A_{si} E \varepsilon_u}{K_u b} \sum d_i$$

Since i = number of tensile forces each carried by A_{si}

$$\sum d_i \simeq i \frac{b}{2} (1 - K_u) \quad \text{and} \quad i A_{si} = A_s^t$$

$$T = \frac{A_s^t E \varepsilon_u}{2K_u} (1 - K_u) \tag{11}$$

Similarly,

$$C = \frac{A_s^c E \varepsilon_u}{2} \tag{12}$$

where:

A_s^t = area of steel in tension;

A_s^c = area of steel in compression;

T = total tensile force carried by steel; and

C = total compressive force carried by steel.

The compressive force carried by masonry, based on the equivalent rectangular stresses (see Fig. 1) is:

$$C_m = K_1 K_u K_3 f'_m bt \tag{13}$$

where:

C_m = total compressive force carried by masonry;

K_1, K_u, K_3 = constants;

f'_m = compressive strength of masonry; and

t = wall thickness.

Taking moments about the extreme fiber in the tensile part of the cross section yields:

$$T\frac{b}{3}(1 - K_u) + N_u\frac{b}{2} - C(b - \frac{K_u b}{3}) - C_m(b - K_2 K_u b) + M_u = 0 \tag{14}$$

The tensile force in Equation 14 was assumed to be distributed (i.e., the distribution of the tensile forces is triangle) or substitute Equations 11, 12 and 13 in Equation 14

$$M_u = \frac{A_s^c E\varepsilon_u b}{2}(1 - \frac{K_u}{3}) + K_1 K_3 K_u b^2 t f'_m(1 - K_2 K_u) - \frac{A_s^t E\varepsilon_u b}{6K_u}(1 - K_u)^2 - \frac{N_u b}{2}$$

But $A_s^t \simeq A_s \frac{b(1 - K_u)}{b} = A_s(1 - K_u)$

and $A_s^c \simeq K_u A_s$

$$M_u = \frac{A_s E\varepsilon_u b}{2}(K_u - \frac{K_u^2}{3}) - \frac{A_s E\varepsilon_u b}{6\,K_u}(1 - K_u)^3 + K_1 K_3 K_u b^2 t f'_m - \frac{N_u b}{2}$$

$$M_u = K_1 K_3 K_u b^2 t f'_m - \frac{A_s E\varepsilon_u b}{12\,K_u}(2 - 12K_u + 8K_u^2 + 2K_u^3) - \frac{N_u b}{2} \tag{15}$$

But $M_u = V_u h$

$$V_u = \frac{1}{h}[K_1 K_3 K_u b^2 t f'_m - \frac{A_s E_u b}{6 K_u}(1 - 6K_u + 4K_u^2 + K_u^3) - \frac{N_u b}{2}] \qquad (16)$$

The ultimate shear force can be calculated using Equation 16 after determining the constants K_1, K_2, K_3, and K_u.

Evaluation of constants (1) The constant "K_u", which determines the location of the neutral axis, can be calculated from the elastic stage (Fig. 1-a) as follows:

$$\frac{K_u b}{b} = (\frac{N_u}{A} + \frac{V_u h}{Z})/2 \; \frac{V_u h}{Z}$$

$$K_u = 0.5 + \frac{N_u h}{2 V_u A h} \qquad (17)$$

where Z is the elastic section modulus.

For a rectangular wall cross section,

$$K_u = 0.5 + \frac{N_u b}{12 V_u h} \qquad (18)$$

For composite masonry walls on the basis of the values in Table 1,

$$K_u = 0.5 + 0.0555 \frac{N_u}{V_u} \qquad (19)$$

For the range of precompression used in the tested walls [6, 7], and based on Equation 19, the value of K_u can be taken as 0.6.

(2) The constant "K_2" determines the location of the compressive force. Based on the stress-strain curve for one wythe [6, 7], the following approximation can be made: The ultimate compressive strength occurred at a strain of 0.00175 (the ultimate strain is 0.003); for simplicity, the stress distribution is assumed to be as shown in Fig. 1-d

$$F_1 = \tfrac{1}{2} \frac{\varepsilon_c}{\varepsilon_u} K_u b \; K_3 f'_m t$$

$$F_1 = 0.292 \; K_u b K_3 t f'_m$$

$$F_2 = K_3 f'_m \left(1 - \frac{\varepsilon_c}{\varepsilon_u}\right) K_u b t$$

$$= 0.42\ K_u b K_3 t f'_m$$

Taking moments for the compressive force only about the neutral axis yields:

$$(F_1 + F_2)(K_u b - K_2 K_u b) = F_1(0.389\ K_u b) + F_2(0.792\ K_u b)$$

$$1 - K_2 = 0.63$$

$$K_2 = 0.37$$

and

$$K_1 = 0.292 + 0.42 = 0.712$$

The actual value of "K_2" should be greater than the calculated one, due to the approximation made in the stress distribution (Fig. 1-d). The value of "K_2" for concrete is equal to 0.5 β_1. If β_1 is equal to 0.85, then

$$K_2 = 0.425 \qquad (20)$$

Since the last value is slightly higher than the calculated one, and probably more accurate, Equation 20 can be used.

(3) The constants K_1 and K_3 determine the compressive force carried by masonry. Table 3, using Equation 16 and the measured ultimate shear loads [6, 7] to evaluate the contant "K_1K_3", shows the different values of K_1K_3.

Fig. 2 shows the relationship between the constant "K_1K_3" and the value N_u/Af'_m. The figure indicates that:

Table 3. Values for the constant "K_1K_3"

Wall	W1	W3	W5	W7	W9	W2	W4	W6	W8	W10
K_1K_3	0.6568	0.404	0.502	0.65	0.5396	0.3905	0.4394	0.4349	0.5566	0.543

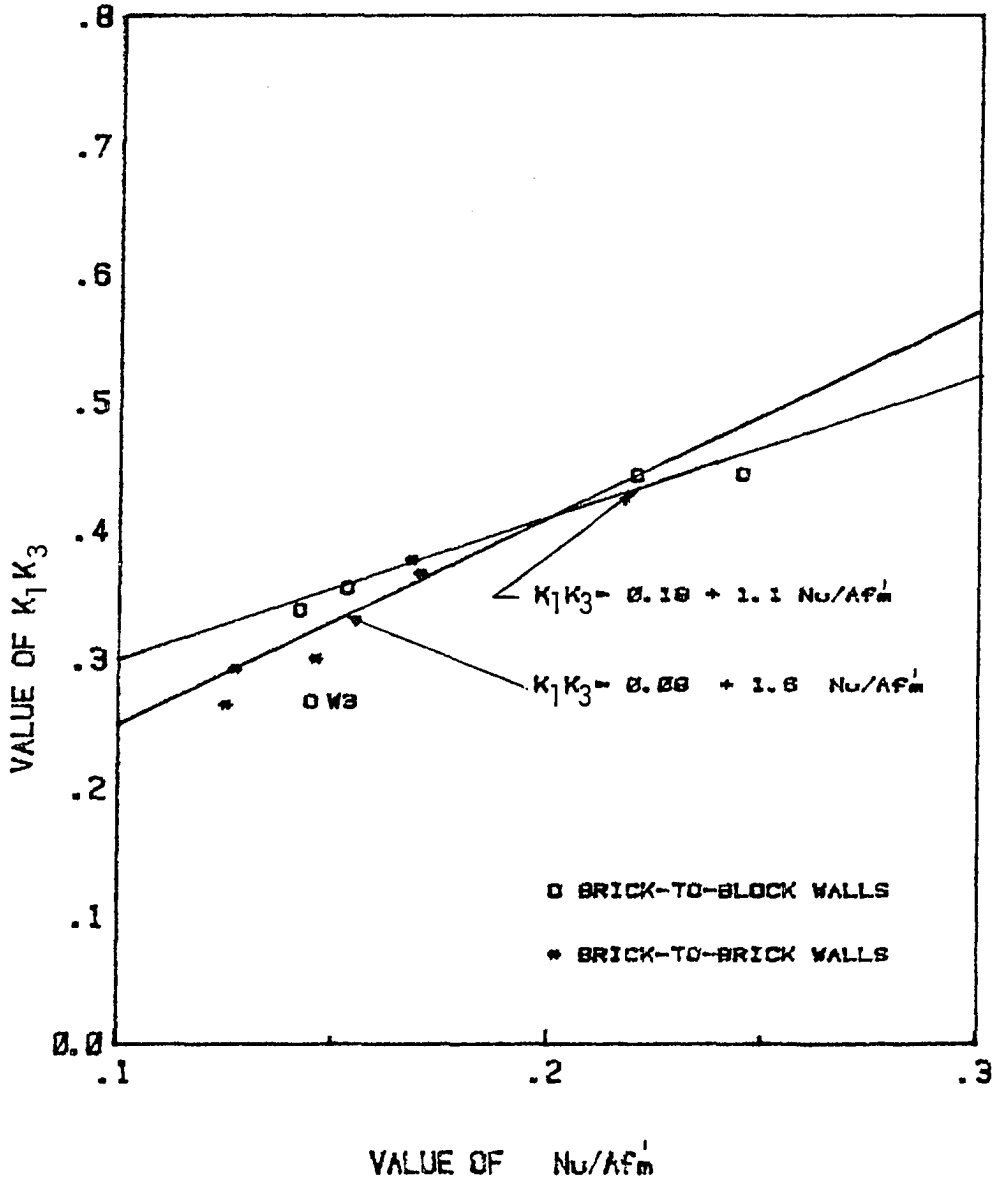

Figure 2. The relationship between "K_1K_3" and N_u/Af'_m

For brick-to-block walls, $K_1K_3 = 0.19 + 1.1 \frac{N_u}{Af'_m}$ (21)

For brick-to-brick walls, $K_1K_3 = 0.09 + 1.6 \frac{N_u}{Af'_m}$ (22)

Based on the following values of the constants:

$K_u = 0.6$

$K_2 = 0.425$

$E = 29{,}000$ ksi

$\varepsilon_u = 0.003$

K_1K_3 = as given in Equations 21 and 22,

Equation 16 can be written as

Brick-to-block walls: $V_u = \frac{1}{h}[0.114\ b^2tf'_m + 22.81\ A_sb + 0.16\ N_ub]$ (23)

Brick-to-brick walls: $V_u = \frac{1}{h}[0.054\ b^2tf'_m + 22.81\ A_sb + 0.46\ N_ub]$ (24)

where N_u, V_u and f'_m in these equations have to be in kips.

Table 4 shows the ultimate shear loads calculated by Equations 23 and 24 and compares them to the experimental ones. The table indicates good agreement between theoretical and experimental loads.

Table 4. Comparison between Equations 23 or 24 and the experimental ultimate shear loads

Brick-to-block walls				Brick-to-brick walls			
Wall No.	Measured V_u kips	Calculated V_u Eq. 23 kips	Percentage difference	Wall No.	Measured V_u kips	Calculated V_u Eq. 24 kips	Percentage difference
W1	76	80.7	6.2	W2	90	103.3	14.8
W3	64.2	96.3	5.0	W4	94.4	106	12.3
W5	89.5	92.4	3.2	W6	85.3	85.7	0.5
W7	90	87	-3.3	W8	96	89.2	-7.1
W9	78	78.9	1.2	W10	90	88.6	-1.6

Load-Deflection Curve

The load-deflection curve for composite masonry walls can be as trilinear curve [6, 7]. The trilinear curve represents three stages, as follows:

(1) The first stage is the elastic, or uncracked case. The deflection is calculated in this stage using the simple equation of

$$\Delta = \frac{Ph^3}{3EI} + \frac{Ph}{AG} \qquad (1)$$

(2) The second stage is the cracked case, represented by the second portion of the curve. The deflections in this portion were calculated using the cracked section concept assuming that the effective area of the masonry is the uncracked one.

(3) The third stage is the ultimate shear load and can be calculated either using the finite element [9] or using Equation 23 or 24.

Figs. 3 and 4 show the proposed trilinear curve for the masonry walls. Fig. 3 shows this cruve for the brick-to-block walls. The deflections were calculated for the different precompression loads and indicated no significant difference in the results, as shown in Fig. 3. Fig. 4 shows the proposed load-deflection curve for brick-to-brick walls and shows the calculated deflections for different values of precompression.

Figs. 5 through 9 show a comparison between the proposed curve and the experimental results for the composite walls [6, 7]. The figures indicate the following:

(1) The proposed load-deflection curve reasonably represents the actual behavior for the brick-to-block walls.

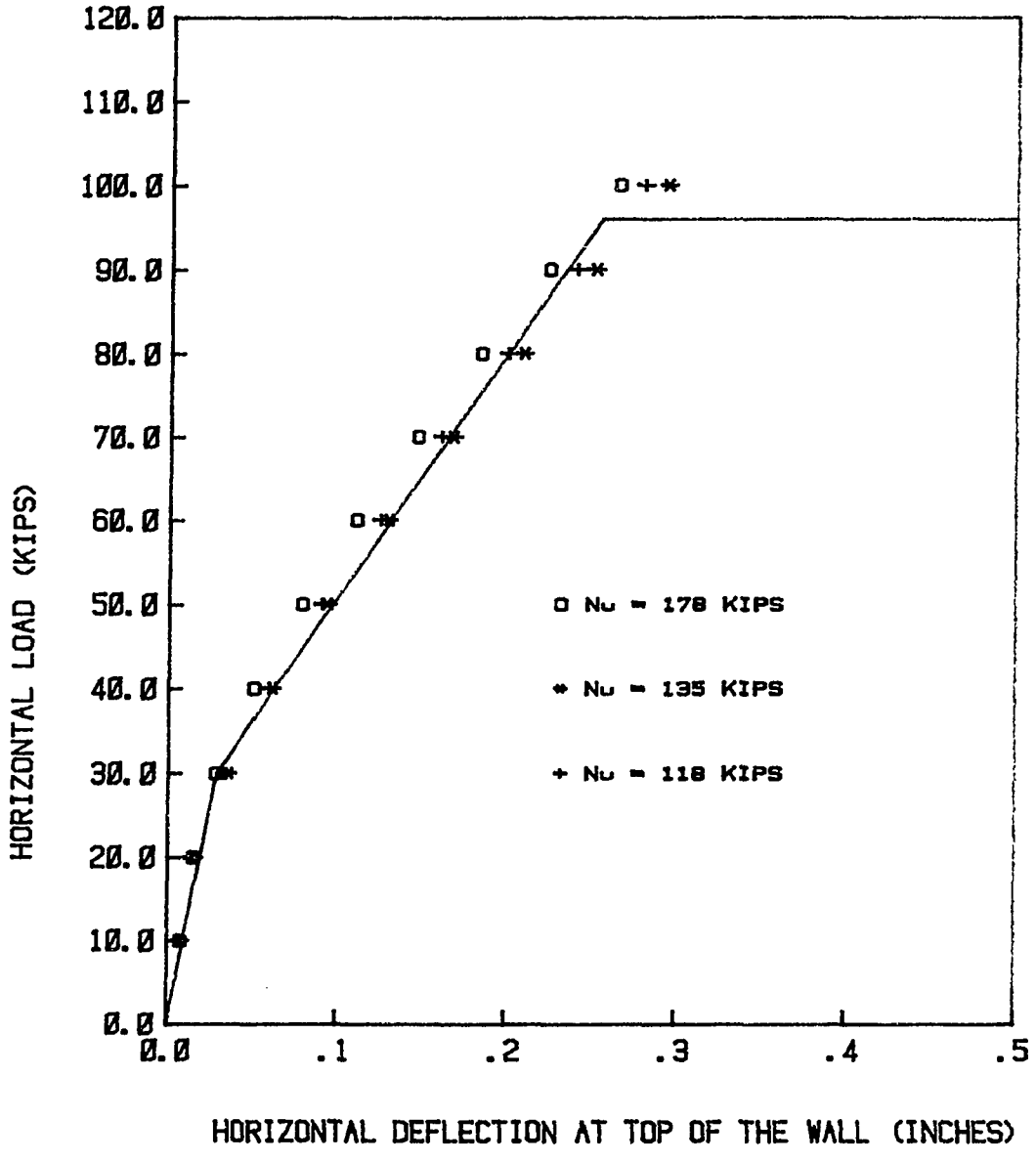

Figure 3. Proposed load-deflection curve for brick-to-block walls

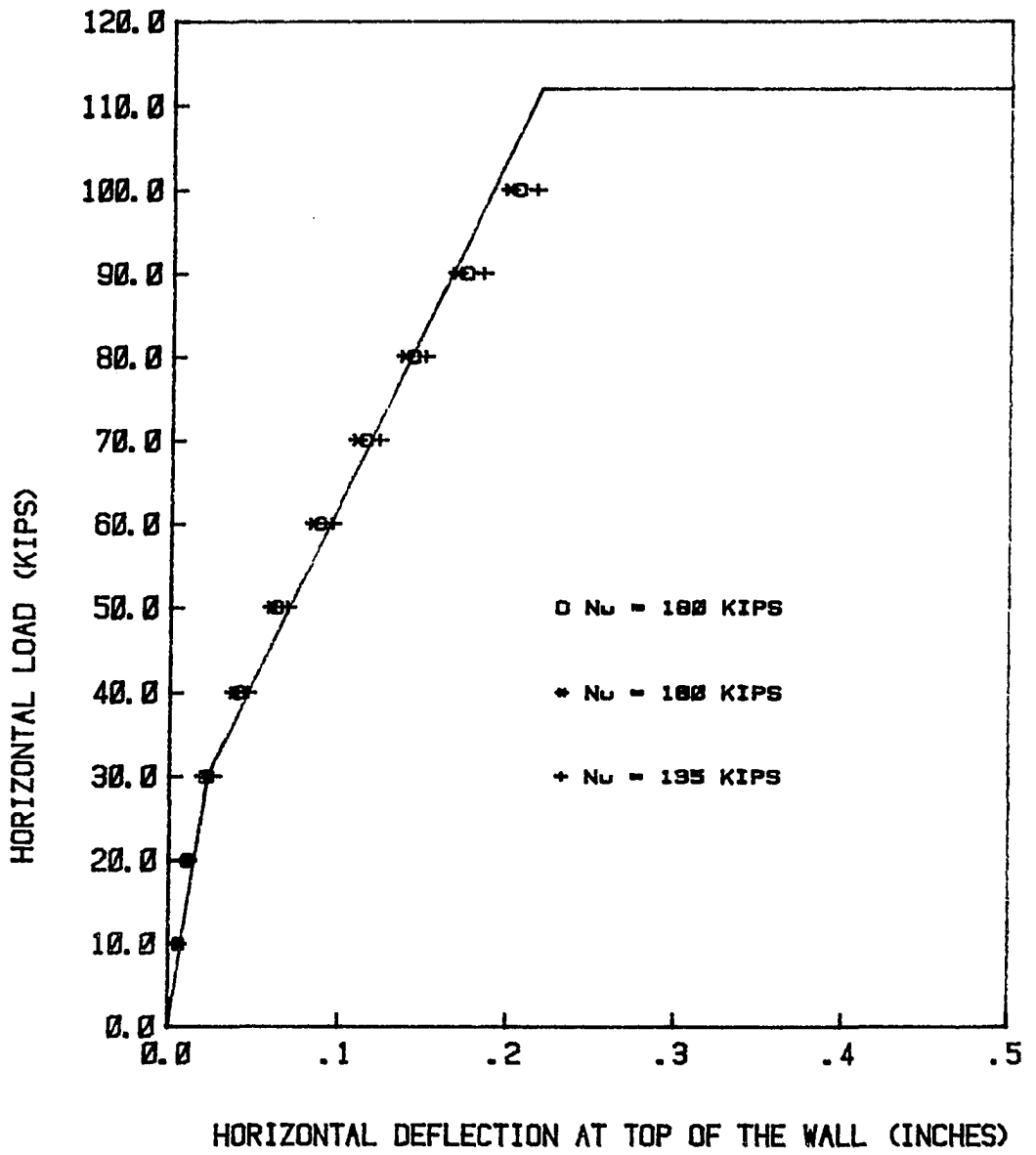

Figure 4. Proposed load-deflection curve for brick-to-brick walls

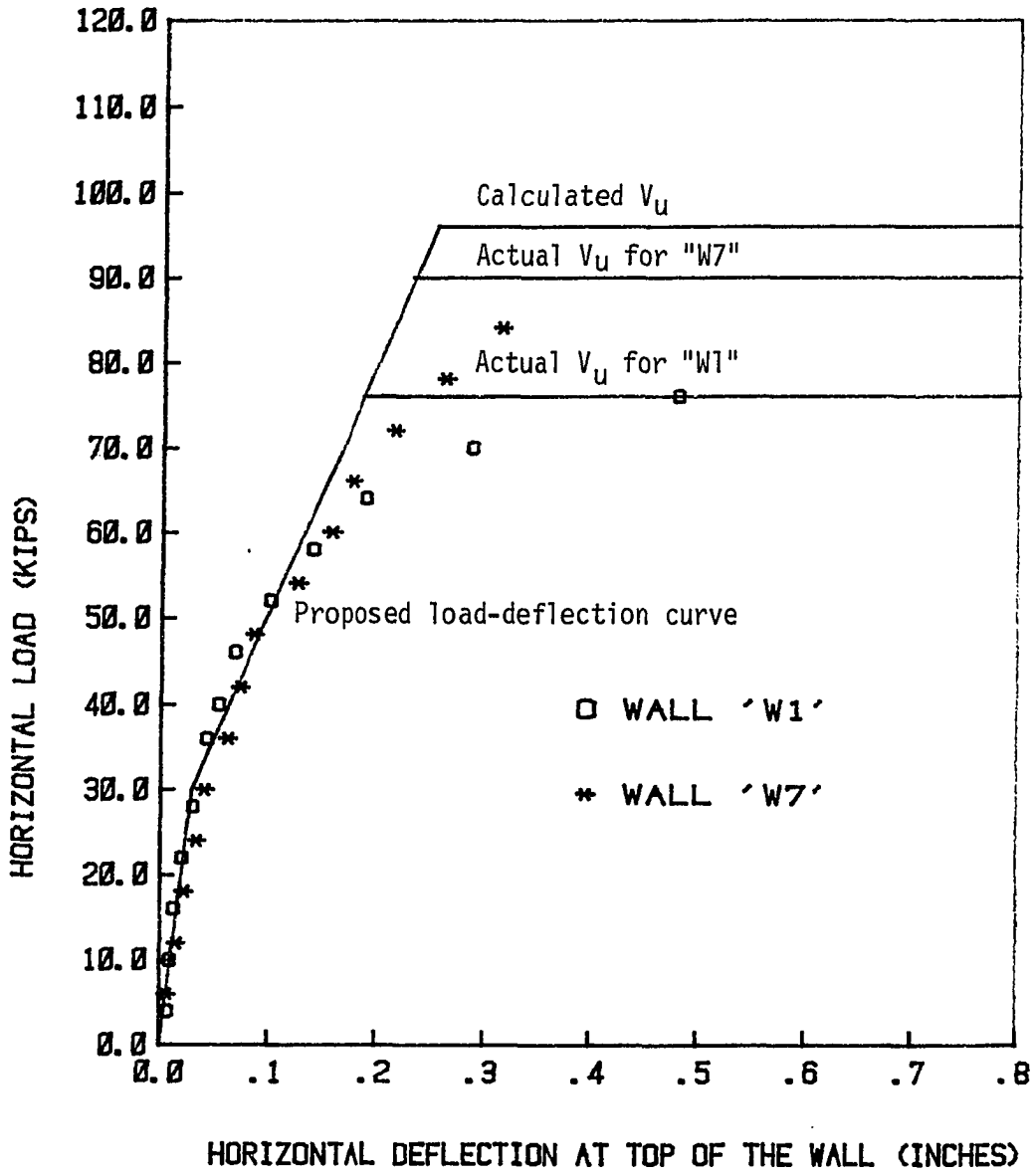

Figure 5. Comparison between the results of "W1" and "W7", and the proposed load-deflection curve

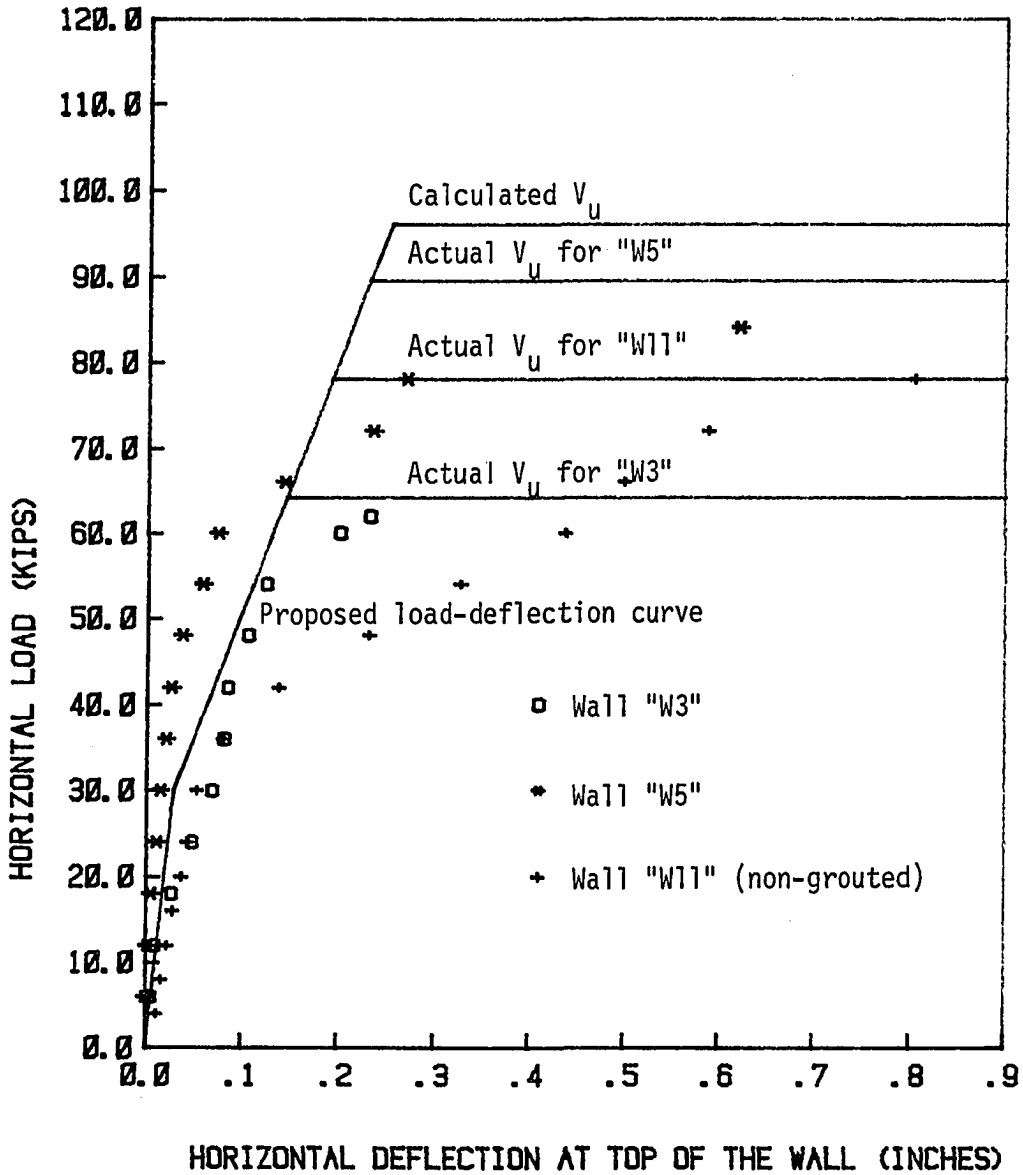

Figure 6. Comparison between the results of "W3", "W5" and "W11", and the proposed load-deflection curve

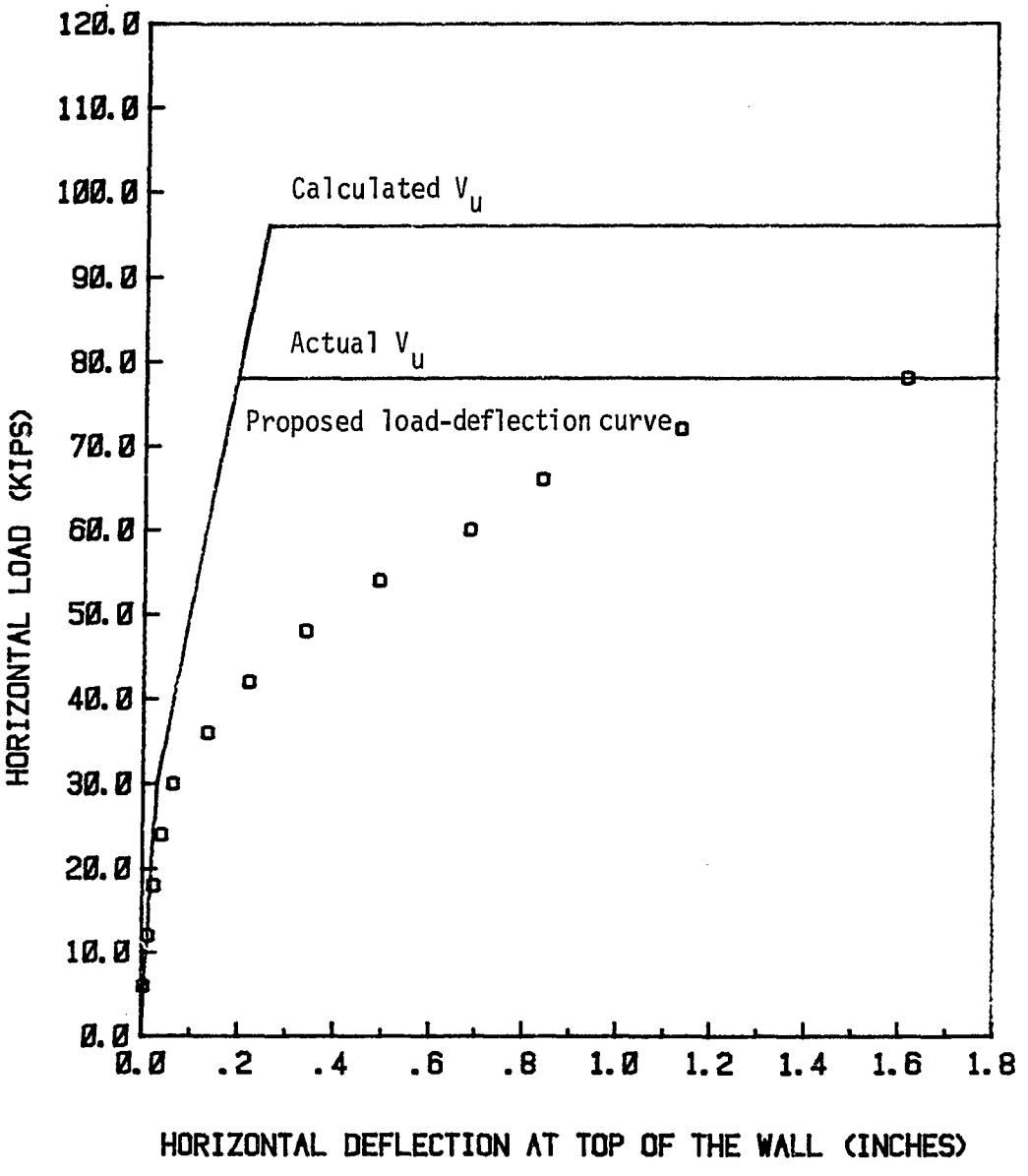

Figure 7. Comparison between the results of "W9" and the proposed load-deflection curve

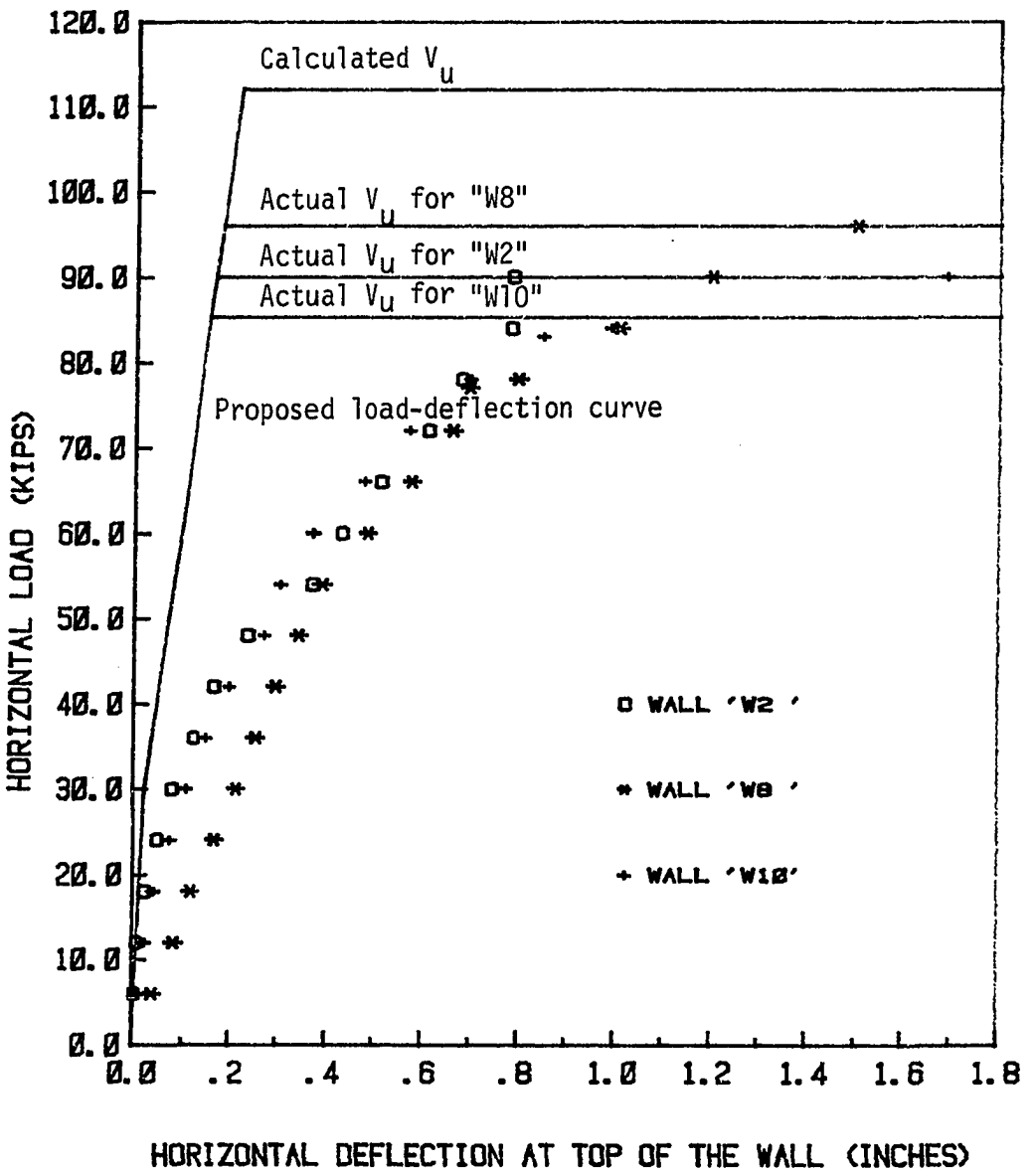

Figure 8. Comparison between the results of "W2", "W8" and "W10", and the proposed load-deflection curve

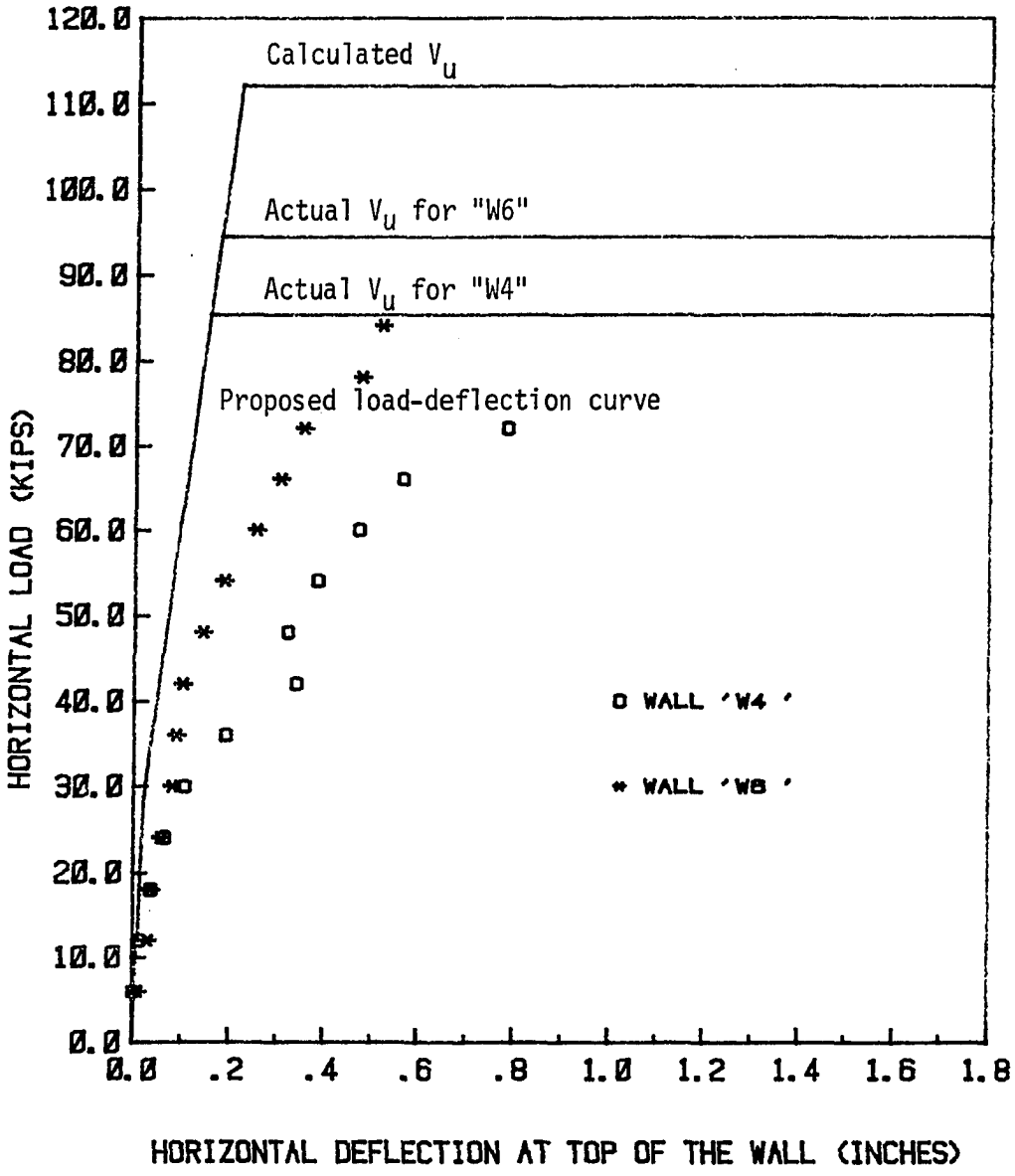

Figure 9. Comparison between the results of "W4" and "W6", and the proposed load-deflection curve

(2) For brick-to-brick walls, the proposed curve deviates from the experimental results in the second stage in particular.

The deviation shown in Fig. 7 from the experimental one may be due to the break of the weld connecting the vertical reinforcement at the far east end, allowing a softening in stiffness (the break occurred at a horizontal load of 72 kips).

Table 5 compares the ultimate calculated horizontal load (using the finite element technique with an assumed strain of 0.003) with the ultimate measured horizontal loads, and with the ones calculated using Equations 23 and 24. Table 5 inciates that the predicted ultimate shear load from Equations 23 and 24 is in good agreement with the experimental results and yields better results than the finite element method.

Table 5. Comparison between calculated "V_{uc}" and measured "V_{um}" ultimate shear loads

Brick-to-block walls				Brick-to-brick walls			
Wall No.	V_{uc} [a]	V_{uc} [b]	V_{um}	Wall No.	V_{uc} [a]	V_{uc} [c]	V_{um}
W1	96	80.7	76	W2	102	103.3	90
W3	96	96.3	64.2	W4	112	106	94.4
W5	96	92.4	89.5	W6	100	85.7	85.3
W7	96	87	90	W8	102	89.2	96
W9	83	78.9	78	W10	102	88.6	90

[a]Ultimate shear load based on finite element results [10].
[b]Ultimate shear load based on Equation 23.
[c]Ultimate shear load based on Equation 24.

Figs. 10 and 11 compare experimental results for both the finite element technique and the theory for flexural strength for shear walls

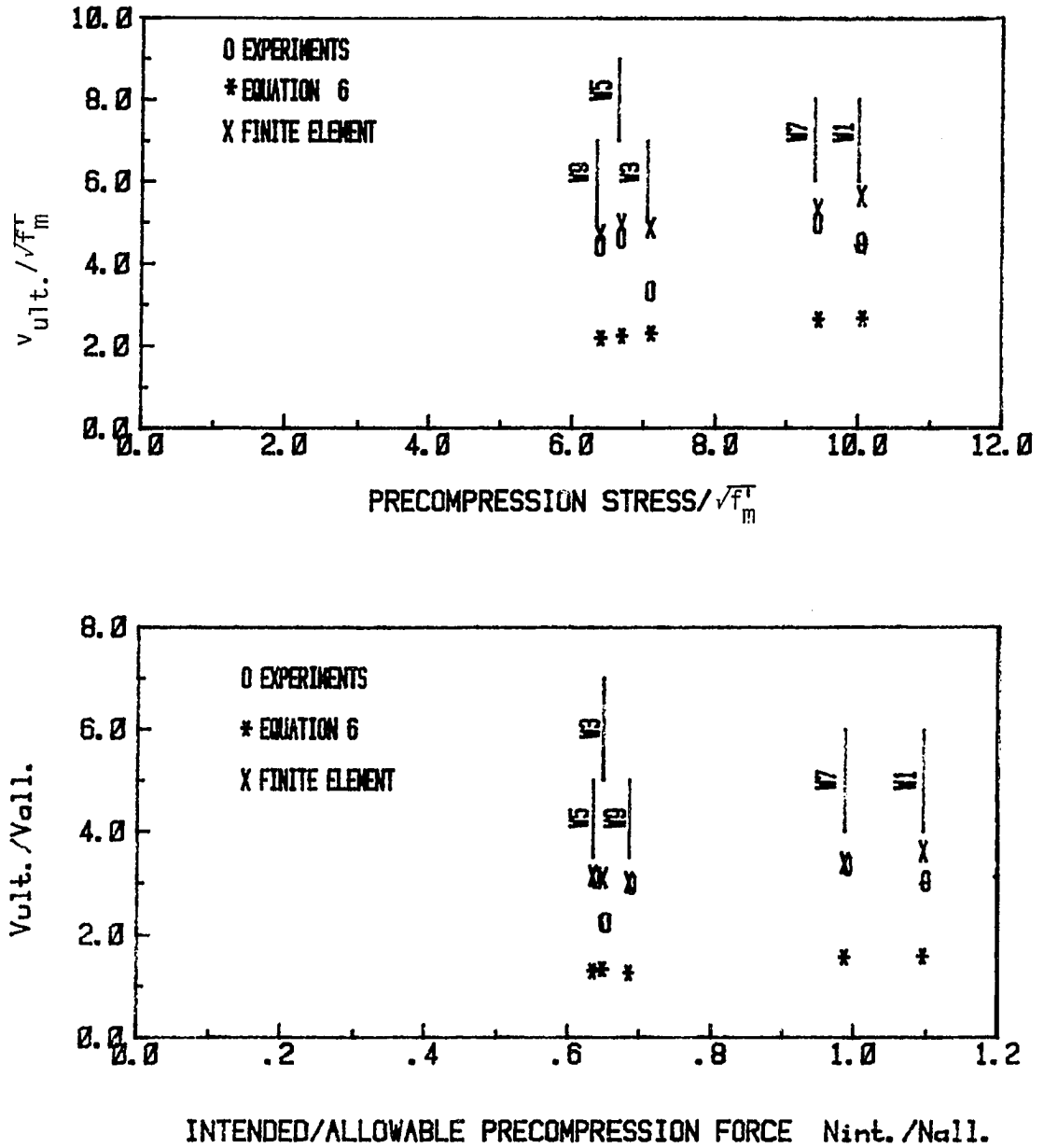

Figure 10. Comparison between the experimental results and shear wall equation versus the finite element for brick-to-block walls

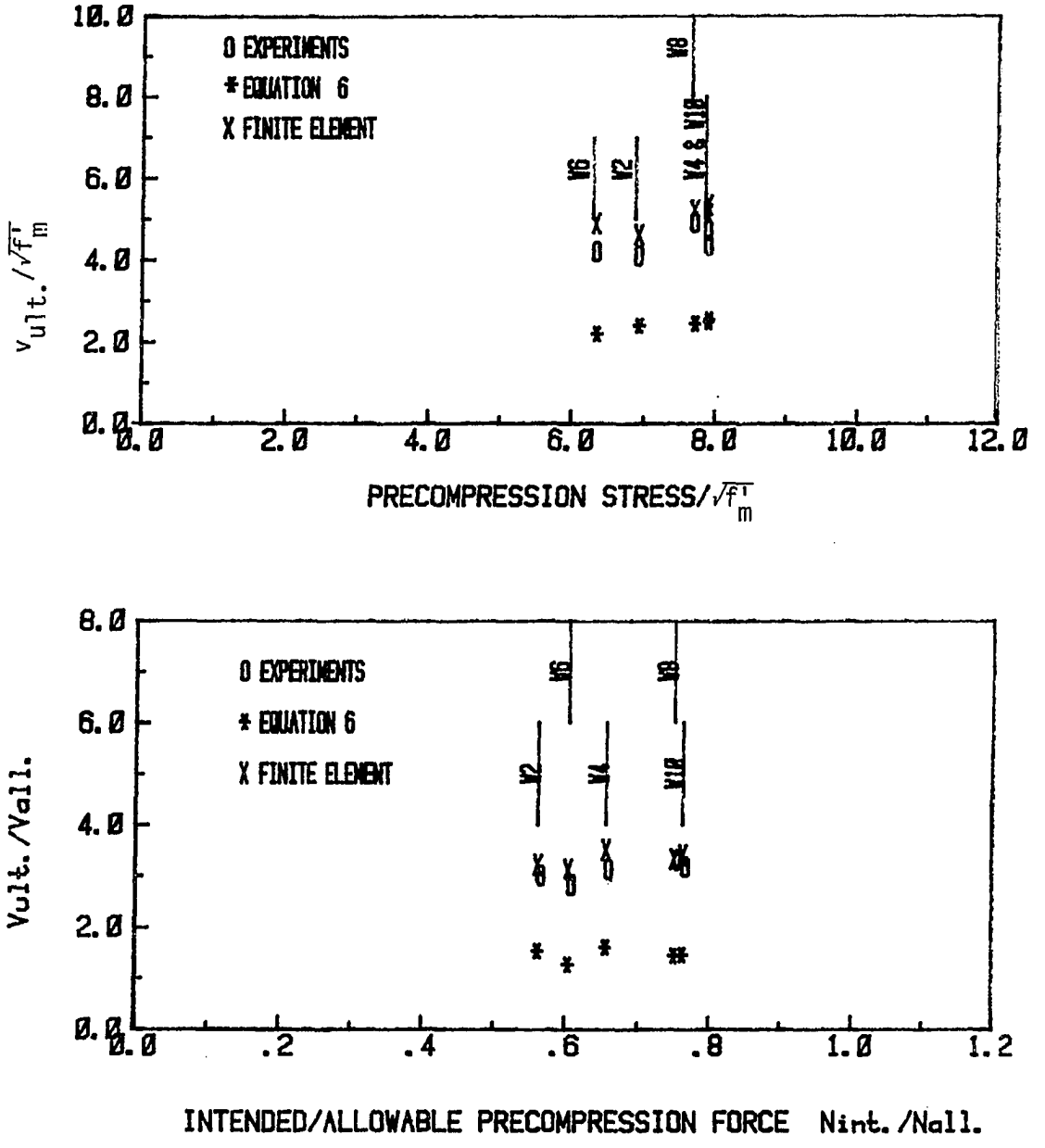

Figure 11. Comparison between the experimental results and shear wall equation versus the finite element for brick-to-brick walls

represented by Equation 6. The allowable vertical stresses were calculated on the basis of ACI 531-79 equation [10]:

$$F_a = 0.225\ f'_m\ [1 - (\frac{h}{40t})^3] \tag{25}$$

The allowable force $N_{all} = F_a$ area (26)

The last two figures (Figs. 10 and 11) and Table 5 indicate that both the finite element using the cracked-uncracked case concept or Equation 23 or 24 can be used to predict the ultimate shear load.

CONCLUSIONS AND RECOMMENDATIONS

On the basis of this study, the following conclusions can be made:

(1) That the ultimate shear load can be predicted by the modified shear wall equation, by the finite element method, or by using the following equations:

$$V_u = \frac{1}{h}[0.114\ b^2 t f'_m + 22.81\ A_s b + 0.16\ N_u b] \quad \text{for brick-to-block walls}$$

$$V_u = \frac{1}{h}[0.054\ b^2 t f'_m + 22.81\ A_s b + 0.46\ N_u b] \quad \text{for brick-to-brick walls}$$

The last two equations give the closest values of ultimate shear loads to actual ones.

(2) The constants K_2, K_1K_3 and K_u can be taken as follows:

$K_2 = 0.425$

$K_u = 0.6$

$K_1K_3 = 0.19 + 1.1\ N_u/Af'_m$ for brick-to-block walls

$K_1K_3 = 0.09 + 1.6\ N_u/Af'_m$ for brick-to-brick walls.

Tests need to be done to evaluate the constants, taking into account the different parameters.

(3) That the trilinear load-deflection curve can represent the actual curve for the brick-to-block walls. Further study is needed for predicting the load-deflections curve for brick-to-brick walls.

ACKNOWLEDGMENTS

The authors express their thanks to the Masonry Institute of Iowa and to the Masons Union of Iowa for providing material and labor for building the specimens. Thanks are also due to the Civil Engineering Department and Engineering Research Institute at Iowa State University. The assistance of Mr. Doug Wood is appreciated.

REFERENCES

1. R. R. Schneider and L. W. Dickey. "Reinforced masonry design." Prentice-Hall, Inc., Englewood Cliffs, New Jersey, 1980.

2. J. E. Amrhein. "Reinforced masonry engineering handbook." Clay and Concrete Masonry, Masonry Institute of America, Los Angeles, California, 1983.

3. R. Park and T. Paulay. "Reinforced concrete structures." John Wiley & Sons Inc., New York, 1975.

4. A. E. Carderas; J. M. Hanson; W. G. Corley and E. Hognestad. "Design provisions for shear walls." Proc. Journal of the American Concrete Institute, 70, No. 3, (March 1973), 221-230.

5. American Concrete Institute. "Building code requirements for reinforced concrete." ACI Standard 318-77, Detroit, Michigan, 1977.

6. M. H. Ahmed, M. L. Porter and A. Wolde-Tinsae. "Behavior of reinforced brick-to-block walls." Part 2A of unpublished Ph.D. dissertation by M. H. Ahmed, Iowa State University, Ames, Iowa, 1983.

7. M. H. Ahmed; M. L. Porter and A. Wolde-Tinsae. "Behavior of reinforced brick-to-brick walls." Part 2B of unpublished Ph.D. dissertation by M. H. Ahmed, Iowa State University, Ames, Iowa, 1983.

8. S. C. Anand; D. T. Young and D. T. Stevens. "A model to predict shearing stresses between wythes in composite masonry walls due to differential movement." Proc. North American Masonry Conference, University of Maryland, College Park, Maryland, August, 1982.

9. M. H. Ahmed; M. L. Porter and A. Wolde-Tinsae. "Analysis of composite masonry walls: Part I." Part 3 of unpublished Ph.D. dissertation by M. H. Ahmed, Iowa State University, Ames, Iowa, 1983.

10. American Concrete Institute. "Building code requirements for reinforced concrete." ACI Standard 318-77, Detroit, Michigan, 1977.

NOTATIONS

a_j Distance of point j from the neutral axis.

A Cross sectional area of the wall (gross section).

A_s Area of vertical steel in the entire wall section.

A_s^c Area of compression steel.

A_s^t Area of tension steel.

A_{si}, A_{sj} Area of steel at points i and j.

b Wall width

c_j Compressive force carried by steel at point j.

C Total compressive force carried by the cross section.

C_m Compressive force carried by the masonry.

d_i Distance of point i from the neutral axis.

E Elastic modulus of elasticity of the composite wall.

f_y Yield stress for steel.

f'_m Ultimate compressive strength for masonry

f_v Allowable shear stress for masonry shear wall.

F_a Allowable compressive stress for masonry shear wall.

F_1,F_2 Compressive forces for the cross section of the wall.

G, G_{xy} Modulus of rigidity of the composite wall

h Wall height

I Moment of inertia about the y-y axis of the wall cross section.

K_1,K_2,K_3 and K_u Constants

M_u Ultimate moment at the base of the wall.

$N_{all.}$ Allowable precompression loads

$N_{int.}$ Intended precompression loads.

N_u Vertical precompression load, kips.

t Thickness of the wall

$t_{b\ell}$ Thickness of block wythe.

t_{br} Thickness of brick wythe.

t_{gr} Thickness of grout wythe.

T Total tensile force carried by the tension steel.

T_i Tensile force carried by the steel at point i.

$v_{ult.}$ Ultimate shear stresses.

V Lateral (in-plane) load applied at top of the wall.

V_{all} Allowable lateral load.

V_u Ultimate lateral load, kips.

V_{uc} Calculated ultimate lateral load, kips.

V_{um} Measured ultimate lateral load, kips.

Z Elastic section modulus of the composite wall.

Δ Horizontal deflection at top of the wall.

ε_{cj} and ε_{ti} Strains at points j and i.

ε_u Ultimate strain of masonry wall.

β_1 Constant.

ν_{xy} Poisson's ratio in the x-y direction.

ν_{yx} Poisson's ratio in the y-x direction.

TENTATIVE DESIGN CRITERIA FOR REINFORCED COMPOSITE MASONRY WALLS

Notations

A_g Gross area for the composite wall cross section.

A_s Area of vertical reinforcement in the wall cross section.

b Wall width.

f_y Yield stress for the steel reinforcement.

f'_m Ultimate compressive strength for composite masonry prisms.

h Height of the wall.

M_u Factored ultimate moment at the wall base, due to the effect of the shear load.

N_u Precompression total vertical load, applied at the top of the wall.

v_u Factored ultimate in-plane shear stresses at top of wall, based on gross area.

V_n Nominal shear load.

V_u Factored ultimate in-plane shear load.

ϕ Constant equal to 0.7 for bearing failure.

Definition

Masonry elements composed of more than one type of masonry are known as "composites". One of the different shapes of composite material is the multi-wythe wall. These wythes can be made of blocks or bricks. The space between the wythes can be grouted and reinforced; so can the holes of the masonry. The composite wall here considered has two wythes with a reinforced grouted joint.

Failure Modes

The possible failure modes are:

(1) flexure;

(2) bearing;

(3) diagonal shear;

(4) sliding shear;

(5) transverse shear;

(6) bond:

  (a) between brick and mortar (along bed joint);

  (b) between brick and collar joint;

  (c) between block and collar joint;

  (d) between block and mortar (along bed joint); and

  (e) between steel and grout.

(7) buckling of reinforcement.

The following design criterion was developed based on the flexure failure mode.

Shear Strength

(1) The ultimate shear load shall be based on:

$$V_n - \frac{V_u}{\phi} \tag{1a}$$

$$M_n - \frac{M_u}{\phi} \tag{1b}$$

(2) The factored ultimate shear force shall be calculated as:

$$V_u = \frac{M_u}{h} = \frac{\phi M_n}{h}$$

where: $M_u = 0.114\ b^2 t f'_m + 22.81\ A_s b + 0.16\ N_u b$ (2)

or $M_u = 0.054\ b^2 t f'_m + 22.81\ A_s b + 0.46\ N_u b$ (3)

where Equation 2 is used for brick-to-block walls and Equation 3 is used for brick-to-brick walls.

(3) The factored ultimate shear stresses should be calculated on the basis of total actual gross area of the wall cross section, or

$$v_u = V_u/A_g \qquad (4)$$

(4) The allowable loads and stresses should not exceed the values calculated from Equations 2 through 4, taking into account a safety factor of 3.0.

Compressive Strength

(1) A minimum of three composite prisms in accordance with ASTM Specifications [5] should be built for each type of wall, using materials and thicknesses similar to those of the walls. The ultimate compressive strength can be determined by testing these prisms. For design and analysis, f'_m should not exceed the least f'_m of the individual wythes.

Reinforcements

(1) Reinforcement shall be placed in the collar joint. Reinforcement may be needed in the masonry wythes for other purposes.

(2) Reinforcement needed for such walls is the minimum reinforcement for masonry walls (i.e., 0.002 times the gross area as total reinforcement, but not less than 0.007 times the gross area in either horizontal or vertical directions).

(3) Horizontal reinforcement is not necessarily needed in the bed

joints. Metal ties can be used to hold the two masonry wythes before grouting.

(4) The reinforcement should be continuous through the floors.

Method of Analysis

(1) The wall should be treated as a cantilever beam fixed at the base and free at the top.

(2) Equation 2 or 3 is recommended for use in the calculation of ultimate and allowable loads and stresses.

(3) The finite element analysis for two-dimensional stresses can be used in conjunction with the concept of the cracked-uncracked section to better understand the wall's behavior.

Building the Wall

The wall may be built as follows:

(1) Build the first wythe completely;

(2) Place the reinforcement in the collar joint and hold to the metal ties;

(3) Build part of the second wythe and wait for one complete day;

(4) Grout the complete first part and finish building the second; and

(5) After another complete day, grout the rest of the wall.

CONCLUSIONS AND RECOMMENDATIONS

Conclusions

Based on this investigation, the following conclusions can be made:

(1) Using the composite masonry wall with grouting and reinforcing the collar joint versus the block wythe increases ultimate shear force by 15%, the initial stiffness by more than 300%, and the first crack load by 43%.

(2) The finite element technique with the cracked-uncracked case concept can be used to predict the ultimate shear capacity and load-deflection for composite brick-to-block reinforced masonry walls.

(3) Ultimate shear load can be predicted based on an assumed ultimate strain of 0.003, using the finite element method or the composite masonry wall equation. These equations are as follows:

$$V_u = \frac{1}{h}[0.114\ b^2 t f'_m + 22.81\ A_s b + 0.16\ N_u b] \quad \text{(brick-to-block wall)}$$

$$V_u = \frac{1}{h}[0.054\ b^2 t f'_m + 22.81\ A_s b + 0.46\ N_u b] \quad \text{(brick-to-brick wall)}$$

The composite masonry wall equations gave the best estimate for the ultimate shear load.

(4) The load-deflection curve for the composite masonry wall can be assumed trilinear.

(5) The assumption of composite action for the wall was valid.

(6) The allowable stresses (v_{all}) can be calculated for brick-to-brick walls using a safety factor of 3 as follows:

$$v_{all} = 47 + 0.0625\ \sigma_c$$

where: σ_c is the precompressive stress (psi); and

v_{all} is in psi.

(7) The effect of precompression load on both the load-deflection curve and the ultimate shear load is small for the range that is used in these tests.

(8) The allowable value of the shear stresses given in the UBC Codes is applied for the composite wall.

(9) The ultimate shear stresses for the tested walls ranged as:

Brick-to-block walls - 150.7-204.6 psi

Brick-to-brick walls - 196.8-221.3 psi

(10) Joint reinforcement reduces the ultimate shear load but not significantly ($\simeq$ 6%). This reduction agrees with similar conclusions for load bearing single wythe walls.

(11) The allowable shear-bond stresses (V_{SB}) can be calculated, based on safety factor of 3.0, as follows:

$$V_{SB} = 38.9 + 0.0103\ f'_m$$

where V_{SB} and f'_m are in psi.

(12) The steel did not yield in any wall, even though it was the minimum amount allowed by the ACI Code.

Recommendations

Application of the finite element method in conjunction with the theory for flexural strength resulted in good agreement between predicted

ultimate shear load and behavior of the composite masonry wall when compared to the experimental results. The following recommendations for further studies can be taken into consideration.

Experimental studies

For experimental tests to be conducted for composite masonry walls, the following parameters need to be considered:

(1) Wide range of height-to-width and height-to-thickness ratios.

(2) Wide range of precompression stresses.

(3) Different values for reinforcement.

(4) Different types of mortars, joint thicknesses, and strengths for masonry joints.

(5) The effect of the collar joint thickness.

(6) Conducting control tests to determine:

   (a) Ultimate strength for mortars, grout and masonry in compression, tension, and shear.

   (b) Stress-strain curves for different materials and for the composite section; and

   (c) Bond strengths between both mortar and grout, with both brick and block, in both shear and tension.

(7) The effect of different boundary conditions should be investigated.

(8) Tests need to be conducted to evaluate the constants K_2, K_1K_3 and K_u for the rectangular stress block.

(9) The actual stress distribution for the wall base needs to be known.

Analytical studies

For analytical studies to be made, the following parameters need to be considered:

(1) analysis of the composite wall using the finite element method with a wider range of actual strengths for different materials used in the composite wall; and

(2) different boundary conditions.

ACKNOWLEDGMENTS

The investigation contained here was conducted with the help of many sources. The author wishes to express his appreciation to all of those sources, in particular to the Civil Engineering Department under direction of Prof. C. E. Ekberg, and to the Engineering Research Institute, under the direction of Prof. W. W. Sanders for making this study possible.

The author wishes to thank most highly Prof. M. L. Porter for his contributions, encouragement and help while serving as Major Professor for this project. His encouragement and understanding throughout this study is greatly appreciated.

The author wishes to express his thanks and appreciation to Prof. A. Wolde-Tinsae for his help and contribution while serving as Co-Major Professor for this investigation. The author also wishes to thank the hourly employees in the lab who aided in preparing and conducting the test under the direction of Mr. Doug Wood. A special thanks is due to the masonry employees who contributed their time and effort in building the specimens. Thanks are also due to the Agency for International Development, the Masons Union of Iowa and the Masonry Institute of Iowa for their help in completing this project.

The author wishes to thank most highly Prof. F. W. Klaiber for his contribution. He is a genius to the extent that he could judge the whole work by only reading the first paper. Without his contribution, the author could have graduated six months earlier.

Last, the author would like to thank all of the unmentioned people who contributed in any way towards completion of this study.

REFERENCES

1. A. R. R. Schneider and L. W. Dickey. "Reinforced masonry design." Prentice-Hall, Inc., Englewood Cliffs, New Jersey, 1980.

2. Masonry Research Foundation. "Request for proposal." Masonry Research Foundation, Washington, D.C., 1980.

3. National Concrete Masonry Association. "Concrete masonry load bearing walls." NCMA-TEK, Rosslyn Station, Virginia, n. 61, 1974.

4. Iowa State University. "The graduate college thesis manual." Iowa State University, Ames, Iowa, Revised 1981.

5. Masonry Institute of America. "1979 Masonry Codes and Specifications." Masonry Institute of America, Los Angeles, California, 1979.

APPENDIX. SHEAR WALL DESIGN [3]

Consider a 25-story building, as shown in the figure below. Calculate forces on walls B & C at the 10th floor level, assuming:

Story height = 10 ft.

Effective wall thickness = 9" with 80% solid loads:

L.L. Roof = 30 psf

Floor = 40 psf

D.L. Roof = 80 psf

Floor = 100 psf

Floors assumed to span in E-W direction

Walls = 60 psf.

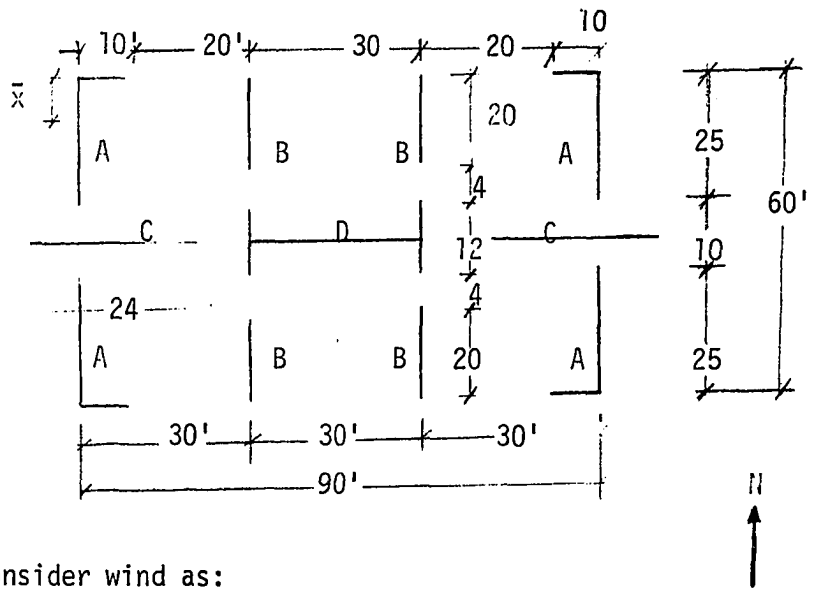

Consider wind as:

(a) wind pressure, 50 psi

(b) wind pressure, 25 psi

Wall Properties

Effective thickness = 0.8x9 = 7.2" = 0.6 ft.

Wall A

N-S direction Effective flange length (3.8.10.2 NCMA Specification for the design and construction of load bearing concrete masonry)

$\leq 6\ t_{eff.} = 6(0.6) = 3.6$ ft.

Area = $3.6(0.6) + 25(0.6) = 17.16\ ft^2$

$\Sigma A\bar{x} = 3.6(0.6)\ \frac{t}{2} + 25(0.6)(\frac{25}{2}) = 188.15\ ft^3$

$\bar{x} = \frac{188.15}{17.16} = 10.96$ ft.

$I = \frac{1}{3}\ (3.6x0.6)(0.6)^2 + \frac{1}{3}\ (25x0.6)(25)^2 - 17.16(10.96)^2$

$= 1063.97\ ft^4$

$S = \frac{I}{25-10.96} = 75.78\ ft^3$

E-W direction

Area = $3.6(0.6) + 0.6(10) = 8.16\ ft^2$

$A\bar{x} = 3.6(0.6)(0.3) + 0.6(10)(5) = 30.65\ ft^3$

$\bar{x} = \frac{30.65}{8.16} = 3.76$ ft

$I = \frac{1}{3}\ (3.6x0.6)(0.6)^2 + \frac{1}{3}\ (.6x10)(10)^2 - 8.16(3.76)^2$

$= 84.9\ ft^4$

$S = \frac{84.9}{10-3.76} = 13.61\ ft^3$

Wall B

N-S direction

Area = $20(0.6) = 12\ ft^2$

$I = \frac{12(20)^2}{12} = 400\ ft^4$

$S = \frac{12(20)}{6} = 40\ ft^3$

E-W direction

$S \simeq 0$

Wall C

N-S direction

$S \simeq 0$

E-W direction

Area = $25(0.6) = 15\ ft^2$

$I = \frac{15(25)^2}{12} = 781.25$

$S = \frac{15(25)}{6} = 62.5\ ft^3$

Wall D

N-S direction Neglect the web

Area = $2(12)(0.6) = 14.4\ ft^2$

$I = \frac{14.4(12)^2}{12} = 172.8\ ft^4$

$S = \frac{14.4(12)}{6} = 28.8\ ft^3$

E-W direction

$A = (30\text{-}0.6)0.6 + 2(12)(0.6) = 32.04\ ft^2$

$$I = \frac{29.4(0.6)(29.4)^2}{12} + 24(0.6)(15)^2 = 4510.6 \text{ ft}^4$$

$$S = \frac{4510.6}{15} = 300.7 \text{ ft}^3$$

Wall	N-S direction			E-W direction		
	Area	I	S	Area	I	S
A	17.16	1063.97	75.78	8.16	84.9	13.61
B	12	400	40	--	0	0
C	--	0	0	15	781.25	62.5
D	14.4	172.8	28.8	32.04	4510.6	300.7

Distribution of Lateral Load

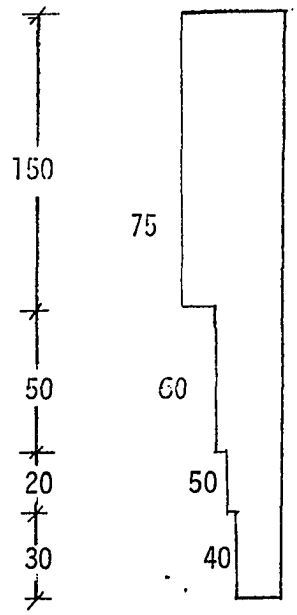

Case (a) for 50 psi wind pressure

10th floor level

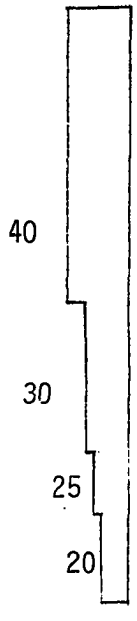

Case (b) for 25 psi wind pressure

	Case (a)	Case (b)
	N-S direction	
Total V	$\frac{75(150)(90)}{1000}$ = 1012.5 k	$\frac{40(150)(90)}{1000}$ = 540 k
Total Mo	$\frac{75(150)(75)(90)}{1000}$ = 75,938 k-ft	$\frac{40(150)(75)(90)}{1000}$ = 40,500 k-ft
	E-W direction	
Total V	$\frac{75(150)(60)}{1000}$ = 675 k	$\frac{40(150)(60)}{1000}$ = 360 k
Total Mo	$\frac{75(150)(75)(60)}{1000}$ = 50,625 k-ft	$\frac{40(150)(75)(60)}{1000}$ = 27,000 k-ft

Wall	I	# of walls	Total I	% of load	Case (a)		Case (b)	
					V	Mo	V	Mo
			N-S direction					
A	1063.97	4	4255.88	70.6	714.8	53,612	381.2	28,593
B	400	4	1600	26.5	268.3	20,124	143.1	10,733
D	172.8	1	172.8	2.9	29.4	2,202	15.7	1,175
			E-W direction					
A	84.9	4	339.6	5.3	35.8	2,683	19.1	1,431
C	781.25	2	1562.5	24.4	164.7	12,353	87.8	6,588
D	4510.6	1	4510.6	70.3	474.5	35,589	253.1	18,981
	ΣN-S		6028.68					
	ΣE-W		6412.7					

Vertical Load

Wall B

Total D.L. = 22[(80)(30) + 14(100)(30)] + (20)(15)(10)(60)

= 1156.8 k

Total L.L. = 22 [(30)(30) + 14(40)(30)]

= 389.4 k

Total reduced L.L. (R.L.L.)

= 22[(30)(30) + (40)(30)] + 13(22)(0.4)(40)(30)

= 183.5 k

Total V.L. load = 1340.3 k

Wall C

Total D.L. = (80)(5)(15) + 14(100)(5)(15) + 15(60)(10)(25)

= 336 k

Total L.L. = (30)(5)(15) + 14(40)(5)(15)

= 44.25 k

No reduction in L.L. permitted because of small contributing area per floor.

Total V.L. load = 380.25 k

For Wall B

N-S direction

V = 268.3 k (Case a)

V = 143.1 k (Case b)

N_u = 1340.3 k

or

V = 3.3 k/ft (Case a)

V = 4.29 k/ft (Case b)

N_u = 16.75 k/ft

For Wall C

E-W direction

V = 164.7 k (Case a)

V = 87.8 k (Case b)

N_u = 380.25 k

or

V = 3.3 k/ft long (Case a)

V = 1.75 k/ft long (Case b)

N_u = 7.6 k/ft

For panels of 4-ft. wide, the actual forces will be as follows:

Wall	Case a		Case b	
	V (k)	N_u (k)	V (k)	N_u (k)
B	13.4	67	17.16	67
C	13.2	30.4	7	30.4

NOTATIONS

A	Cross sectional area of the wall; $in.^2$.
I	Moment of inertia about the N-S axis; $in.^4$.
M_o	Bending moment at the wall base; k-ft.
N_u	Ultimate vertical load; kips.
S	Elastic section modulus; $in.^3$.
t_{eff}.	Effective thickness of the wall; in.
V	Horizontal shear load; kips.